Modeling magnetic materials using advanced DFT functionals: Hubbard, hybrids, meta-GGA, and van der Waals

Iurii Timrov

Laboratory for Materials Simulations, and National Centre for Computational Design and Discovery of Novel Materials (MARVEL), Paul Scherrer Institut, Villigen, Switzerland

PAUL SCHERRER INSTITUT

MARVEL

NATIONAL CENTRE OF COMPETENCE IN RESEARCH

22 April 2024

1st European School on Superconductivity and Magnetism in Quantum Materials

A word of introduction

2004 - 2009

Taras Shevchenko National University of Kyiv (Ukraine)

BSc & MSc degrees with honours

Theoretical physics

2013 - 2016

Scuola Internazionale Superiore di Studi Avanzati (Italy)

Postdoctoral researcher

Advisor: Prof. Stefano Baroni

TDDFT: absorption spectroscopy, magnetic excitations

2009 - 2013

École polytechnique (France)

PhD degree in physics with honours

Supervisor: Dr. Nathalie Vast

DFT, pump-probe experiments, EELS

2016 - 2023

École polytechnique fédérale de Lausanne (Switzerland)

Postdoctoral researcher (2016 - 2021)

Senior research scientist (2021 - present)

Advisor: Prof. Nicola Marzari

DFT+U+V, phonons, complex materials

A word of introduction

2004 - 2009

Taras Shevchenko National University of Kyiv (Ukraine)

BSc & M

T

2013 - 2016

Scuola Internazionale Superiore di Studi Avanzati (Italy)

oral researcher

f. Stefano Baroni

orption spectroscopy,
citations

2023 - present

Paul Scherrer Institut (Switzerland)

Tenure-track scientist

LMS lab head : Prof. Nicola Marzari

Development of novel computational methods, support of experiments, etc.

2009

École polytech

PhD degre

Supervisor: Dr. Nathalie Vast

DFT, pump-probe experiments, EELS

023

de Lausanne (Switzerland)

researcher (2016 - 2021)

Senior research scientist (2021 - present)

Advisor: Prof. Nicola Marzari

DFT+U+V, phonons, complex materials

Paul Scherrer Institut

- Named after the Swiss nuclear physicist Paul Scherrer (1890 - 1969)
- Was created in 1988 by merging two institutes, Swiss Federal Institute for Reactor Research (1960) and Swiss Institute for Nuclear Research (1968).

Facts about the Paul Scherrer Institut

- PSI is *the largest* research institute for natural and engineering sciences in Switzerland
- Conducting cutting-edge research in four main fields: future technologies, energy and climate, health innovation and fundamentals of nature
- PSI develops, builds and operates complex large research facilities: Swiss Light Source SLS, the free-electron X-ray laser SwissFEL, the SINQ neutron source, the SµS muon source and the Swiss research infrastructure for particle physics CHRISP
- PSI employs 2200 people
- Every year, more than 2500 scientists from Switzerland and around the world come to PSI to use our unique facilities to carry out experiments that are not possible anywhere else.
- Annual budget of approximately EUR 430 million

Director: Christian Rüegg

Large-scale facilities at PSI

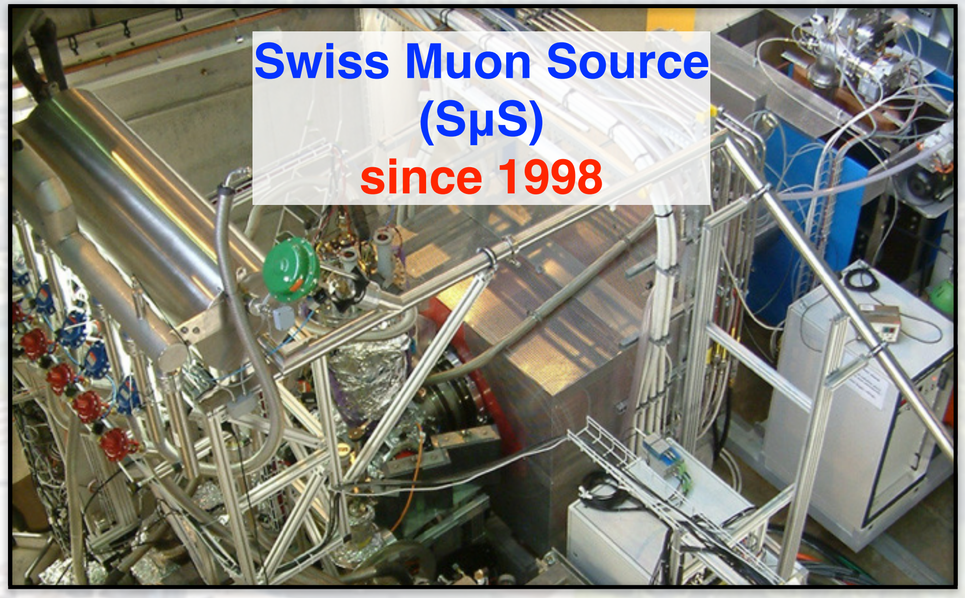

Laboratory for Materials Simulations

- Was created in 2021
- Part of the new Division for Scientific Computing, Theory and Data (SCD)
- The Laboratory currently hosts three groups: Materials Software and Data group, Multiscale Materials Modelling group, and Light Matter Interaction group
- 22 people (the lab grows fast)

Lab head: Nicola Marzari

- Mission: to develop, integrate, and disseminate in the PSI community and the scientific community at large the computational capabilities required to understand, predict, and characterize materials as studied at PSI research facilities with photons, neutrons, muons, and electrons

Arosa (Grisons, Switzerland), 27th December 1925

"At the moment I am struggling with a new atomic theory. I am very optimistic about this thing and expect that if I can only… solve it, it will be very beautiful"

Erwin Schrödinger

The Nobel Prize in Chemistry 1998

Walter Kohn
(1923 - 2016)

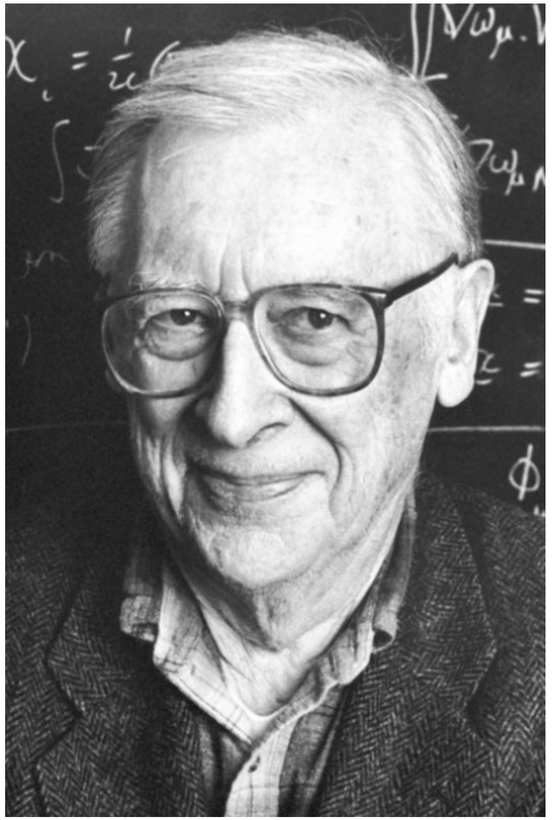

John A. Pople
(1925 - 2004)

The Nobel Prize in Chemistry 1998 was divided equally between Walter Kohn "for his development of the density-functional theory" and John A. Pople "for his development of computational methods in quantum chemistry"

Most cited papers in the history of the American Physical Society (from 1893)

	Journal	# cites	Title	Author(s)
1	PRL (1996)	78085	Generalized Gradient Approximation Made Simple	Perdew, Burke, Ernzerhof
2	PRB (1988)	67303	Development of the Colle-Salvetti Correlation-Energy …	Lee, Yang, Parr
3	PRB (1996)	41683	Efficient Iterative Schemes for Ab Initio Total-Energy …	Kresse and Furthmuller
4	PR (1965)	36841	Self-Consistent Equations Including Exchange and Correlation …	Kohn and Sham
5	PRA (1988)	36659	Density-Functional Exchange-Energy Approximation …	Becke
6	PRB (1976)	31865	Special Points for Brillouin-Zone Integrations	Monkhorst and Pack
7	PRB (1999)	30940	From Ultrasoft Pseudopotentials to the Projector Augmented …	Kresse and Joubert
8	PRB (1994)	30801	Projector Augmented-Wave Method	Blochl
9	PR (1964)	30563	Inhomogeneous Electron Gas	Hohenberg and Kohn
10	PRB (1993)	19903	Ab initio Molecular Dynamics for Liquid Metals	Kresse and Hafner
11	PRB (1992)	17286	Accurate and Simple Analytic Representation of the Electron …	Perdew and Wang
12	PRB (1990)	15618	Soft Self-Consistent Pseudopotentials in a Generalized …	Vanderbilt
13	PRB (1992)	15142	Atoms, Molecules, Solids, and Surfaces - Applications of the …	Perdew, Chevary, …
14	PRB (1981)	14673	Self-Interaction Correction to Density-Functional Approx. …	Perdew and Zunger
15	PRB (1986)	13907	Density-Functional Approx. for the Correlation-Energy …	Perdew
16	RMP (2009)	13513	The Electronic Properties of Graphene	Castro Neto et al.
17	PR (1934)	12353	Note on an Approximation Treatment for Many-Electron Systems	Moller and Plesset
18	PRB (1972)	11840	Optical Constants on Noble Metals	Johnson and Christy
19	PRB (1991)	11580	Efficient Pseudopotentials for Plane-Wave Calculations	Troullier and Martins
20	PRL (1980)	10784	Ground-State of the Electron-Gas by a Stochastic Method	Ceperley and Alder

The top 100 papers

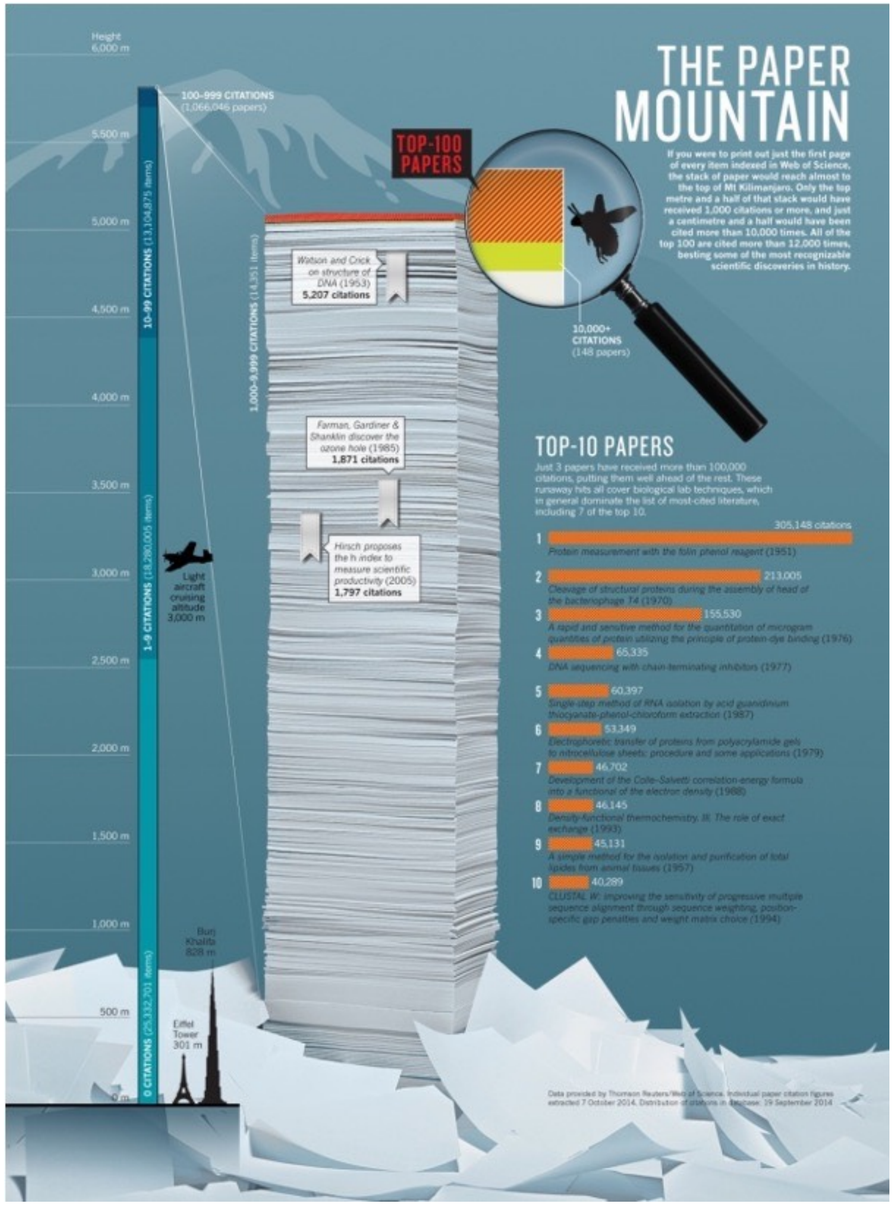

12 papers on density functional theory in the top-100 most cited papers in the entire scientific, medical, engineering literature, ever.

Nature, Oct 2014

From a many-body to a one-body problem

$$\Psi(\mathbf{r}_1, \mathbf{r}_2, ..., \mathbf{r}_N)$$

$$\varphi(\mathbf{r})$$

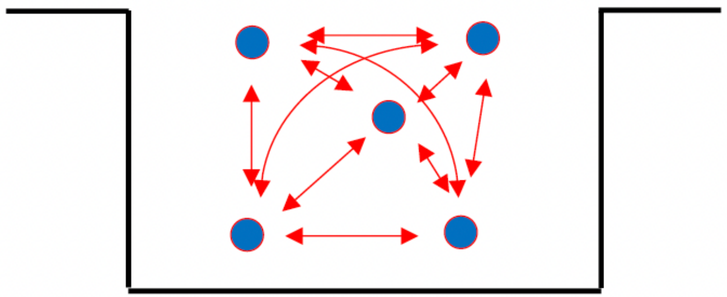

$$n(\mathbf{r})$$

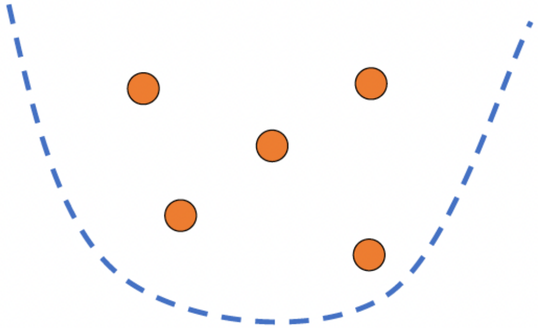

electrons

interaction

external potential $v_{ext}(\mathbf{r})$

Kohn-Sham particles (non-interacting)

effective potential $v_{KS}(\mathbf{r})$

$$n(\mathbf{r}) = \sum_i^{occ} \int |\Psi_i(\mathbf{r}, \mathbf{r}_2, ..., \mathbf{r}_N)|^2 d\mathbf{r}_2 ... d\mathbf{r}_N$$

$$n(\mathbf{r}) = \sum_i^{occ} |\varphi_i(\mathbf{r})|^2$$

Hohenberg-Kohn theorems

Theorem I

For any system of interacting particles in an external local potential $V_{ext}(\mathbf{r})$, the potential $V_{ext}(\mathbf{r})$ is determined uniquely, except for a constant, by the ground state particle density $n_0(\mathbf{r})$.

Theorem II

A universal functional for the energy $E_{HK}[n]$ in terms of the density $n(\mathbf{r})$ can be defined, valid for any external potential $V_{ext}(\mathbf{r})$:

$$E_{HK}[n] = F_{HK}[n] + \int V_{ext}(\mathbf{r})\, n(\mathbf{r})\, d\mathbf{r},$$

where $F_{HK}[n]$ is a universal functional of the density which does not depend on $V_{ext}(\mathbf{r})$. For any particular $V_{ext}(\mathbf{r})$, the exact ground-state energy of the system is the global minimum value of the functional $E_{HK}[n]$, and the density $n(\mathbf{r})$ that minimizes this functional is the exact ground state density $n_0(\mathbf{r})$.

Density-functional theory

Kohn-Sham equation:

$$\boxed{\left(-\frac{\hbar^2}{2m_0}\nabla^2 + V_{KS}(\mathbf{r})\right)\varphi_i(\mathbf{r}) = \varepsilon_i\,\varphi_i(\mathbf{r})}$$

$$\begin{aligned} V_{KS}(\mathbf{r}) &= V_H(\mathbf{r}) + V_{\mathrm{xc}}(\mathbf{r}) + V_{ext}(\mathbf{r}) \\ &= e^2\int \frac{n(\mathbf{r}')}{|\mathbf{r}-\mathbf{r}'|}\,d\mathbf{r}' + \frac{\delta E_{\mathrm{xc}}[n]}{\delta n(\mathbf{r})} + V_{ext}(\mathbf{r}) \end{aligned}$$

?

Density-functional theory

Kohn-Sham equation:

$$\boxed{\left(-\frac{\hbar^2}{2m_0}\nabla^2 + V_{KS}(\mathbf{r})\right)\varphi_i(\mathbf{r}) = \varepsilon_i\,\varphi_i(\mathbf{r})}$$

$$\begin{aligned} V_{KS}(\mathbf{r}) &= V_H(\mathbf{r}) + V_{\mathrm{xc}}(\mathbf{r}) + V_{ext}(\mathbf{r}) \\ &= e^2\int \frac{n(\mathbf{r}')}{|\mathbf{r}-\mathbf{r}'|}\,d\mathbf{r}' + \frac{\delta E_{\mathrm{xc}}[n]}{\delta n(\mathbf{r})} + V_{ext}(\mathbf{r}) \end{aligned}$$

?

Local density approximation (LDA):

$$E_{\mathrm{xc}}^{LDA}[n] = \int \varepsilon_{\mathrm{xc}}^{hom}(n(\mathbf{r}))\,n(\mathbf{r})\,d\mathbf{r}$$

Generalized-gradient approximation (GGA):

$$E_{\mathrm{xc}}^{GGA}[n] = \int \varepsilon_{\mathrm{xc}}(n(\mathbf{r}), \nabla n(\mathbf{r}))\,n(\mathbf{r})\,d\mathbf{r}$$

PBE, PBEsol, …

Some drawbacks of LDA / GGA

- Self-interaction errors

  Consequences: - over-delocalization of electrons (*d* and *f*)
  - incorrect description of charge transfer
  - incorrect energetics of chemical reactions
  - underestimation of band gaps
  - …

- Lack of non-locality

  Consequences: - incorrect description of weak long-range (van der Waals) interactions
  - inadequate description of bond breaking and formation
  - no Rydberg series
  - …

Some advanced exchange-correlation functionals

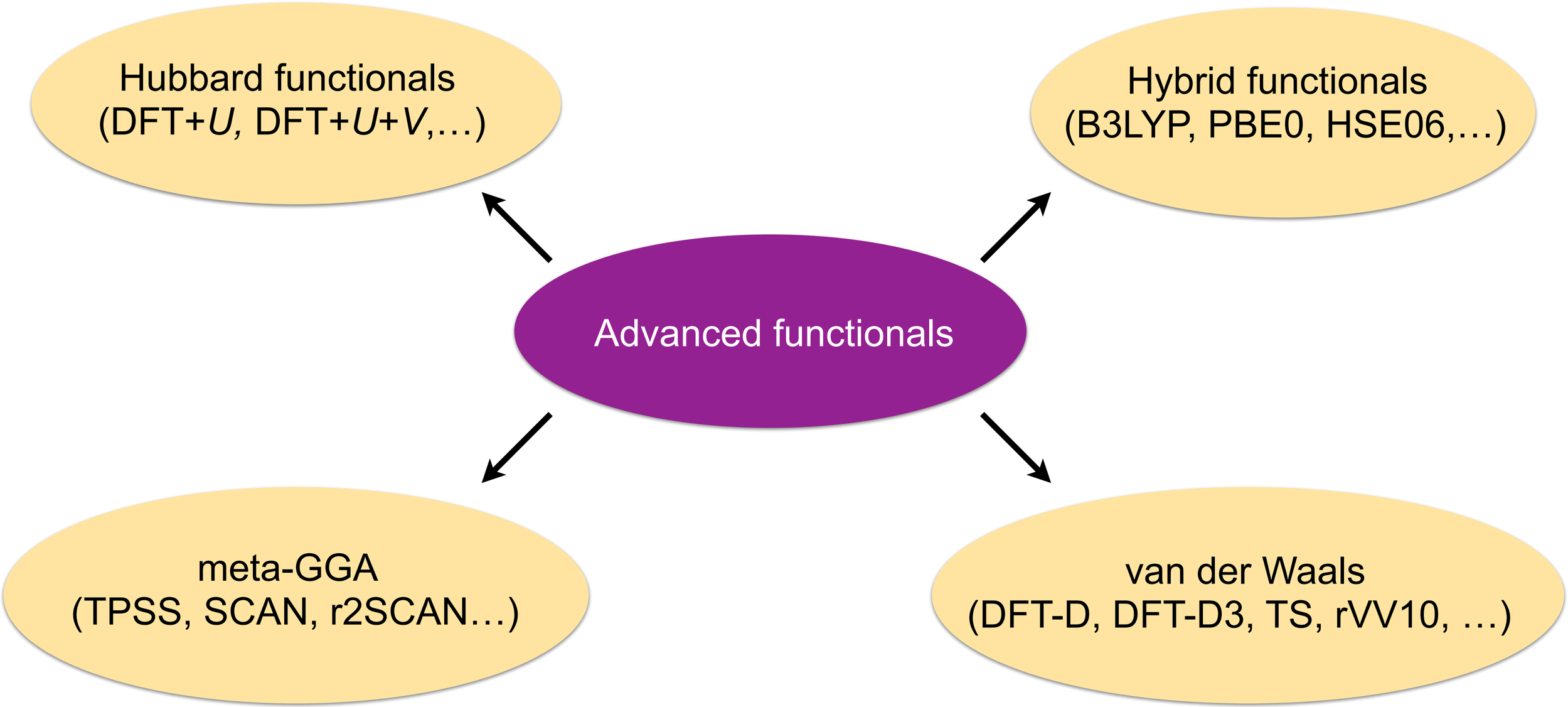

Self-interaction error

Self-interaction errors arrise from an incomplete cancellation of self-Coulomb terms by the approximate exchange-correlation energy terms

total charge density

Hartree potential felt by each electron

$$V_H(\mathbf{r}) = e^2 \int \frac{n(\mathbf{r}')}{|\mathbf{r} - \mathbf{r}'|} d\mathbf{r}'$$

An electron interacts with itself → self-interaction (unphysical)

Self-interaction error

The simplest example: the dissociation of H_2^+

The problem: approximate DFT gives only one solution - equal splitting of the charge

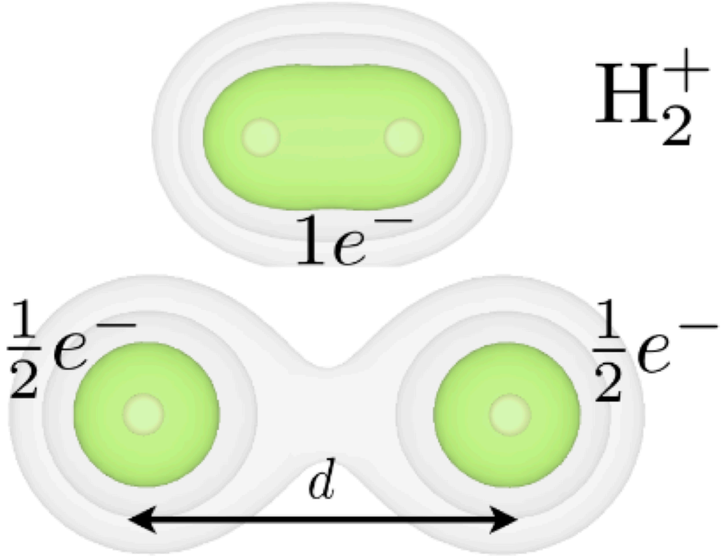

Perdew, Parr, Levy, Balduz, PRL (1982).

Self-interaction error

The simplest example: the dissociation of H_2^+

The problem: approximate DFT gives only one solution - equal splitting of the charge

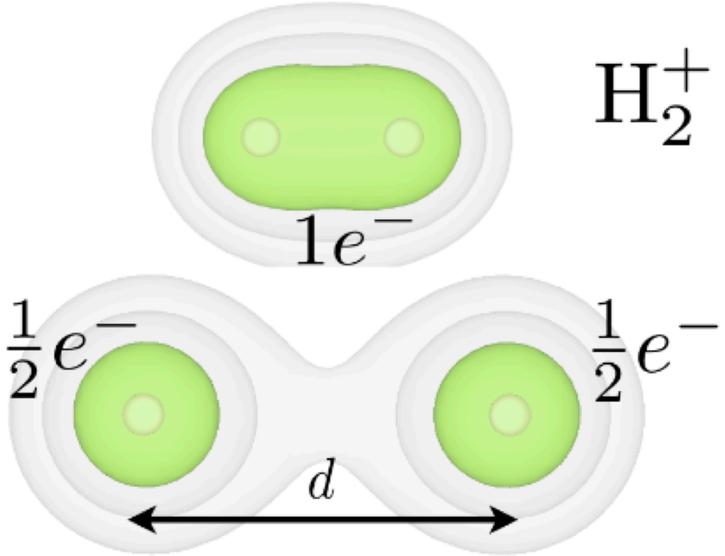

Perdew, Parr, Levy, Balduz, PRL (1982).

Origin of the problem: self-interaction error (**spurious quadratic energy change** when adding/removing a fraction of an electron)

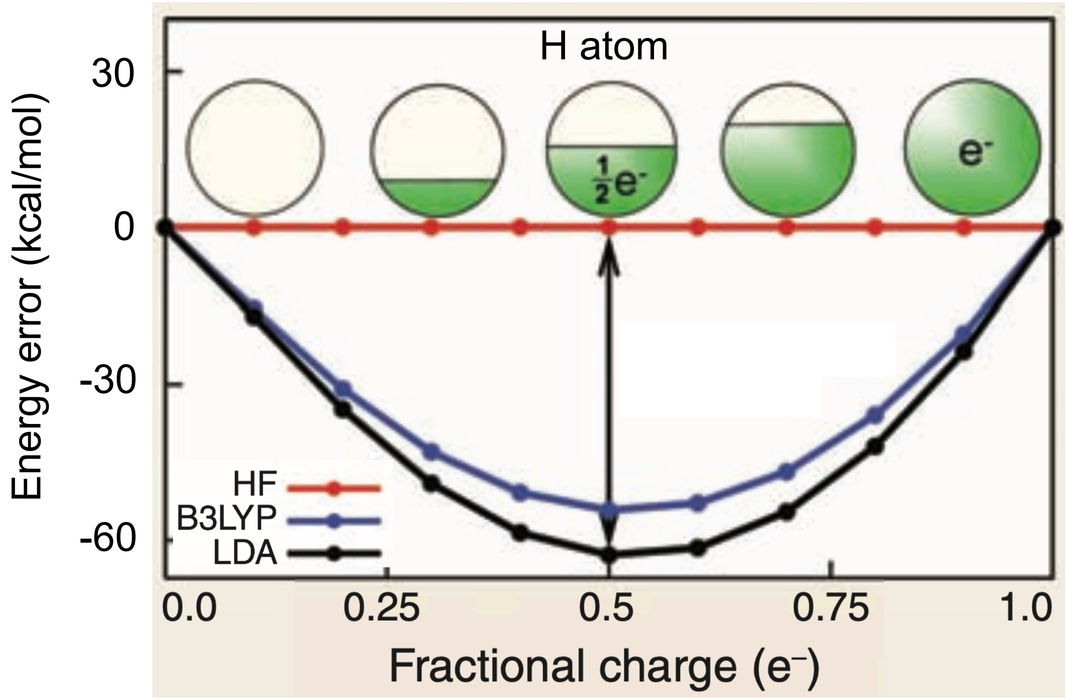

Cohen, Mori-Sanchez, Yang, Science (2008).

Self-interaction error in materials

Correct

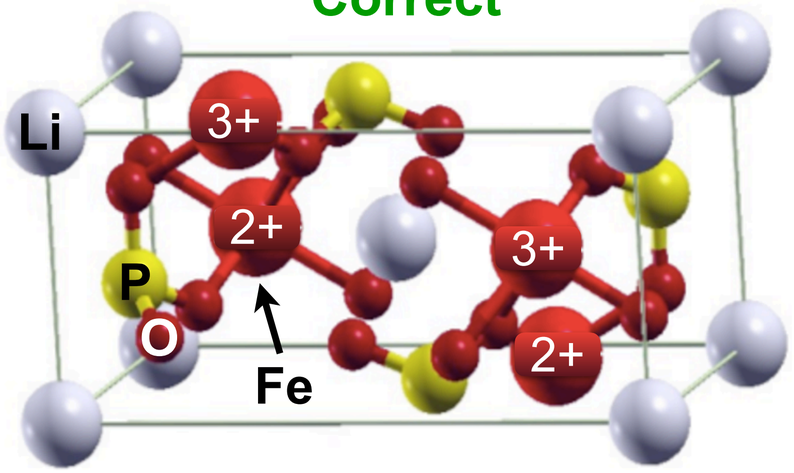

$Li_{0.5}FePO_4$

Incorrect

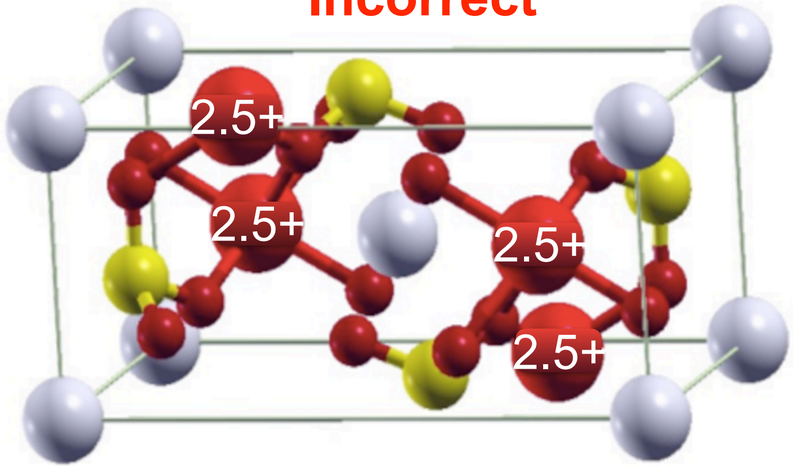

Self-interaction error in materials

Correct

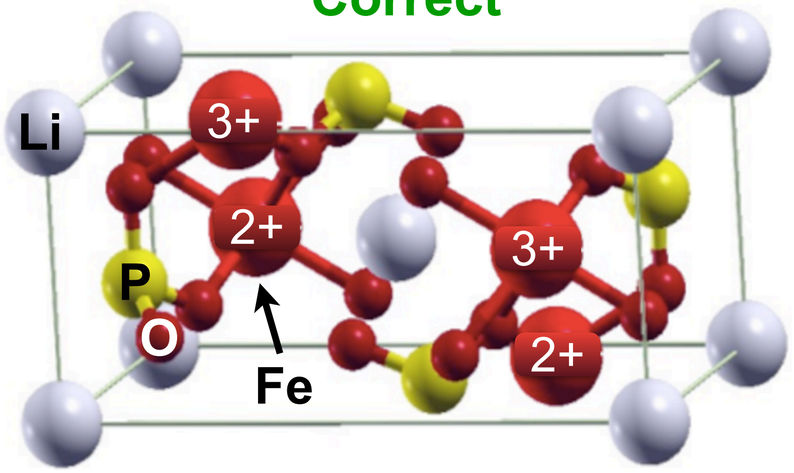

$Li_{0.5}FePO_4$

Incorrect

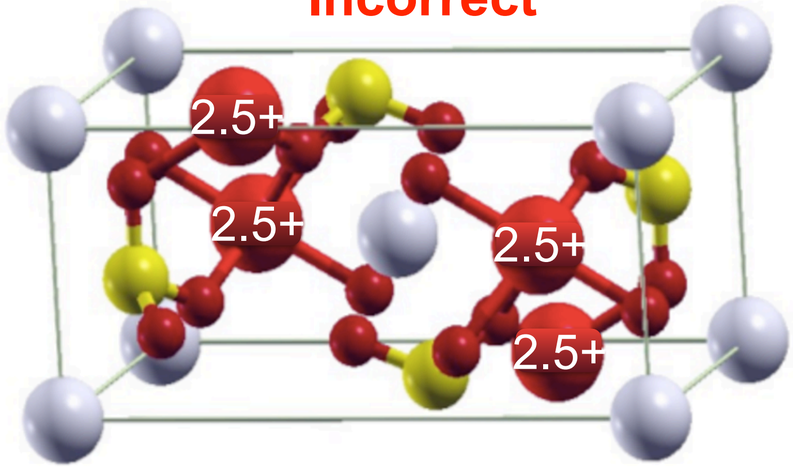

Fe^{2+}: $3d^6$

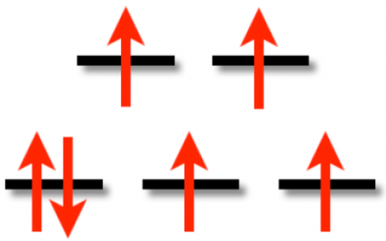

Fe^{3+}: $3d^5$

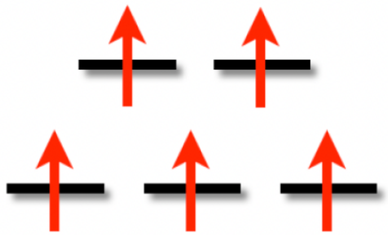

Self-interaction error in materials

Correct

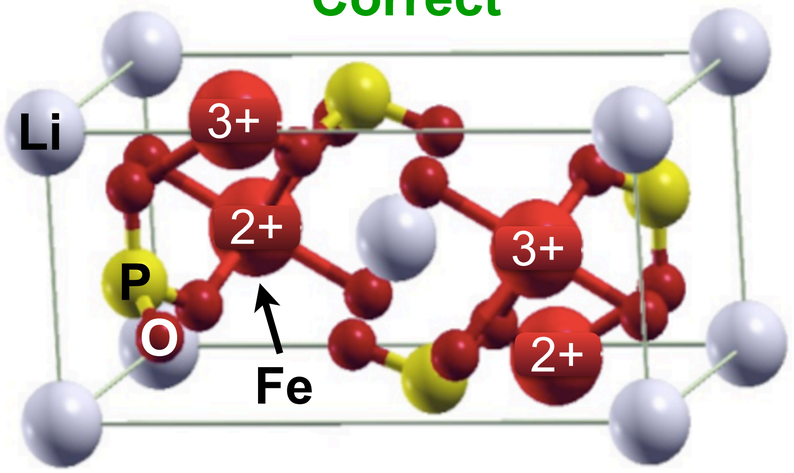

$Li_{0.5}FePO_4$

Incorrect

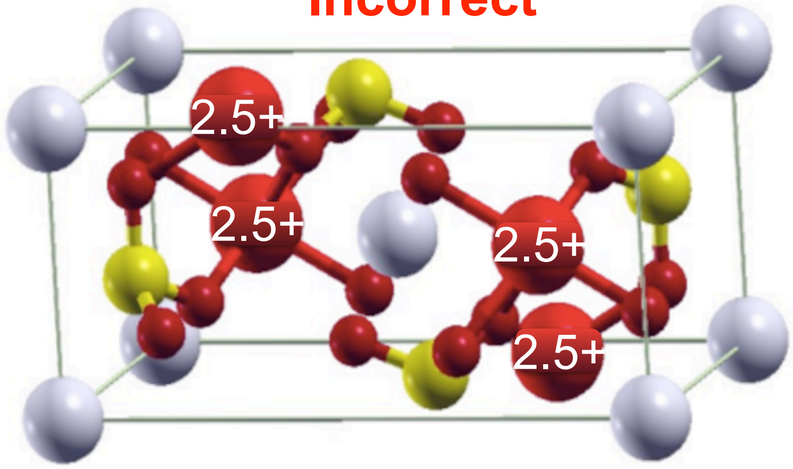

Self-interaction error

Fe-*3d* electrons are delocalized and spread around

Wrong average oxidation state of 2.5+ for Fe ions

Self-interaction error in materials

Correct

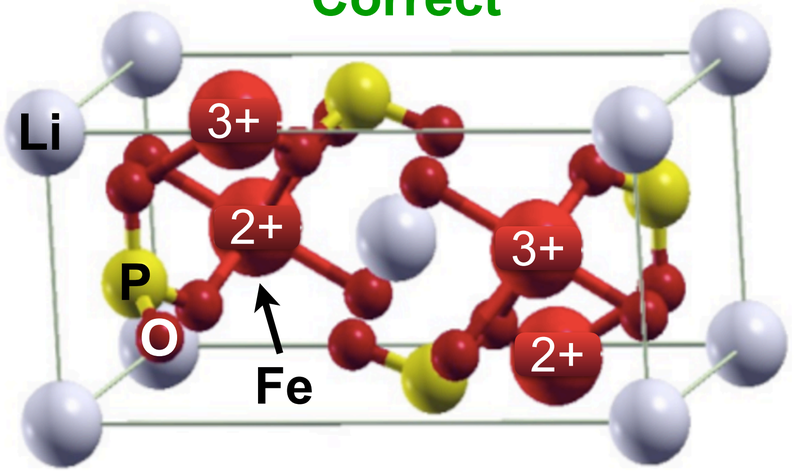

$Li_{0.5}FePO_4$

Incorrect

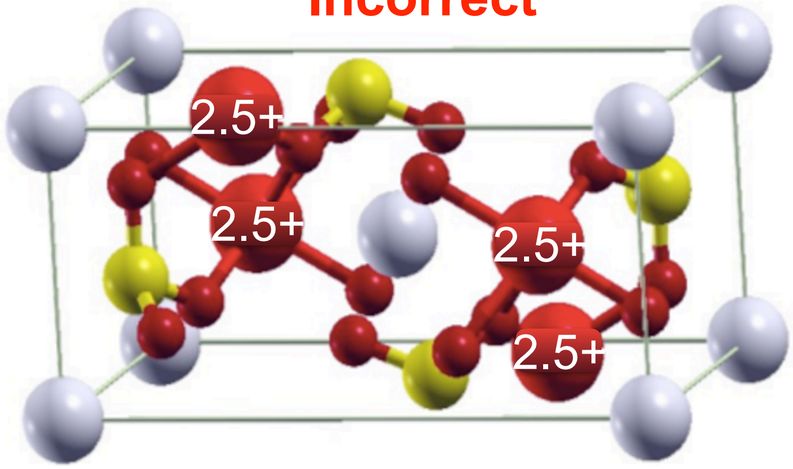

Spurious quadratic energy change when adding/removing a fraction of an electron to Fe

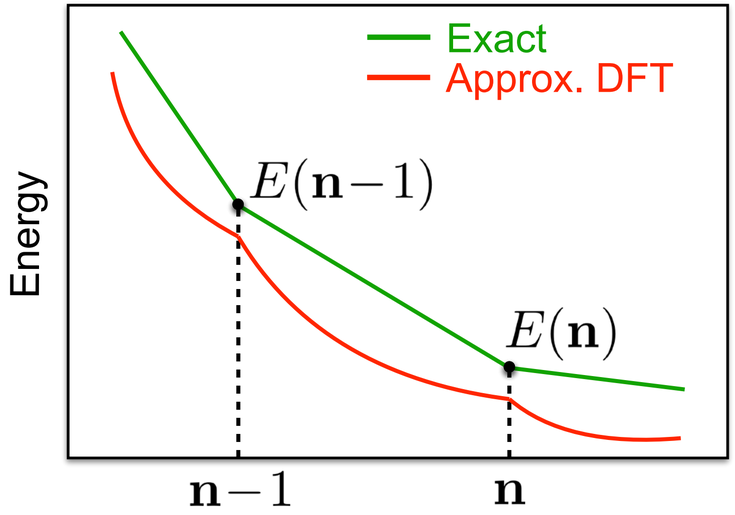

Self-interaction error

Fe-*3d* electrons are delocalized and spread around

Wrong average oxidation state of 2.5+ for Fe ions

Hubbard functionals

What is DFT+U ?

W. Kohn

DFT

(1964 - 1965)

The Hubbard model

(1963 - 1967)

J. Hubbard

~25 years

DFT+*U*

V.I. Anisimov, J. Zaanen, O.K. Andersen,
Phys. Rev. B **44**, 943 (1991)

Hubbard functionals

DFT+*U* : $$E = E_{\mathrm{DFT}} + \frac{1}{2}\sum_{I,\sigma} U^I \,\mathrm{Tr}\left[\left(\mathbf{1} - \mathbf{n}^{I\sigma}\right)\mathbf{n}^{I\sigma}\right]$$

$$(\mathbf{n}^{I\sigma})_{m_1 m_2} = \sum_i f_i \,\langle \psi_{i\sigma} | \varphi^I_{m_2} \rangle \langle \varphi^I_{m_1} | \psi_{i\sigma} \rangle$$

Anisimov et al., PRB (1991). *Liechtenstein et al., PRB (1995).* *Dudarev et al., PRB (1998).*

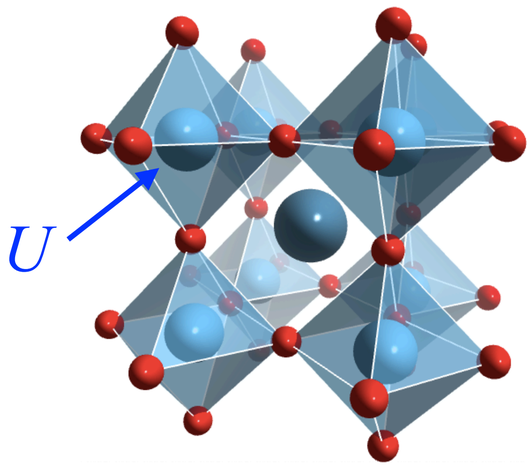

on-site localisation (*U*)

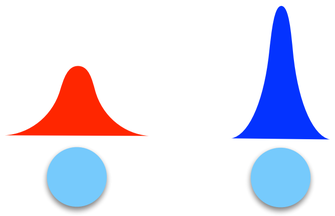

DFT DFT+*U*

Hubbard functionals

DFT+*U* : $$E = E_{\mathrm{DFT}} + \frac{1}{2}\sum_{I,\sigma} U^I \,\mathrm{Tr}\left[\left(\mathbf{1} - \mathbf{n}^{I\sigma}\right)\mathbf{n}^{I\sigma}\right]$$

$$(\mathbf{n}^{I\sigma})_{m_1 m_2} = \sum_i f_i \,\langle \psi_{i\sigma} | \varphi^I_{m_2} \rangle \langle \varphi^I_{m_1} | \psi_{i\sigma} \rangle$$

Anisimov et al., PRB (1991). *Liechtenstein et al., PRB (1995).* *Dudarev et al., PRB (1998).*

DFT+*U*+*V* : $$E = E_{\mathrm{DFT}} + \frac{1}{2}\sum_{I,\sigma} U^I \,\mathrm{Tr}\left[\left(\mathbf{1} - \mathbf{n}^{I\sigma}\right)\mathbf{n}^{I\sigma}\right] - \frac{1}{2}\sum_{I,J,\sigma} V^{IJ}\,\mathrm{Tr}\left[\mathbf{n}^{IJ\sigma}\mathbf{n}^{JI\sigma}\right]$$

Campo Jr and Cococcioni, JPCM (2010).

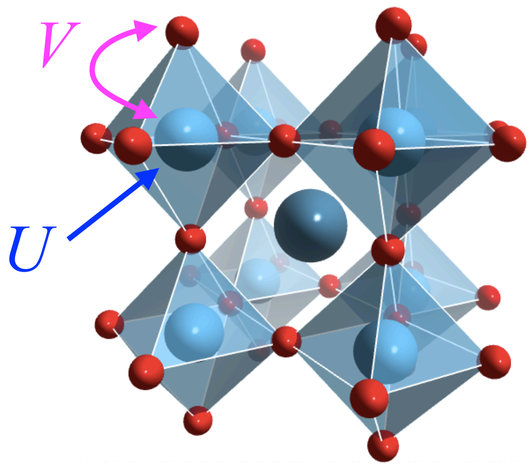

on-site localisation (*U*) &
inter-site hybridisations (*V*)

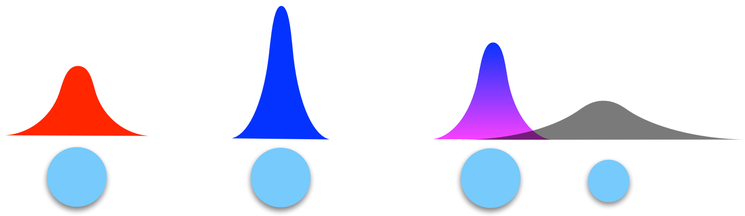

DFT DFT+*U* DFT+*U*+*V*

When do we need Hubbard corrections?

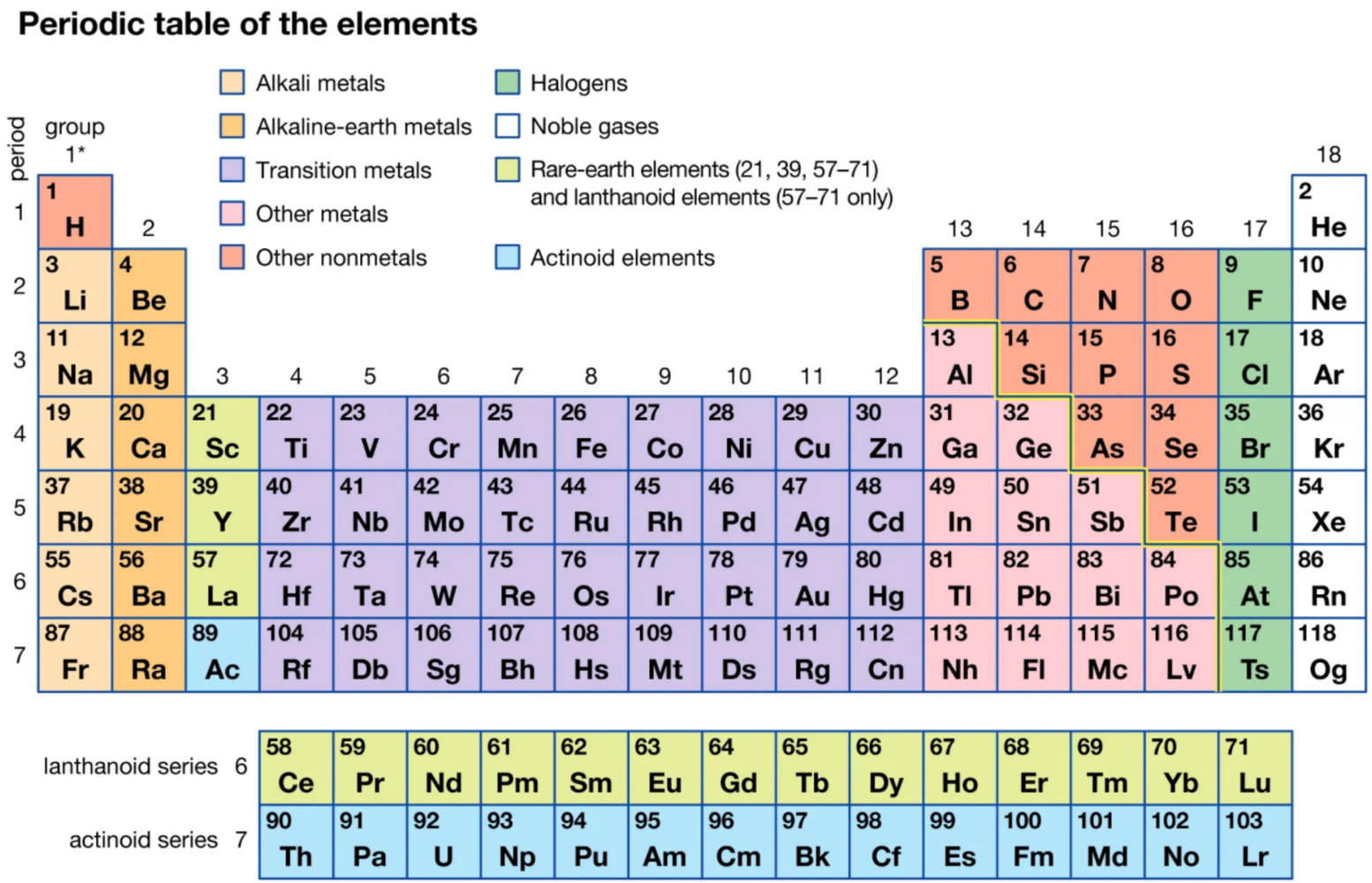

When do we need Hubbard corrections?

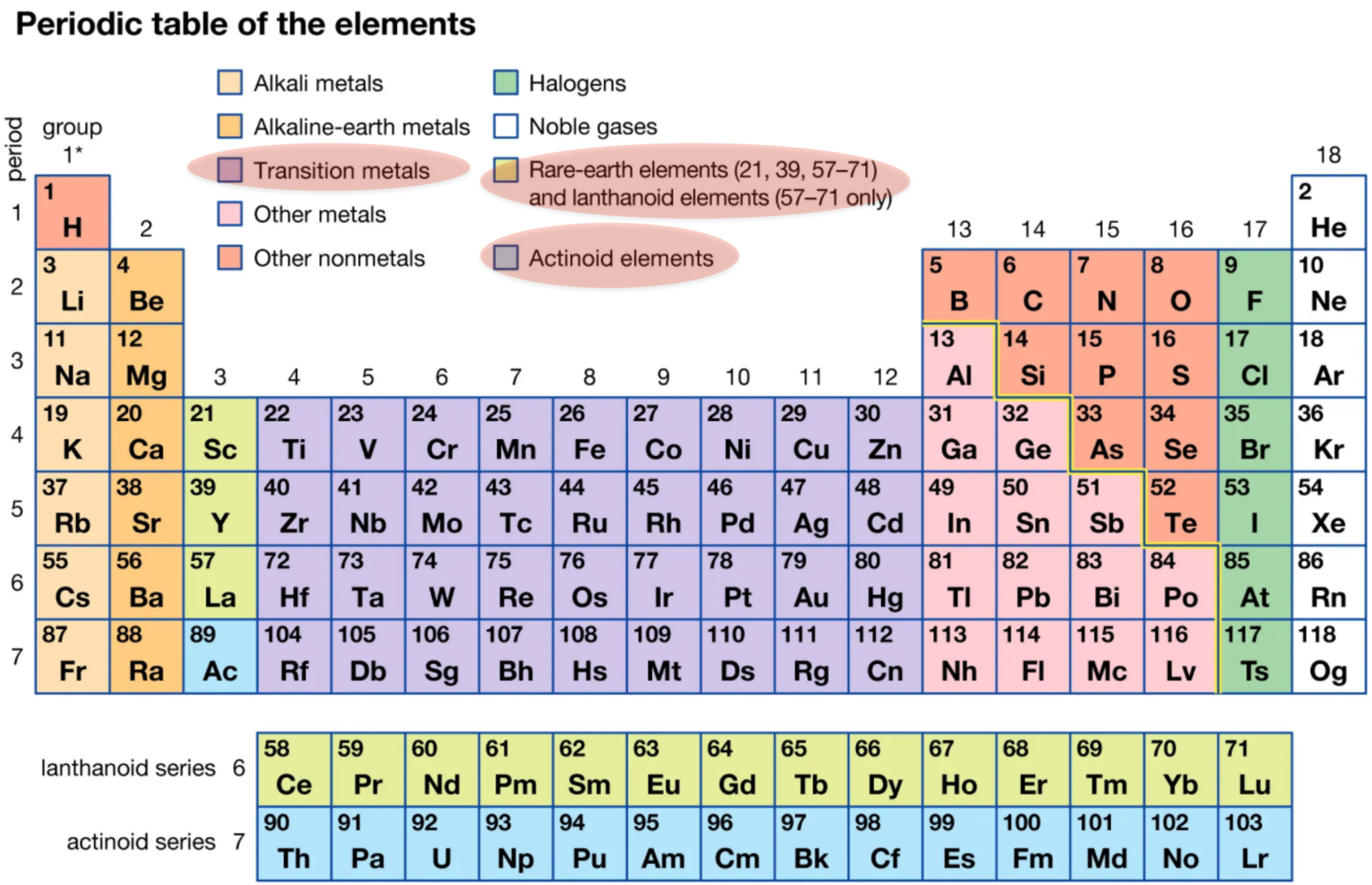

Answer: For elements with partially filled *d* and/or *f* electrons

Two (strongly-interconnected) key aspects of DFT+*U*(+*V*)

$$E = E_{\mathrm{DFT}} + \frac{1}{2}\sum_{I,\sigma} U^I \,\mathrm{Tr}\left[\left(\mathbf{1} - \mathbf{n}^{I\sigma}\right)\mathbf{n}^{I\sigma}\right] - \frac{1}{2}\sum_{I,J,\sigma} V^{IJ}\,\mathrm{Tr}\left[\mathbf{n}^{IJ\sigma}\mathbf{n}^{JI\sigma}\right]$$

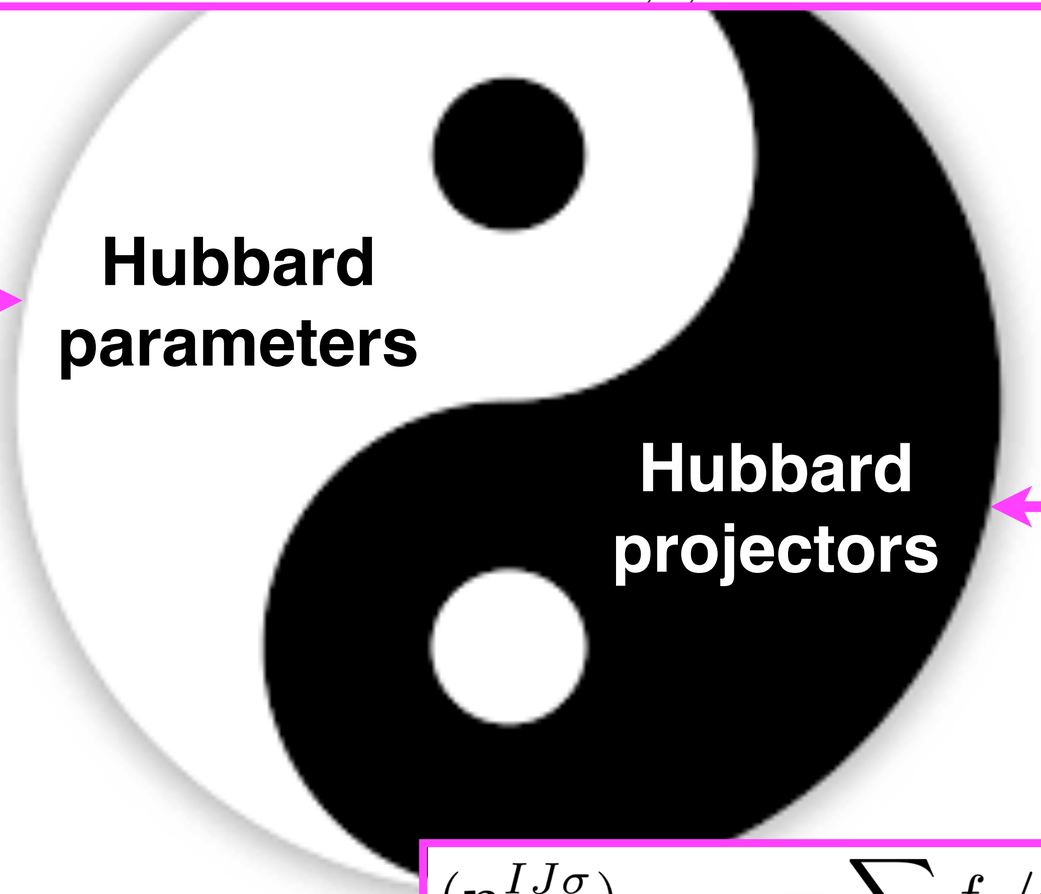

$$(\mathbf{n}^{IJ\sigma})_{m_1 m_2} = \sum_i f_i \,\langle\psi_{i\sigma}|\varphi^J_{m_2}\rangle\langle\varphi^I_{m_1}|\psi_{i\sigma}\rangle$$

Which values for the Hubbard parameters?

The values of Hubbard parameters are not known *a priori*

Which values for the Hubbard parameters?

The values of Hubbard parameters are not known *a priori*

Two strategies

Which values for the Hubbard parameters?

The values of Hubbard parameters are not known *a priori*

Two strategies

(Semi-)empirical

Tune *U* to reproduce, for example:

- Band gaps
- Magnetic moments
- Lattice parameters
- Oxidation enthalpies
- …

Requires the availability of the experimental data!

Which values for the Hubbard parameters?

The values of Hubbard parameters are not known *a priori*

Two strategies

(Semi-)empirical

Tune *U* to reproduce, for example:

- Band gaps
- Magnetic moments
- Lattice parameters
- Oxidation enthalpies
- …

Requires the availability of the experimental data!

First-principles

- Constrained density-functional theory (cDFT)
- Constrained random phase approximation (cRPA)
- Hartree-Fock-based approaches (e.g. ACBN0)
- Linear-response theory

this talk

Hubbard parameters are not universal

Computed Hubbard parameters depend on:

- **Type of Hubbard projector functions**
  (e.g. atomic, orthogonalized atomic, maximally localized Wannier functions, etc.)

$$(\mathbf{n}^{I\sigma})_{m_1 m_2} = \sum_i f_i \langle \psi_{i\sigma} | \varphi^I_{m_2} \rangle \langle \varphi^I_{m_1} | \psi_{i\sigma} \rangle$$

- **Oxidation state of a pseudized atom (pseudopotentials)** [1]

- **Exchange-correlation functional** (e.g. LDA, GGA, etc.)

- **Self-consistency** (i.e. either “one-shot” or self-consistent)

[1] Kulik and Marzari, JCP (2008).

Hubbard parameters from linear-response theory

$$E = E_{\mathrm{DFT}} + \frac{1}{2} U \, \mathrm{Tr}\left[(\mathbf{1} - \mathbf{n})\, \mathbf{n}\right] \qquad \mathrm{n} = \mathrm{Tr}[\mathbf{n}]$$

The main idea: Hubbard corrections remove spurious curvature of the total energy

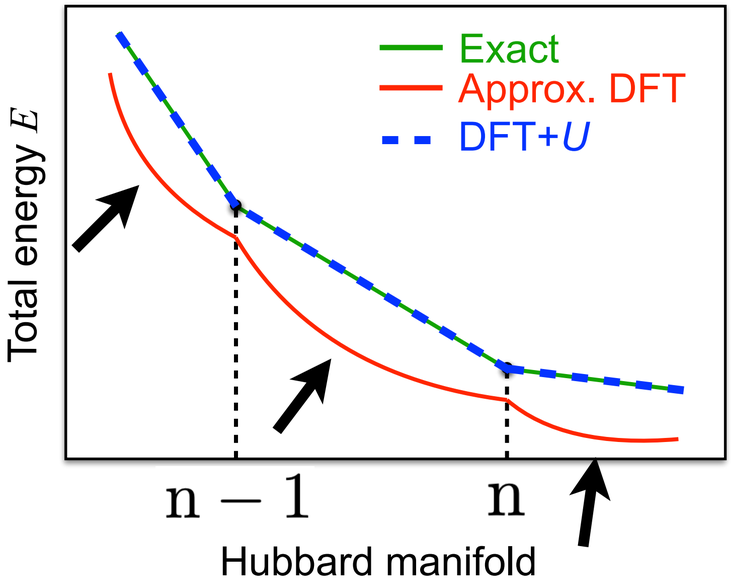

Note: There is no theorem for the piece-wise linearity of E in the Hubbard manifold (only for total number of electrons)

Hubbard parameters from linear-response theory

$$E = E_{\mathrm{DFT}} + \frac{1}{2} U \, \mathrm{Tr}\left[(\mathbf{1} - \mathbf{n})\, \mathbf{n}\right] \qquad \mathrm{n} = \mathrm{Tr}[\mathbf{n}]$$

The main idea: Hubbard corrections remove spurious curvature of the total energy

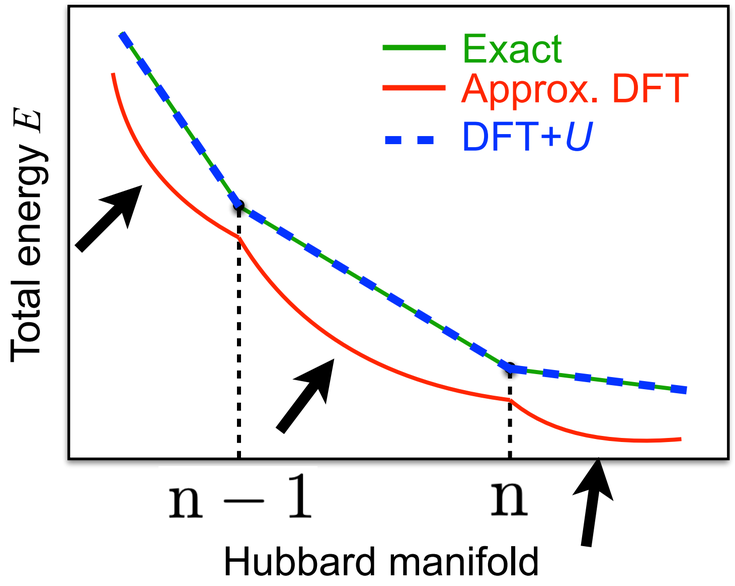

Hubbard parameters can be obtained from the following condition:

$$\frac{d^2 E}{d\mathrm{n}^2} = 0$$

$$U = \frac{d^2 E_{\mathrm{DFT}}}{d\mathrm{n}^2}$$

Note: There is no theorem for the piece-wise linearity of E in the Hubbard manifold (only for total number of electrons)

Cococcioni and de Gironcoli, PRB (2005).

U & *V* from linear-response theory

Old approach: supercells + finite differences (computationally expensive)

Modified Kohn-Sham equations:

$$\left(\hat{H}_\sigma + \lambda^J \hat{V}^J_{\text{pert}}\right)|\psi_{v\mathbf{k}\sigma}\rangle = \varepsilon_{v\mathbf{k}\sigma}|\psi_{v\mathbf{k}\sigma}\rangle$$

Response matrices (from finite differences):

$$\chi_{IJ} = \frac{\Delta n^I}{\Delta \lambda^J}$$

Hubbard parameters:

$$U^I = (\chi_0^{-1} - \chi^{-1})_{II} \quad V^{IJ} = (\chi_0^{-1} - \chi^{-1})_{IJ}$$

M. Cococcioni and S. de Gironcoli, PRB (2005).

New approach: primitive cells + DFPT (computationally much less expensive)

Perturbation theory to 1st order (DFPT):

$$(\hat{H}^\circ_\sigma - \varepsilon^\circ_{v\mathbf{k}\sigma})\left|\frac{d\psi_{v\mathbf{k}\sigma}}{d\lambda^J}\right\rangle = -\left(\frac{d\hat{V}_{\text{Hxc},\sigma}}{d\lambda^J} - \frac{d\varepsilon_{v\mathbf{k}\sigma}}{d\lambda^J} + \hat{V}^J_{\text{pert}}\right)|\psi^\circ_{v\mathbf{k}\sigma}\rangle$$

Response occupation matrices:

$$\frac{dn^{sl\sigma}_{m_1m_2}}{d\lambda^{s'l'}} = \frac{1}{N_\mathbf{q}}\sum_\mathbf{q}^{N_\mathbf{q}} e^{i\mathbf{q}\cdot(\mathbf{R}_l - \mathbf{R}_{l'})}\,\Delta^{s'}_\mathbf{q}\bar{n}^{s\,\sigma}_{m_1m_2}$$

I. Timrov, N. Marzari, M. Cococcioni, PRB (2018) & PRB (2021).

Comparison of the "conventional" linear response and DFPT

Scaling

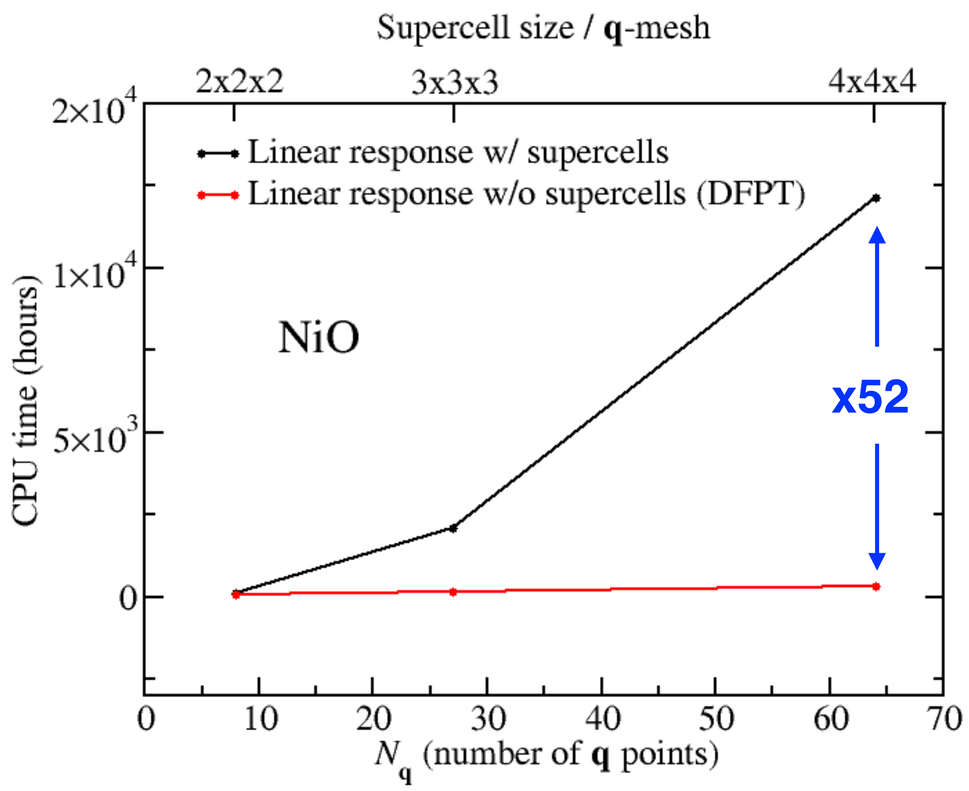

Benchmark of the equivalence between the two approaches

Method	**k**-mesh	SC-size/**q**-mesh	U(Ni-d)
LR-SC	$6 \times 6 \times 6$	$2 \times 2 \times 2$	7.895
DFPT	$12 \times 12 \times 12$		7.900
LR-SC	$4 \times 4 \times 4$	$3 \times 3 \times 3$	8.146
DFPT	$12 \times 12 \times 12$		8.149
LR-SC	$3 \times 3 \times 3$	$4 \times 4 \times 4$	8.168
DFPT	$12 \times 12 \times 12$		8.172

HP code is public and is part of

QUANTUM ESPRESSO

Symmetry → Reduction of $N_{\mathbf{q}}$ in DFPT
(no equivalence in the supercell approach)

Timrov, Marzari, and Cococcioni, PRB (2018), PRB (2021), CPC (2022).

The zoo of Hubbard projectors

1. Nonorthogonalized atomic orbitals

$$\phi^I_{m_1}(\mathbf{r}-\mathbf{R}_I)$$ (contained in pseudopotentials)

Drawback:
Application of Hubbard *U* twice in the overlap regions

2. Orthogonalized atomic orbitals

$$\tilde{\phi}^I_{m_1}(\mathbf{r}-\mathbf{R}_I) = \sum_{Jm_2} \left(\hat{O}^{-\frac{1}{2}}\right)^{JI}_{m_2 m_1} \phi^J_{m_2}(\mathbf{r}-\mathbf{R}_J)$$

$$\left(\hat{O}\right)^{IJ}_{m_1 m_2} = \langle \phi^I_{m_1} | \phi^J_{m_2} \rangle$$

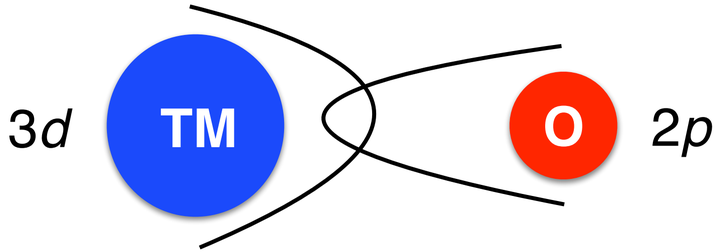

3. Maximally localized Wannier functions

$$w^I_{m_1}(\mathbf{r}-\mathbf{R}_I) = \frac{1}{\sqrt{N_{\mathbf{k}}}} \sum_{\mathbf{k}} e^{-i\mathbf{k}\cdot\mathbf{R}_I} \sum_{n}^{N_{\mathrm{KSbands}}} U^{(\mathbf{k})}_{nm_1} \psi_{n\mathbf{k}}(\mathbf{r})$$

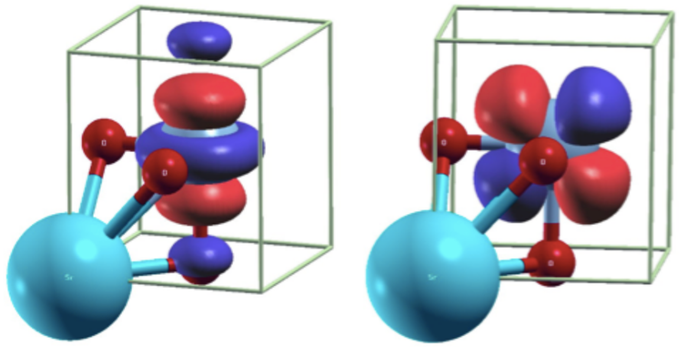

Self-consistent workflow of DFT+*U*+*V*

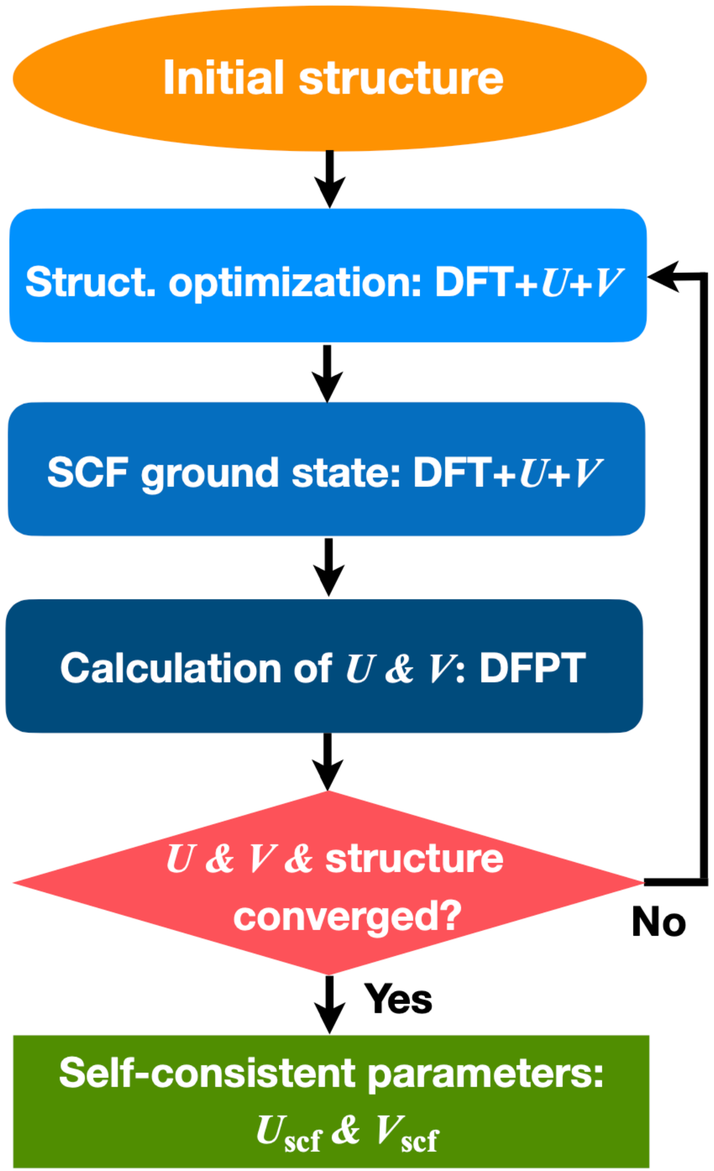

Structural optimization (needs Hubbard forces and stresses)

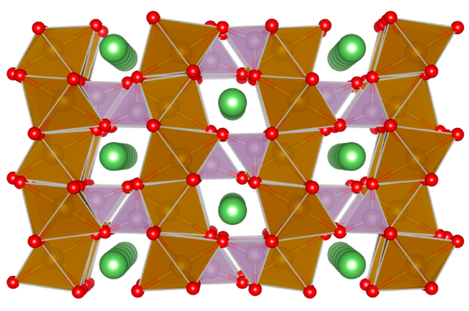

Calculation of Hubbard parameters

$$U^I = (\chi_0^{-1} - \chi^{-1})_{II}$$

$$V^{IJ} = (\chi_0^{-1} - \chi^{-1})_{IJ}$$

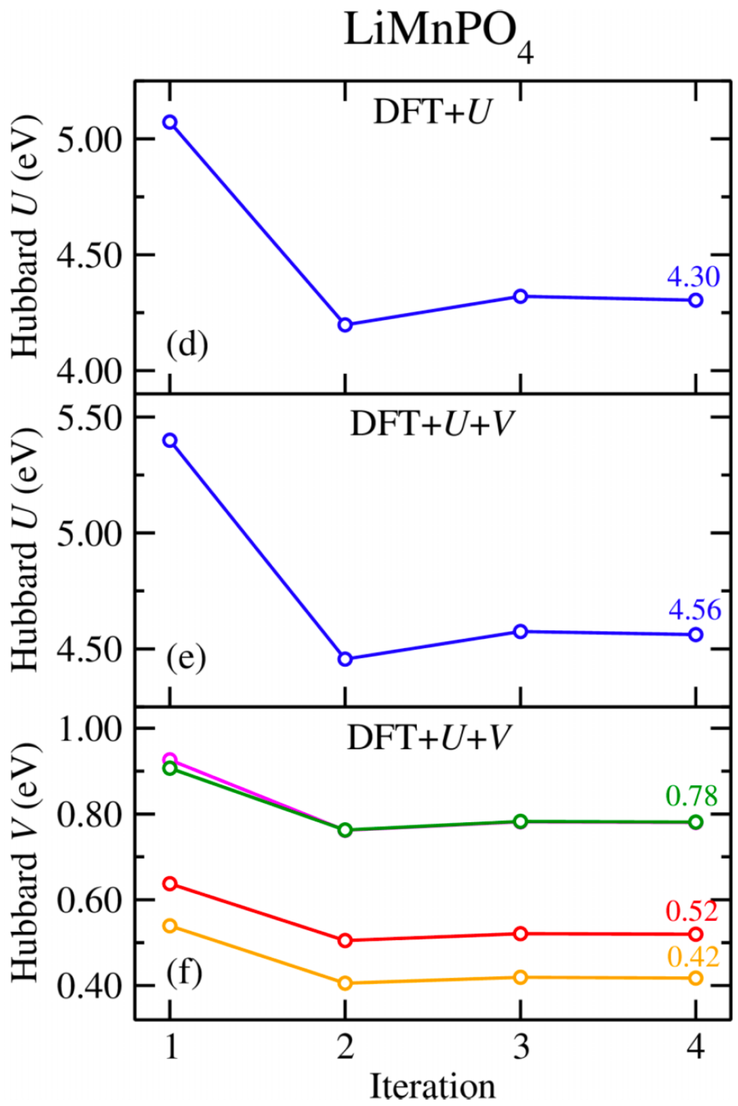

Timrov, Marzari, and Cococcioni, PRB (2021).

Li-ion batteries

Discharging process

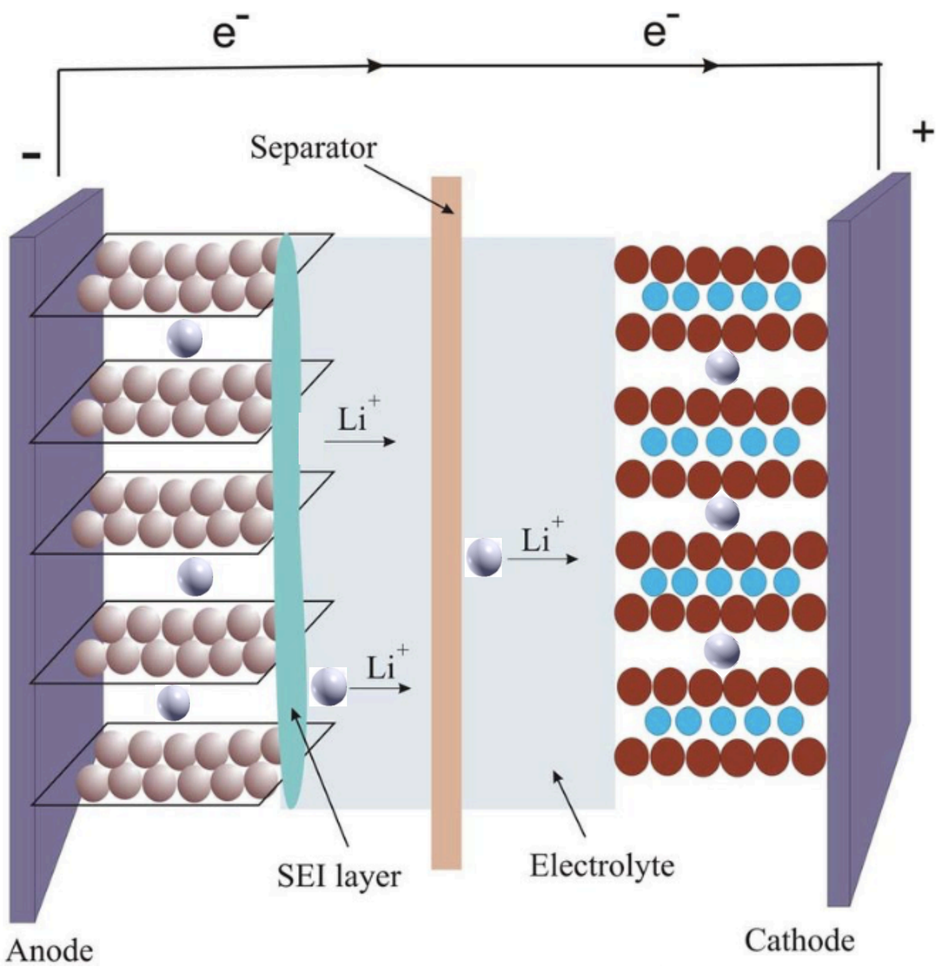

$FePO_4$

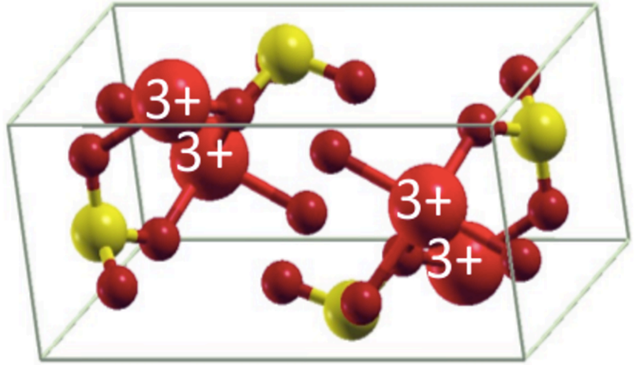

$Li_{0.5}FePO_4$

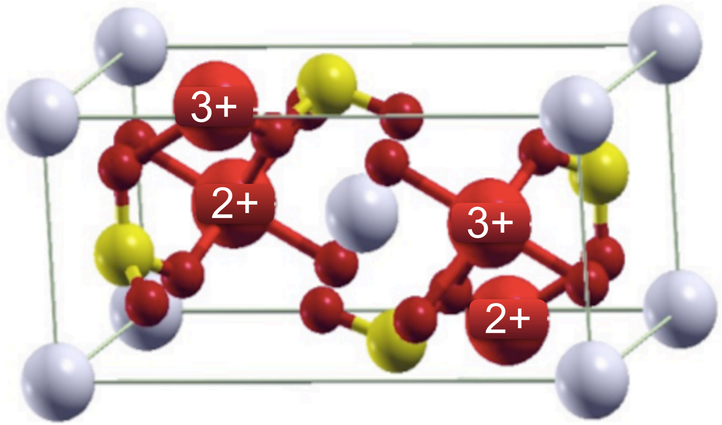

$LiFePO_4$

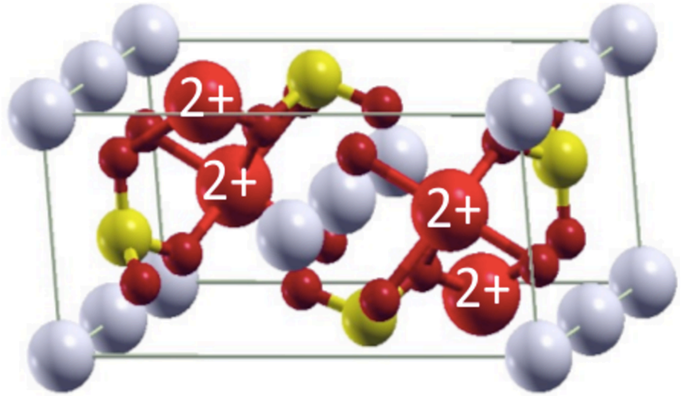

Correct description of change in oxidation state upon lithiation

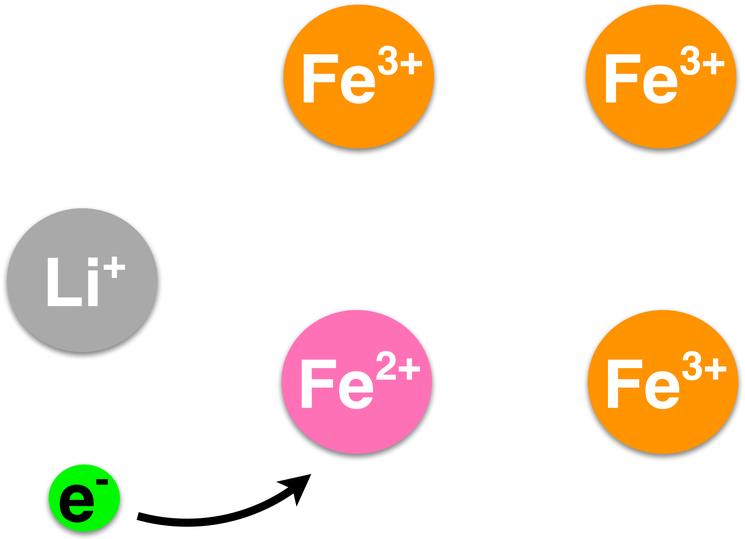

Change in the oxidation state due to accomodation of an extra electron

Correct description of change in oxidation state upon lithiation

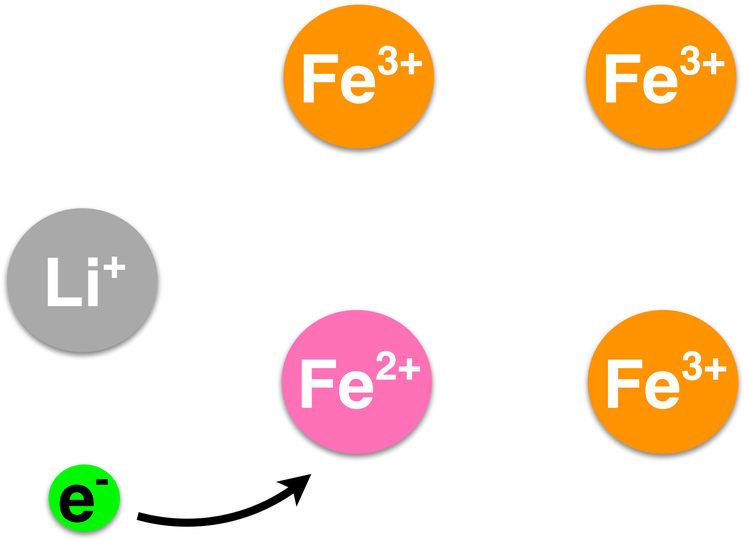

Change in the oxidation state due to accomodation of an extra electron

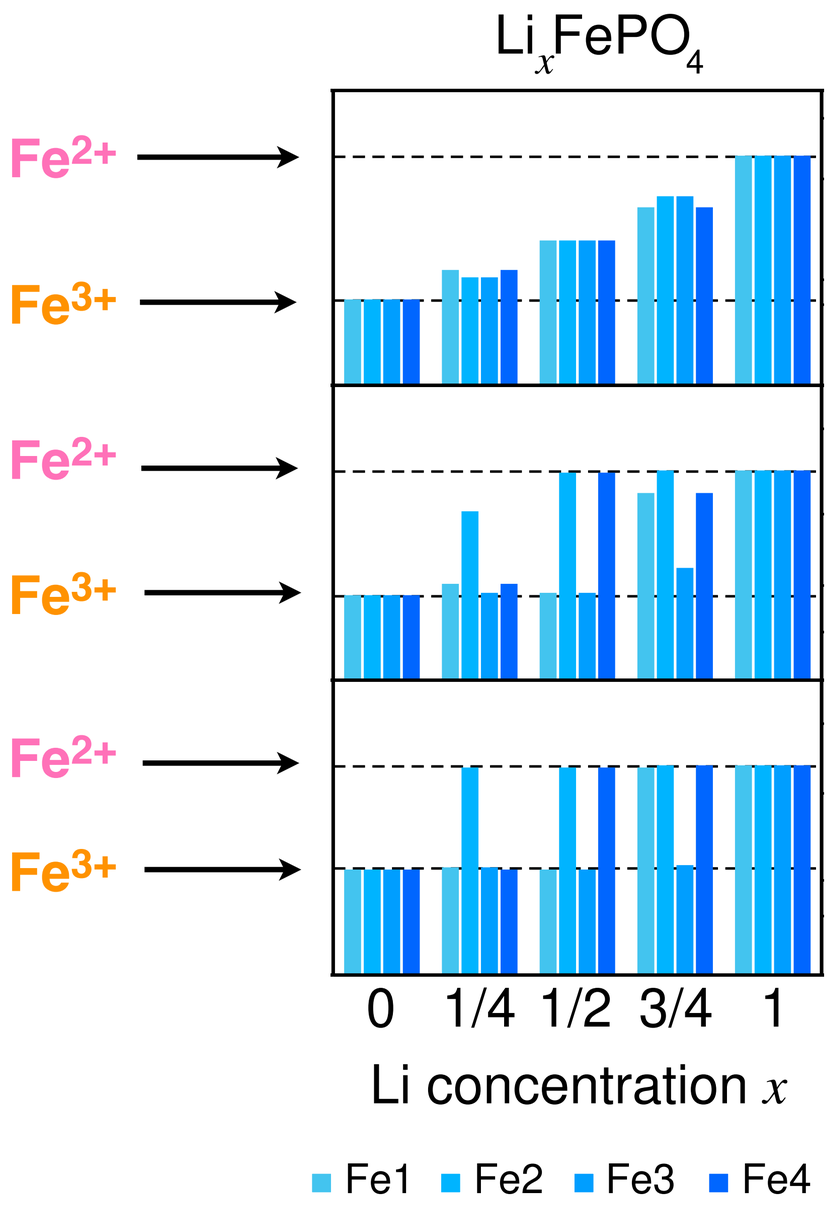

DFT (PBEsol) ❌

Hybrid functional (HSE06) ❌

Extended Hubbard (DFT+*U*+*V*) ✅

Li intercalation voltages

$$\Phi = -\frac{E(\mathrm{Li}_{x_2}\mathrm{S}) - E(\mathrm{Li}_{x_1}\mathrm{S}) - (x_2 - x_1)E(\mathrm{Li})}{(x_2 - x_1)e}$$

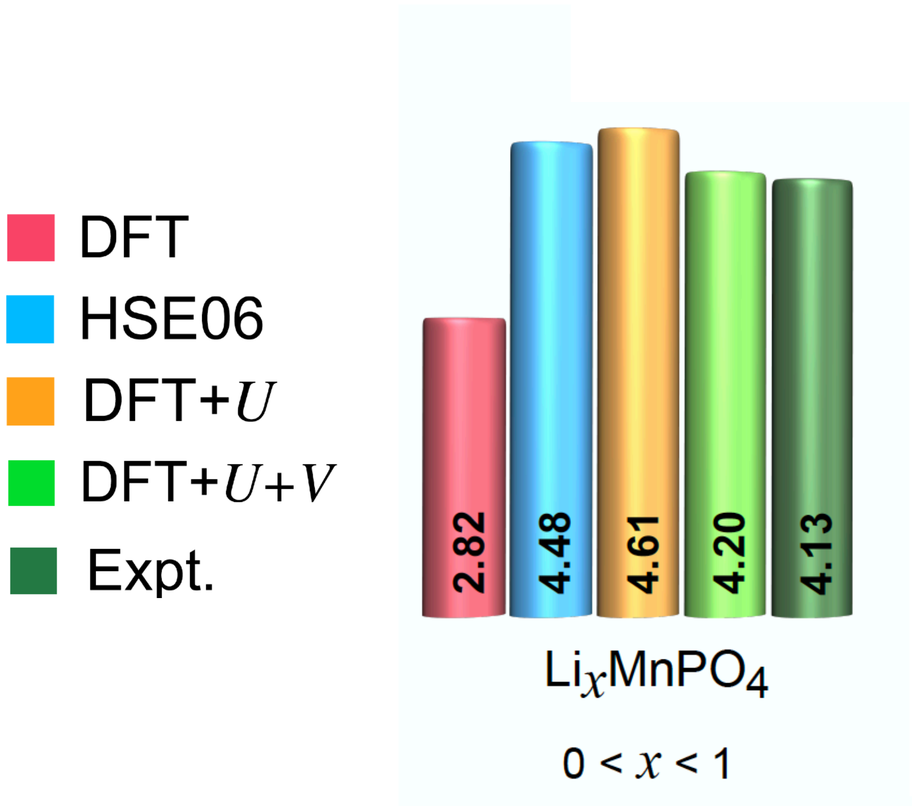

Cococcioni and Marzari, PRM (2019).

Timrov, Aquilante, Cococcioni, Marzari, PRX Energy (2022).

Li intercalation voltages

$$\Phi = -\frac{E(\mathrm{Li}_{x_2}\mathrm{S}) - E(\mathrm{Li}_{x_1}\mathrm{S}) - (x_2 - x_1)E(\mathrm{Li})}{(x_2 - x_1)e}$$

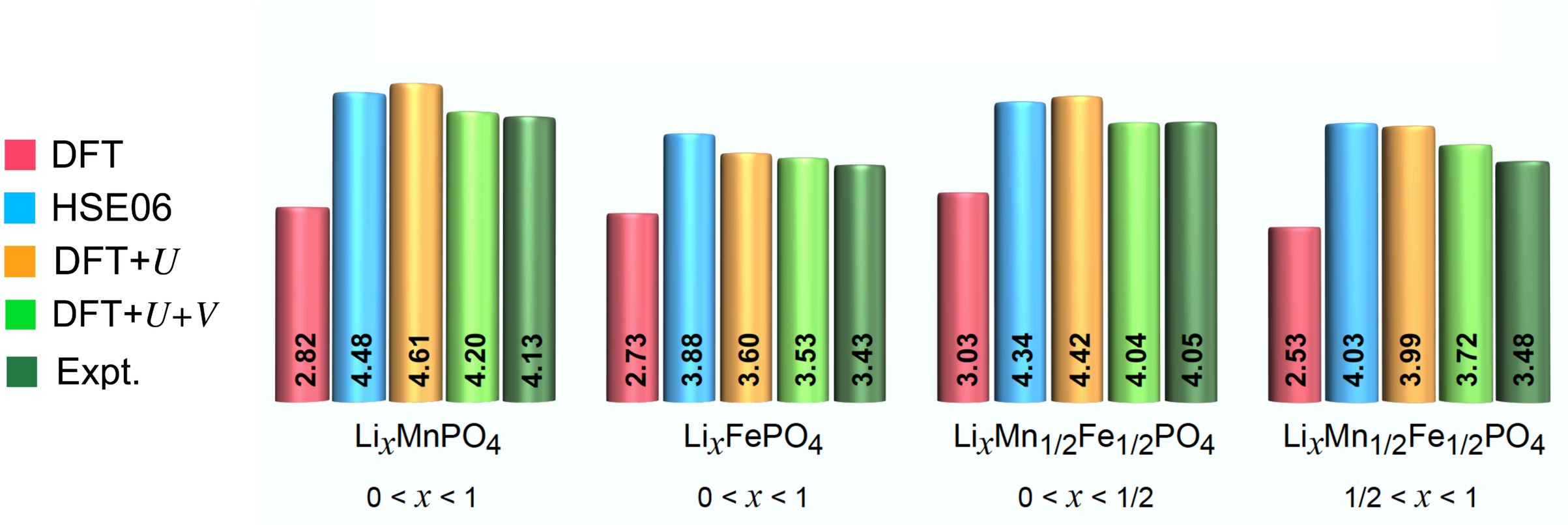

Cococcioni and Marzari, PRM (2019).

Timrov, Aquilante, Cococcioni, Marzari, PRX Energy (2022).

Self-consistent *U* and *V* from linear-response theory

Li_xMnPO_4

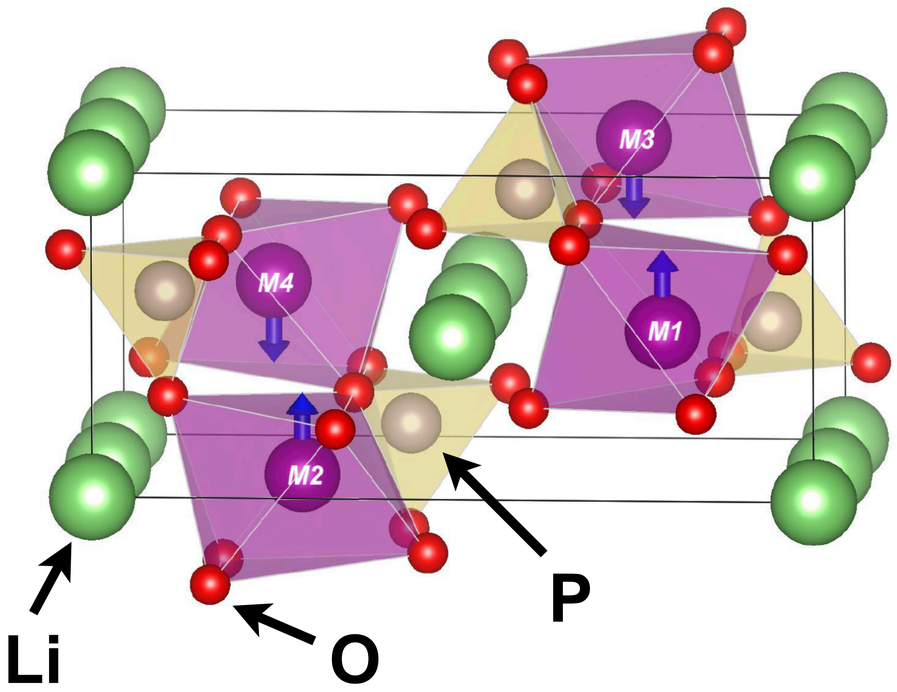

x	HP	Mn1	Mn2	Mn3	Mn4
0	U	6.26	6.26	6.26	6.26
	V	0.54-1.07	0.54-1.07	0.54-1.07	0.54-1.07

***M1 - M4* = Mn1 - Mn4**

Self-consistent *U* and *V* from linear-response theory

Li_xMnPO_4

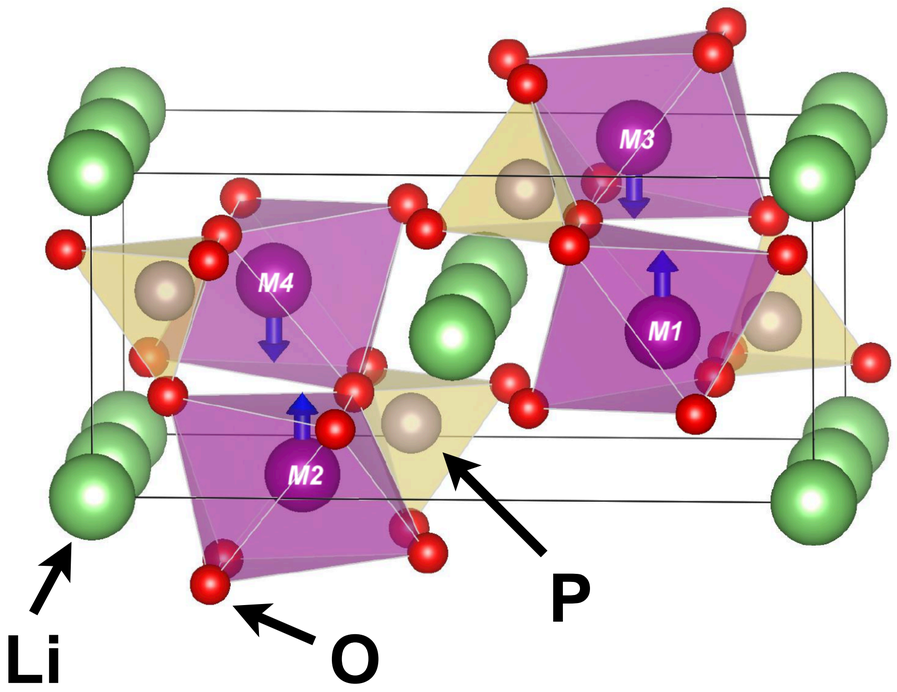

x	HP	Mn1	Mn2	Mn3	Mn4
0	U	6.26	6.26	6.26	6.26
	V	0.54-1.07	0.54-1.07	0.54-1.07	0.54-1.07
1/4	U	6.26	6.25	6.67	5.44
	V	0.40-1.01	0.46-1.05	0.54-1.11	0.39-1.08

***M1 - M4* = Mn1 - Mn4**

Self-consistent *U* and *V* from linear-response theory

Li_xMnPO_4

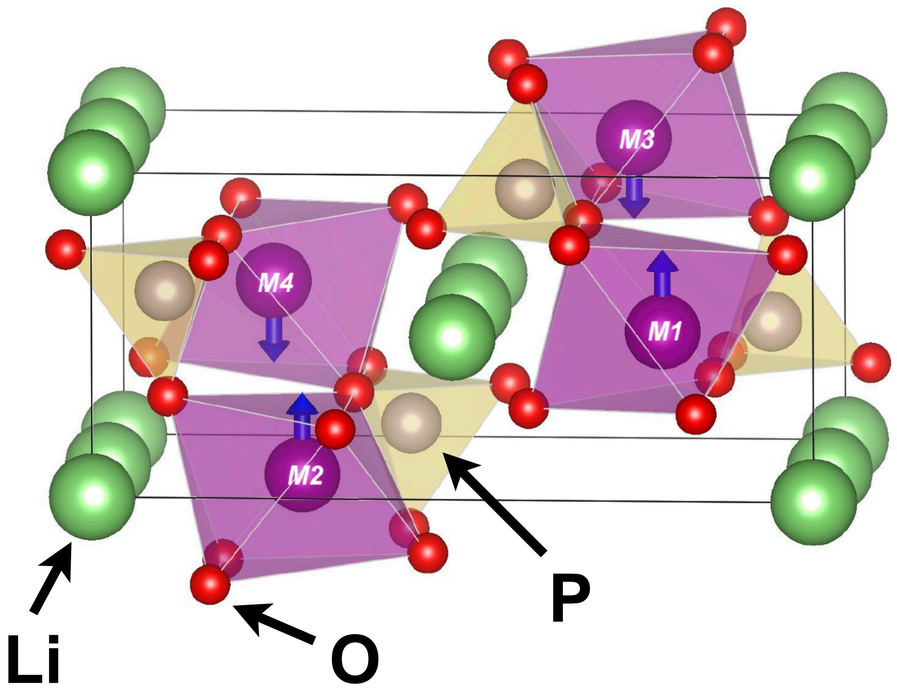

***M1 - M4* = Mn1 - Mn4**

x	HP	Mn1	Mn2	Mn3	Mn4
0	U	6.26	6.26	6.26	6.26
	V	0.54-1.07	0.54-1.07	0.54-1.07	0.54-1.07
1/4	U	6.26	6.25	6.67	5.44
	V	0.40-1.01	0.46-1.05	0.54-1.11	0.39-1.08
1/2	U	6.42	4.95	6.41	4.94
	V	0.34-1.01	0.38-0.96	0.34-1.01	0.38-0.96
3/4	U	4.67	4.64	6.58	4.98
	V	0.48-0.72	0.31-0.91	0.33-1.02	0.41-0.79
1	U	4.56	4.56	4.56	4.56
	V	0.42-0.78	0.42-0.78	0.42-0.78	0.42-0.78

Hubbard parameters are site-dependent and change upon the (de)lithiation

How one would describe the change in *U*&*V* empirically?

Spinel cathode materials

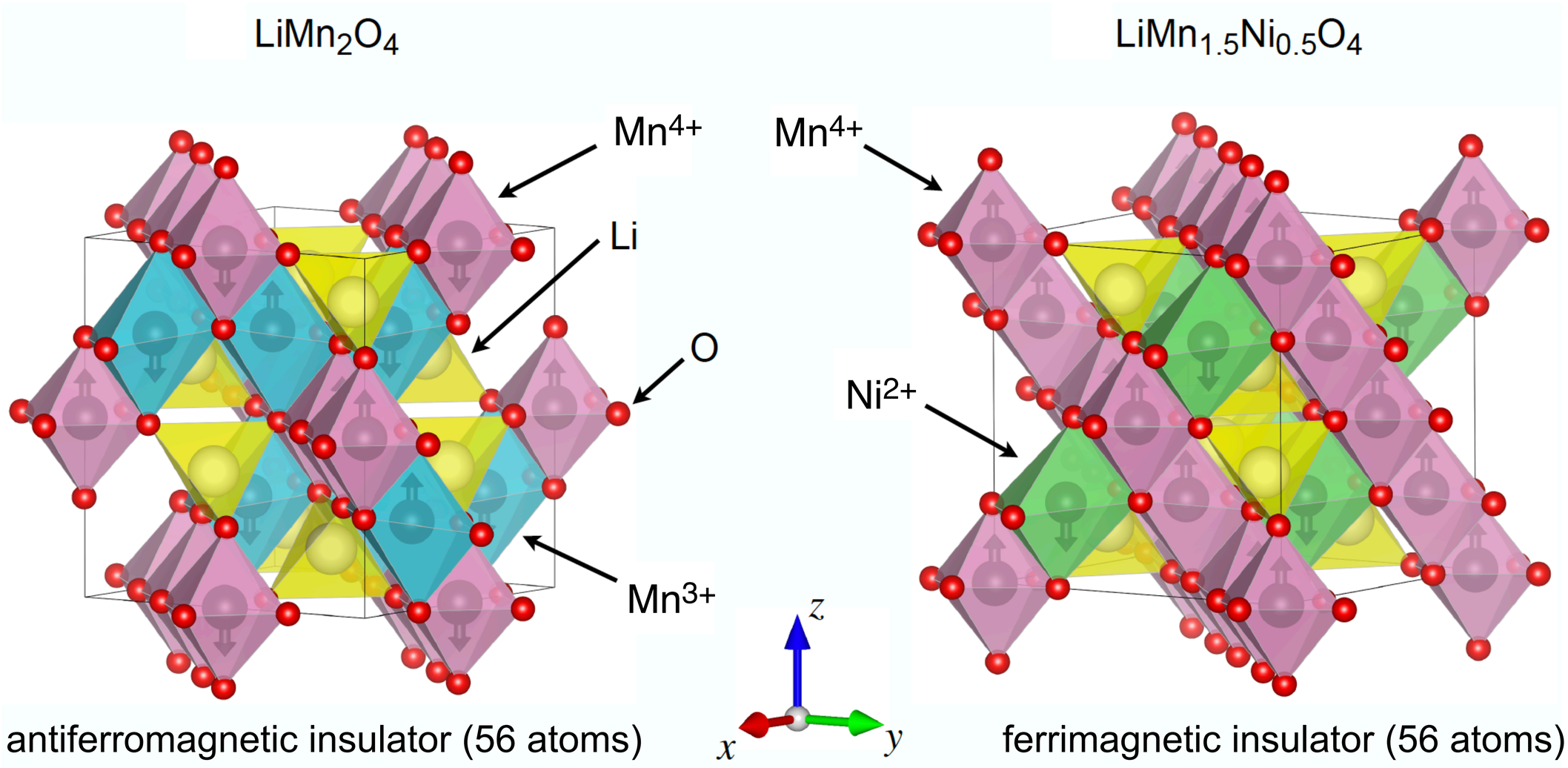

antiferromagnetic insulator (56 atoms)

ferrimagnetic insulator (56 atoms)

These systems are much more expensive computationally for hybrid functionals (and less accurate), but modest for DFT+*U*+*V*

Li intercalation voltages

$$\Phi = -\frac{E(\mathrm{Li}_{x_2}\mathrm{S}) - E(\mathrm{Li}_{x_1}\mathrm{S}) - (x_2 - x_1)E(\mathrm{Li})}{(x_2 - x_1)e}$$

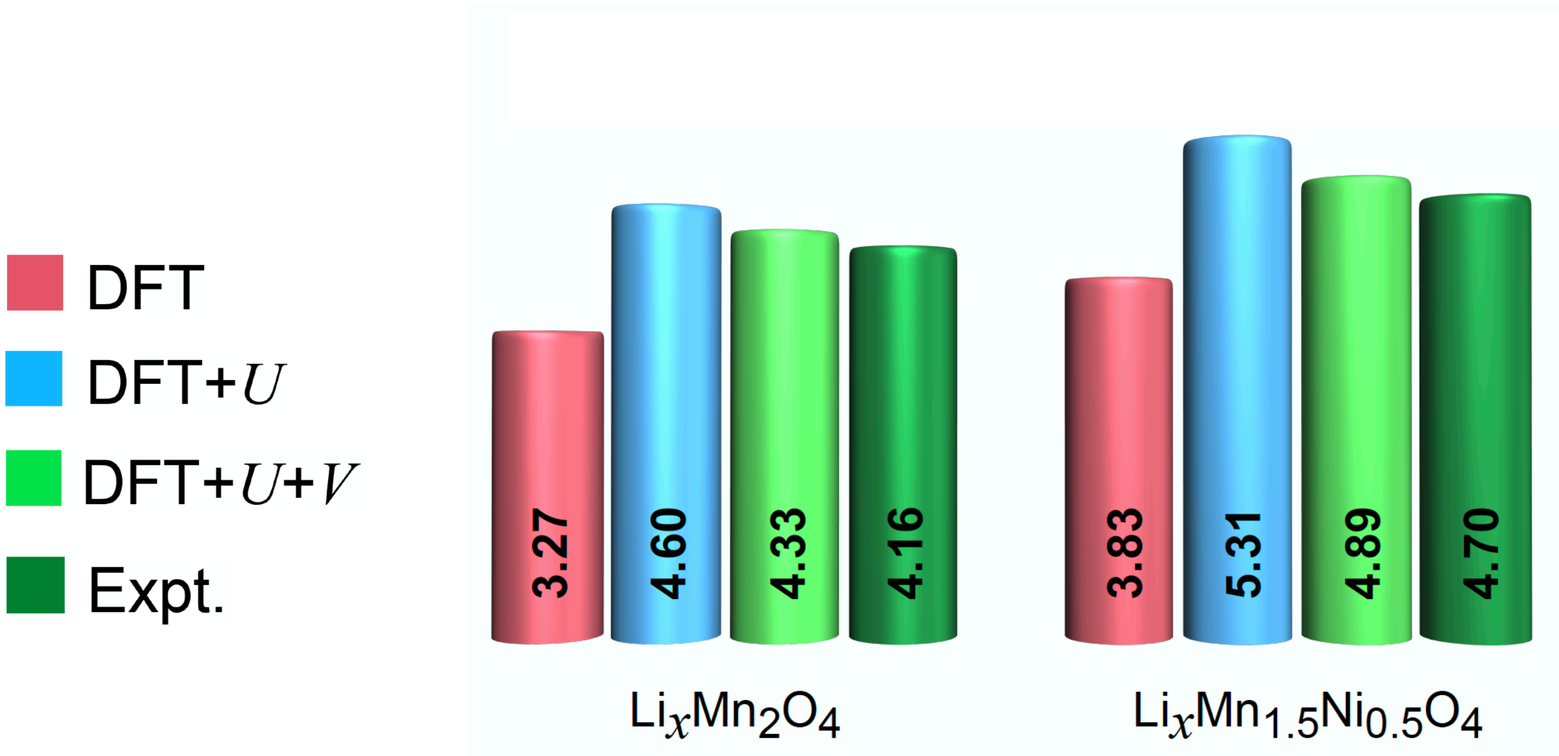

Timrov, Kotiuga, and Marzari, PCCP (2023).

High-throughput search of novel Li-ion battery cathode materials

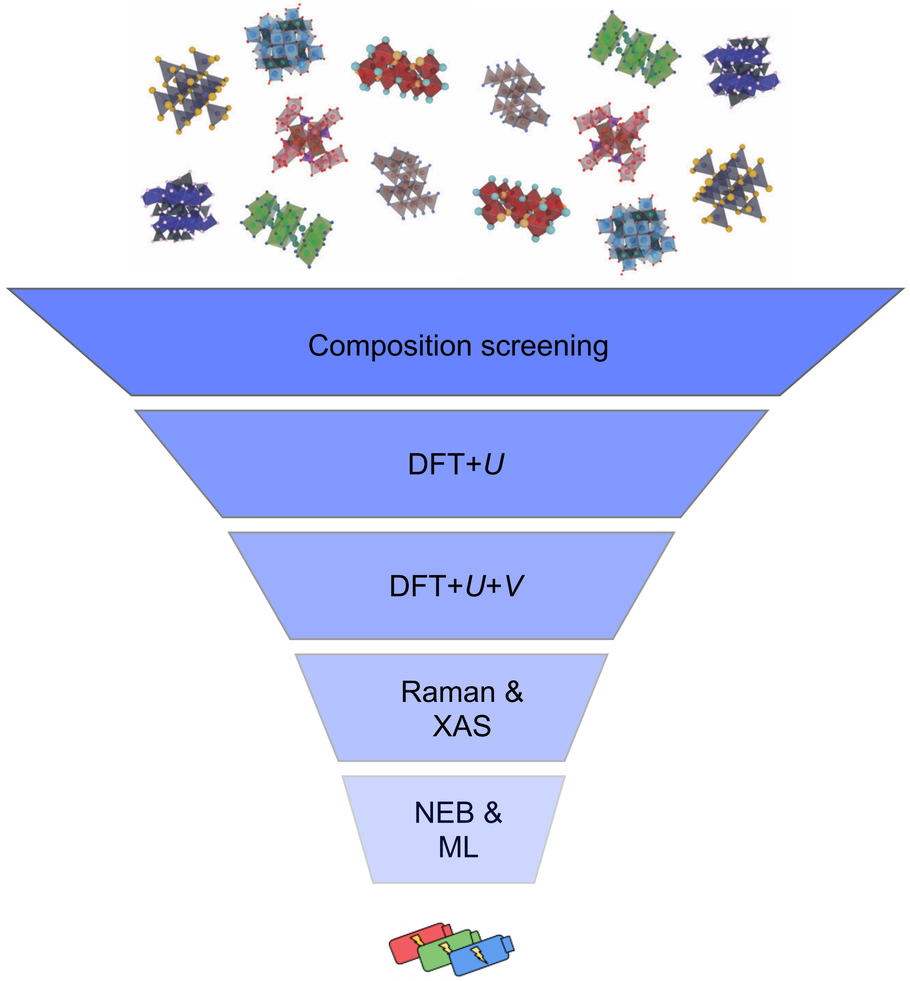

MATERIALS CLOUD

Materials Cloud 3D crystals database

Automation:

AiiDA

Codes & Methods:

QUANTUMESPRESSO

Equivariant
Neural
Networks

Novel Li-ion cathode battery materials

Malica, Bastonero, Bercx, Timrov, Marzari, in preparation

Accelerating Hubbard functionals through machine learning

Distribution of Hubbard *U* values for
Mn, Fe, Co, and Ni in various compounds

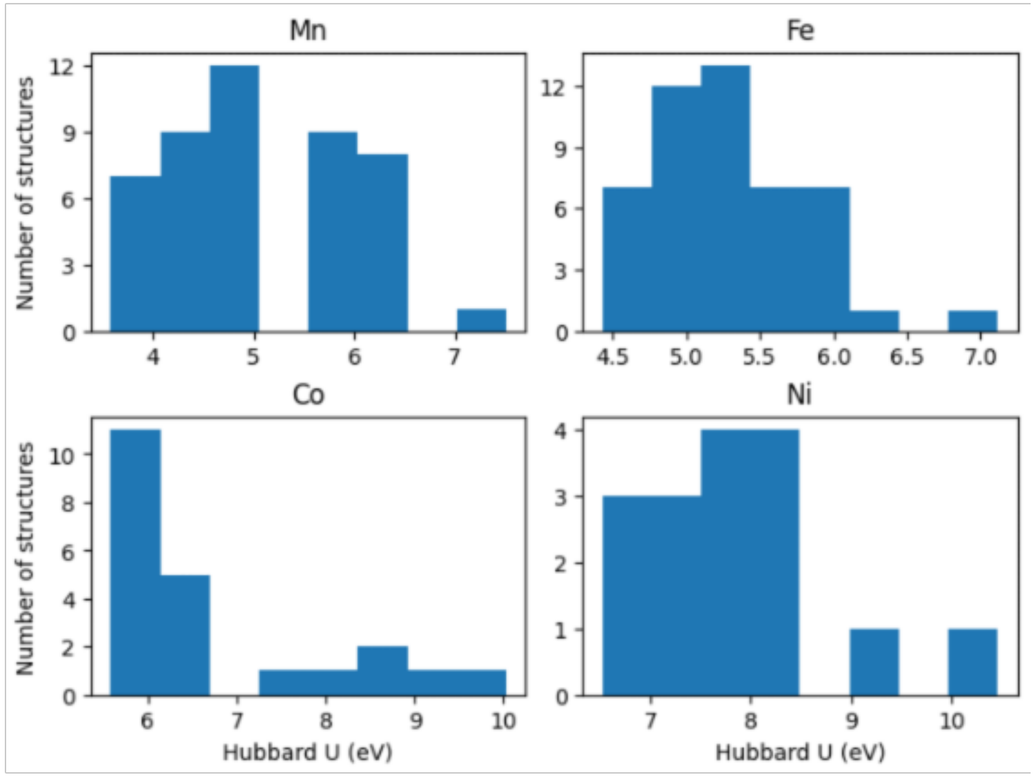

Uhrin, Zadoks, Binci, Marzari, Timrov, in preparation

Accelerating Hubbard functionals through machine learning

Distribution of Hubbard *U* values for
Mn, Fe, Co, and Ni in various compounds

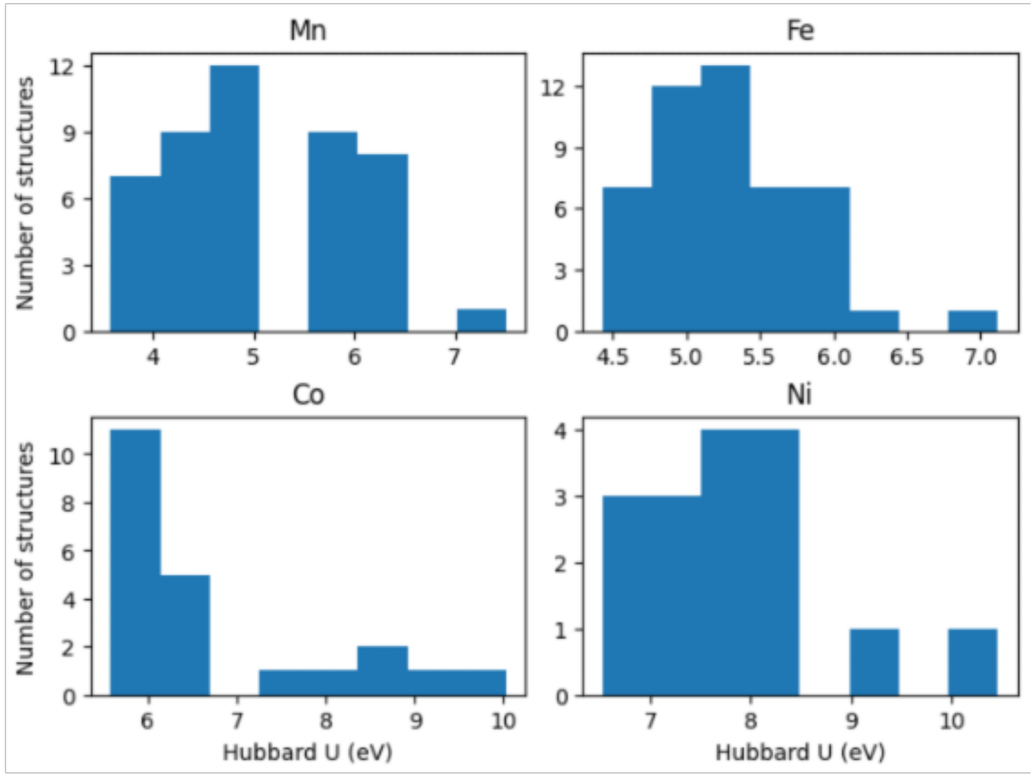

Machine learning

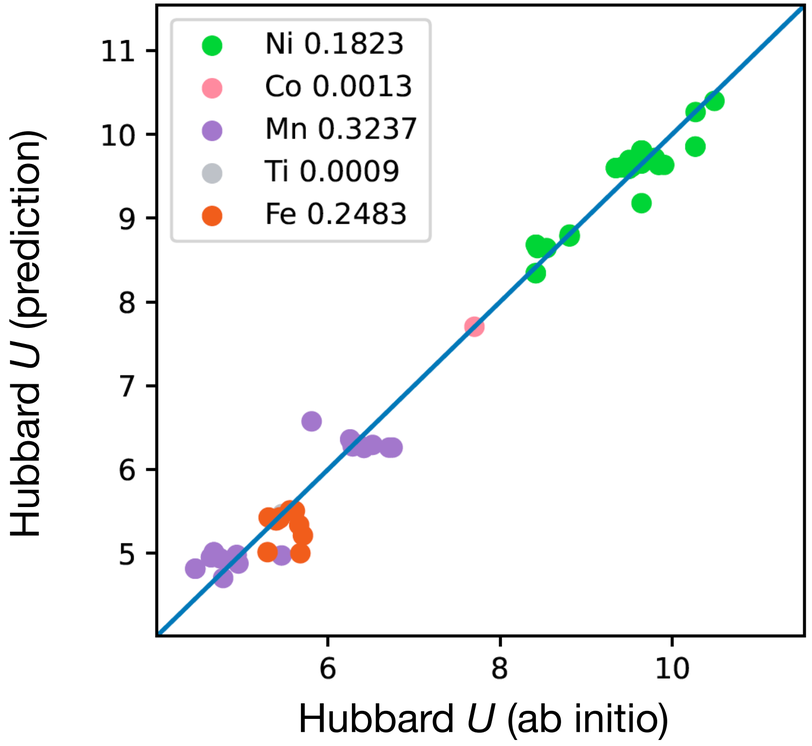

Uhrin, Zadoks, Binci, Marzari, Timrov, in preparation

Formation energies of O vacancies in perovskites

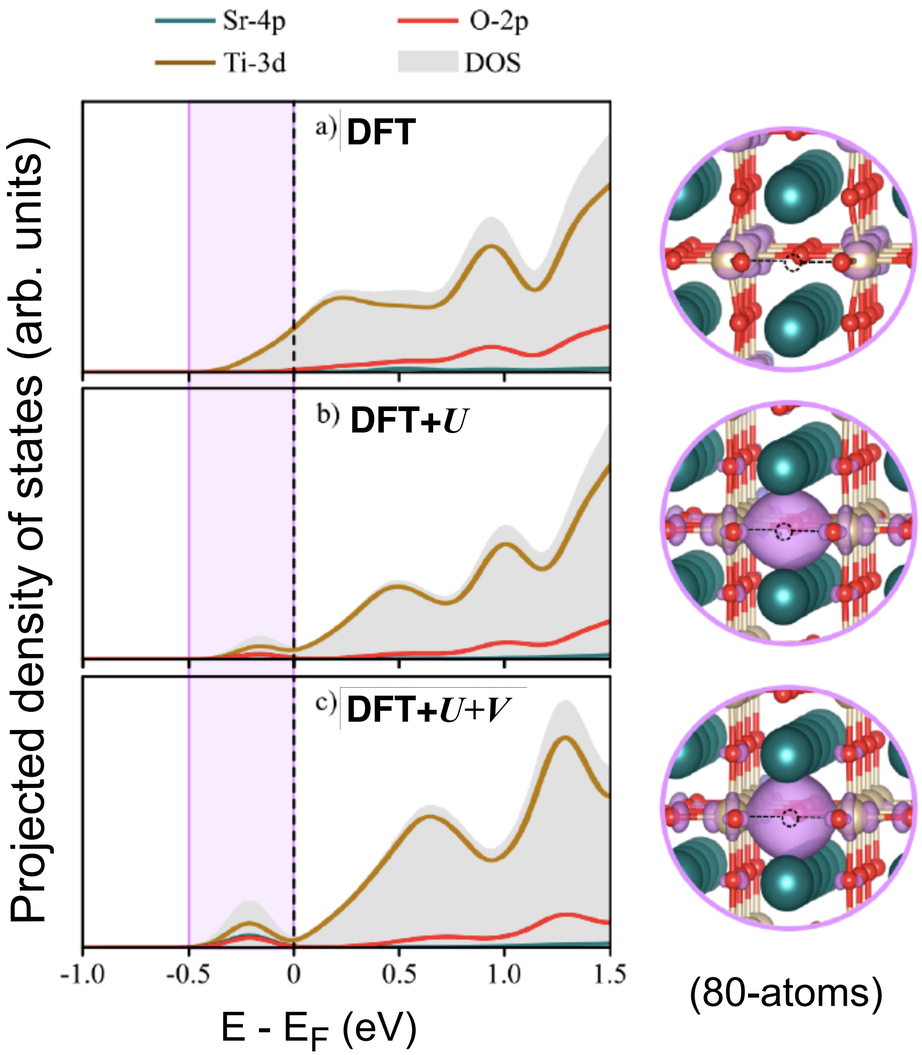

(80-atoms)

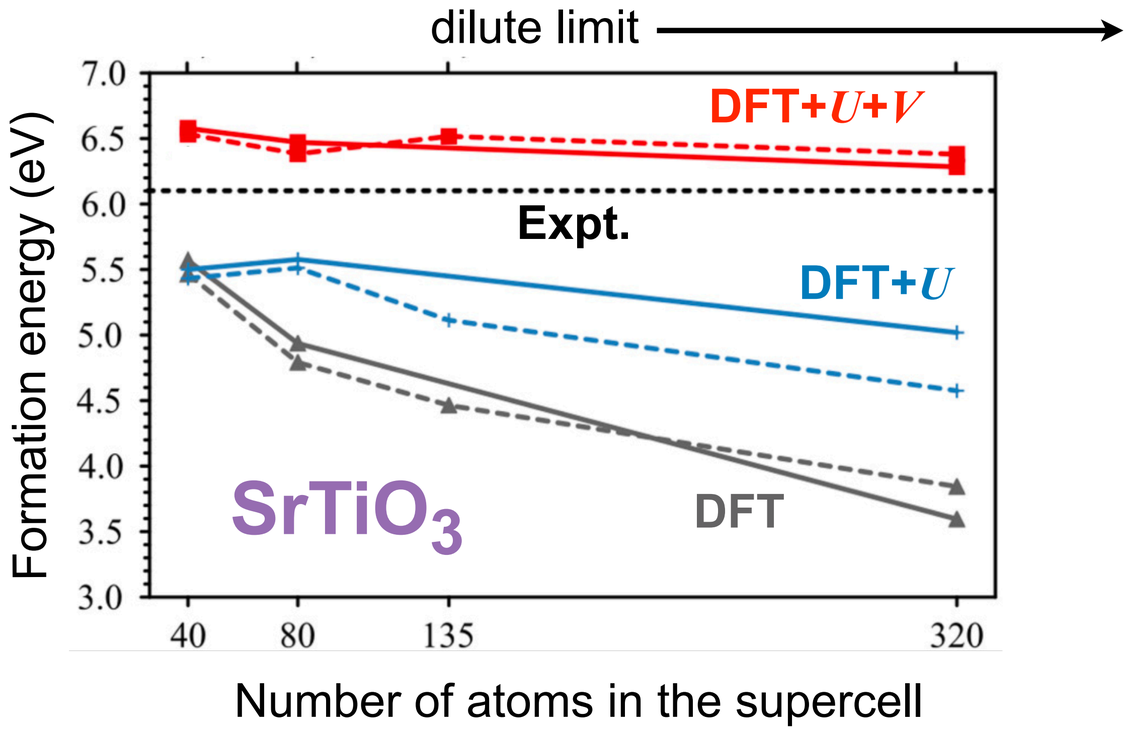

DFT+*U*+*V* accurately predicts the correct formation energies of O vacancies in the dilute limit

C. Ricca, I. Timrov et al., PRB (2019) & PRR (2020).

Phase stability of perovskites

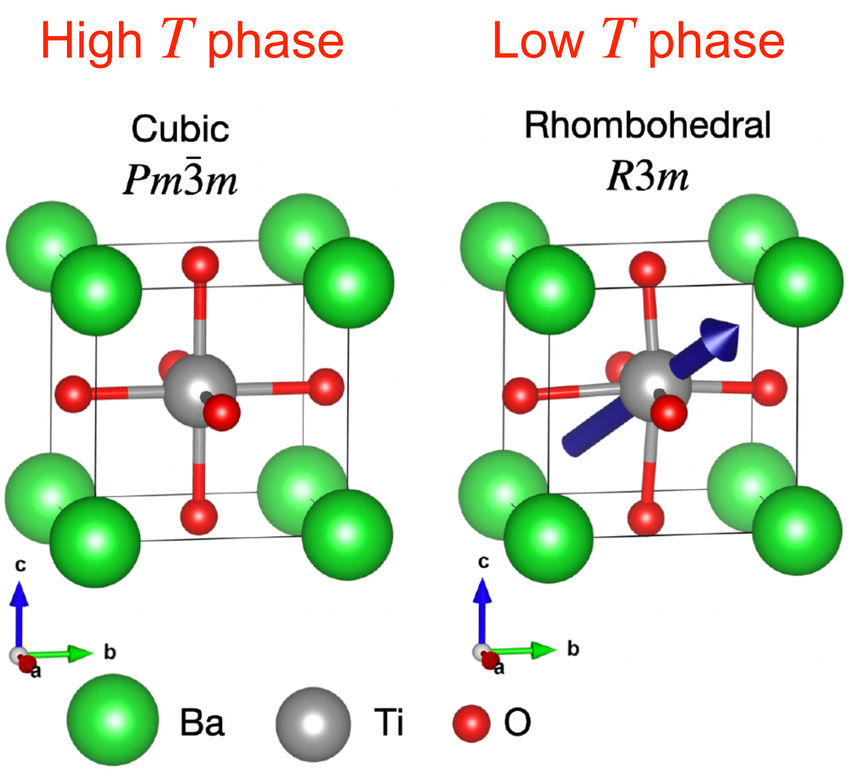

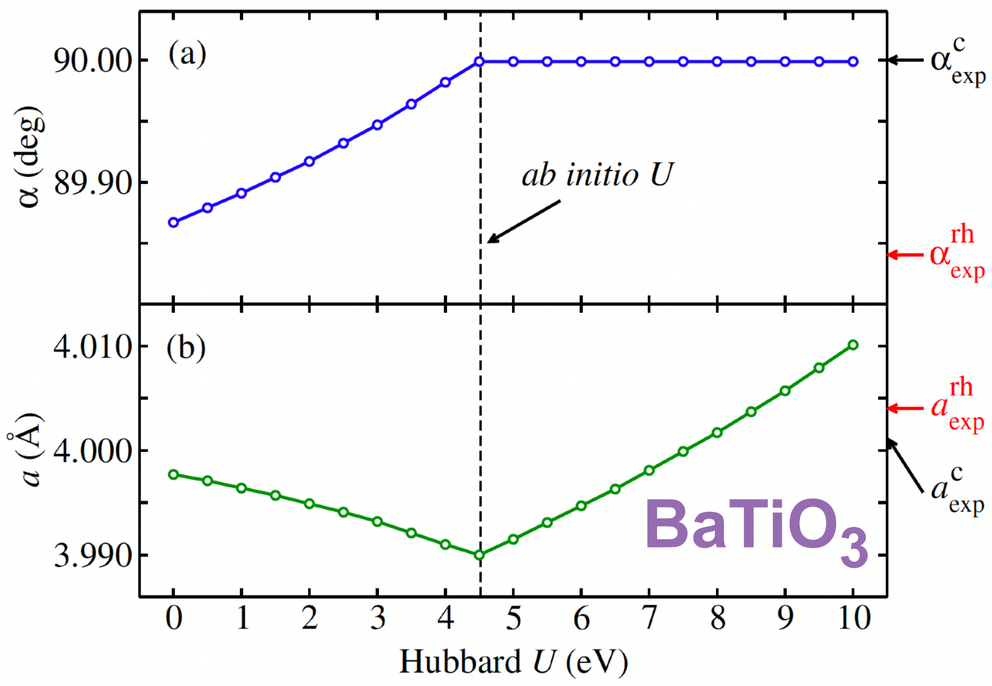

	a (Å)	α (deg)	Δ_{Ti}	Δ_{O}	$\Delta_{O'}$
PBEsol	3.998	89.87	−0.012	0.011	0.018
PBEsol+U	3.990	90.00	0.000	0.000	0.000
PBEsol+U+V	4.017	89.77	−0.014	0.012	0.020
Expt.	4.004	89.84	−0.013	0.011	0.019

At $T = 0$ K, DFT+U incorrectly stabilizes the cubic phase, while DFT+U+V correctly retains the rhombohedral phase

Gebreyesus, Bastonero, Kotiuga, Marzari, Timrov, PRB (2023).

Can Hubbard corrections improve band gaps?

Can we use DFT+*U*(+*V*) to predict band gaps?

Can Hubbard corrections improve band gaps?

Can we use DFT+*U*(+*V*) to predict band gaps?

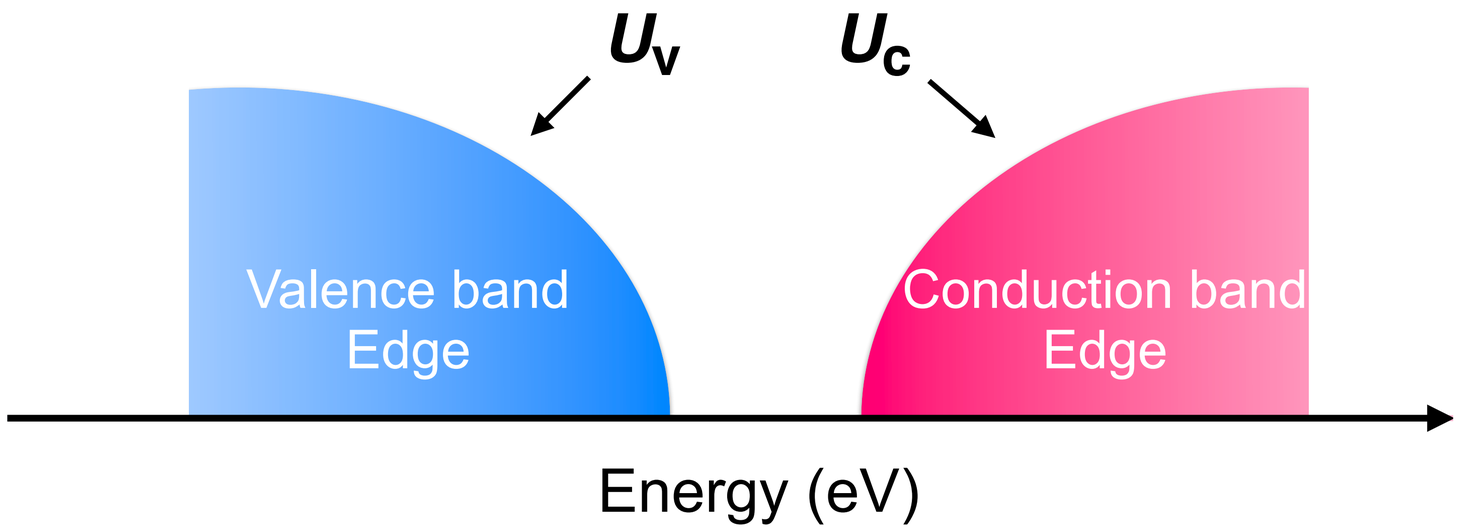

By applying the Hubbard *U* correction to the band edges we might expect improvements in the band gap values with respect to standard DFT

High-throughput search of novel materials for H_2 production

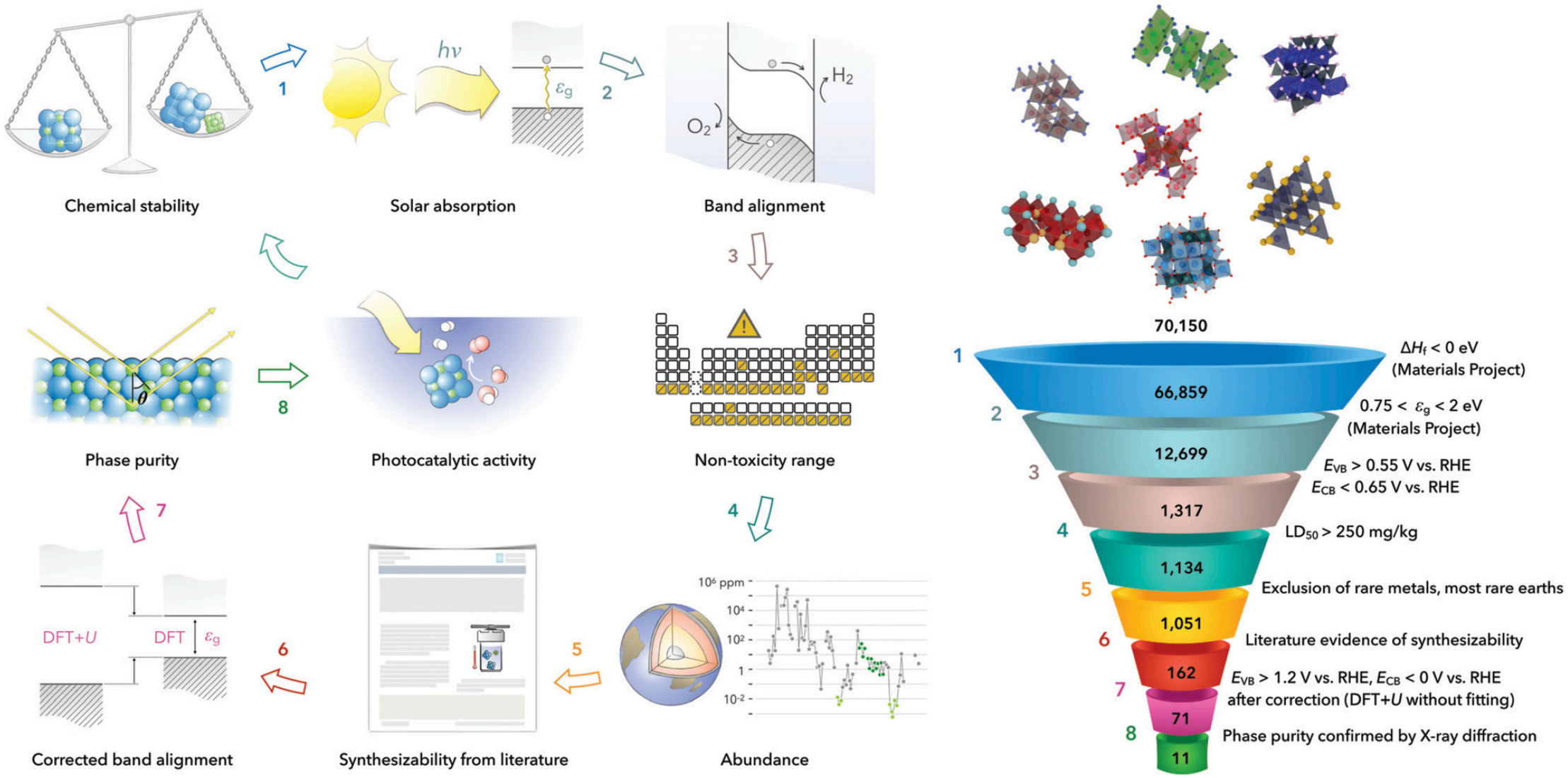

Xiong, …, Timrov,…, Dabo, Energy Environ. Sci. (2021).

High-throughput search of novel materials for H_2 production

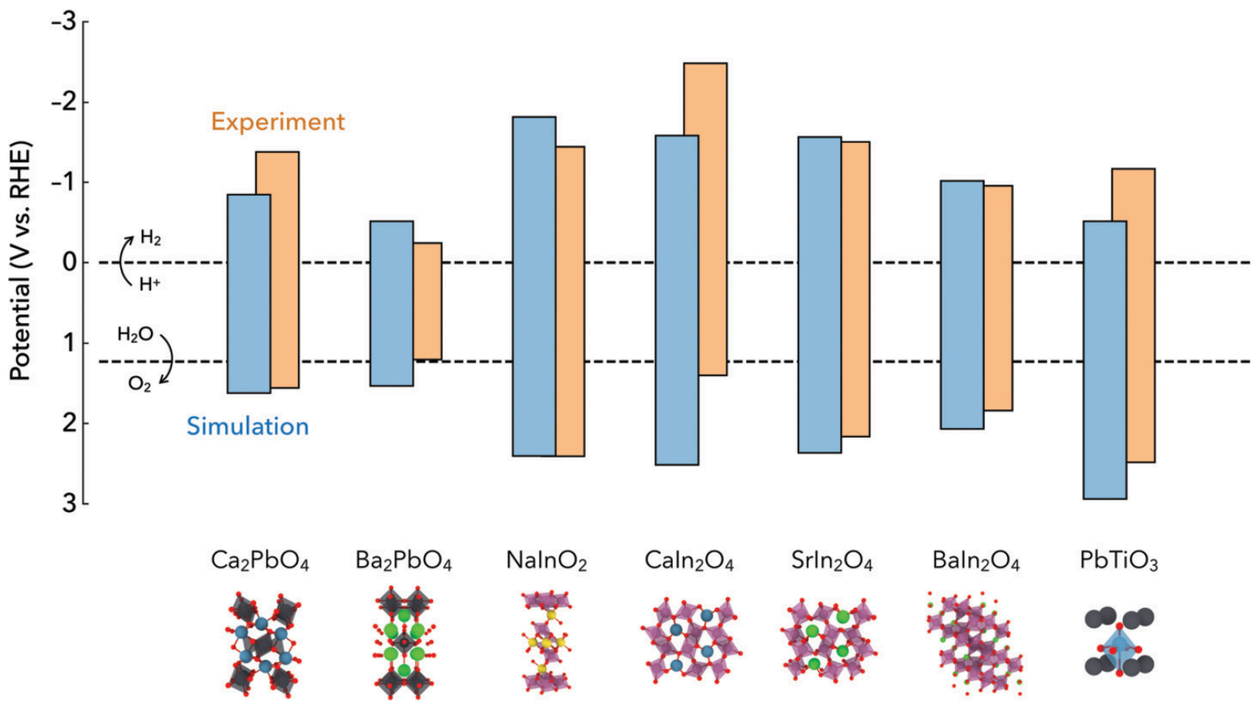

	Space group	DFT ε_g (eV)	DFT+U ε_g (eV)	Expt. ε_g (eV)
Oxides				
$SrCu_2O_2$	$I4_1/amd$	1.81	3.11	3.3[a]
$BaCu_2O_2$	$I4_1/amd$	1.39	3.22	
$CuAlO_2$	$R\bar{3}m$	1.78	3.07	2.99[b]
$CuGaO_2$	$R\bar{3}m$	0.75	2.46	1.97[b]
$Ca_{12}Al_{14}O_{33}$	$C2$	2.01	3.73	4.17[c]
Na_3BiO_4	$P2/c$	1.04	2.21	2.64[d]
Sr_2PbO_4	$Pbam$	1.43	2.31	1.75[e]
Sulfides				
Cu_3SbS_3	$P2_12_12_1$	1.06	1.89	
Cu_2WS_4	$P\bar{4}2m$	1.66	2.06	1.74[f]
Cu_3NbS_4	$P\bar{4}3m$	1.81	1.97	2.5[g]
$CuYS_2$	$Pnma$	1.63	2.18	
Oxychalcogenides				
LaOCuS	$P4/nmm$	1.70	2.65	3.1[h]
LaOCuSe	$P4/nmm$	1.48	2.44	2.82[h]
$La_4O_4Se_3$	$Amm2$	2.01	2.04	1.9[i]
Na_2TeO_4	$P2_1/c$	1.39	3.30	
Oxynitrides				
$CaTaO_2N$	$Pmc2_1$	1.67	2.46	2.6[j]
$LaTiO_2N$	$I2_12_12_1$	1.36	2.42	2.1[k]
Others				
$Na_5CuO_2(OH)_2$	$Pnma$	1.49	3.64	

18 out of 70150 materials were identified as candidates for the photocatalytic water splitting

Xiong, …, Timrov,…, Dabo, Energy Environ. Sci. (2021).

Exploring the energy landscape of magnetic materials

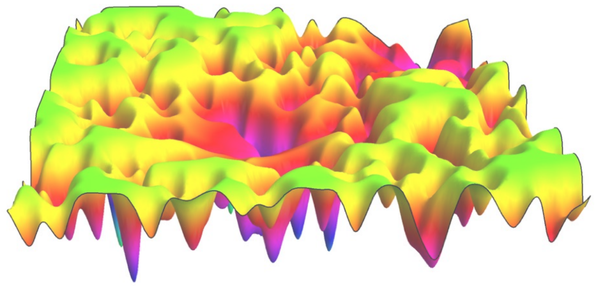

Applying the constraint to the occupations:

$$\tilde{E} = E_{DFT} + \sum_{I,\alpha\beta} \lambda^I_{\alpha\beta}(n^I_{\alpha\beta} - \tilde{n}^I_{\alpha\beta})$$

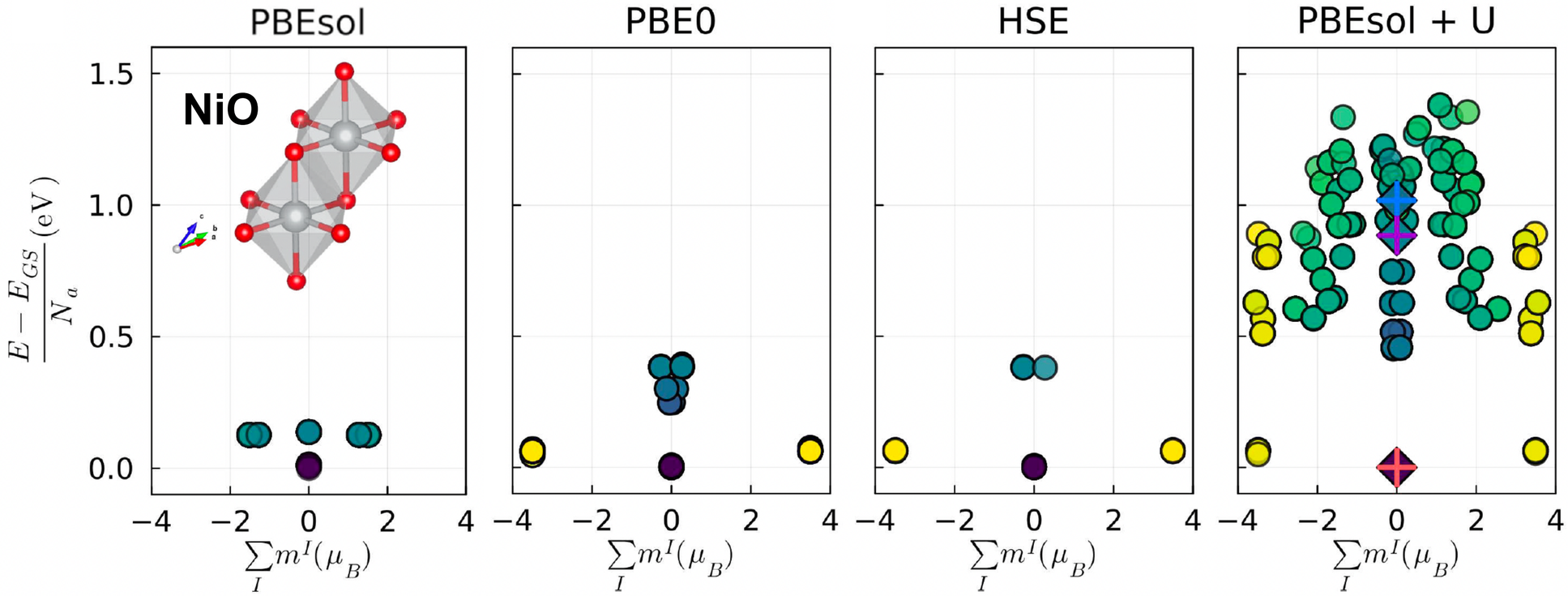

Ponet, Di Lucente, Marzari, https://doi.org/10.21203/rs.3.rs-3358581/v1

Orbital-resolved DFT+*U*

$$E_U = \sum_{I,\sigma} \frac{U^I_{t_{2g}}}{2} \sum_{i\in\{t_{2g}\}} \lambda_i^{I\sigma}(1-\lambda_i^{I\sigma}) + \sum_{I,\sigma} \frac{U^I_{e_g}}{2} \sum_{i\in\{e_g\}} \lambda_i^{I\sigma}(1-\lambda_i^{I\sigma}) \qquad \mathbf{n}^{I\sigma}\mathbf{v}_i^{I\sigma} = \lambda_i^{I\sigma}\mathbf{v}_i^{I\sigma}$$

Different U for t_{2g} and e_g orbitals of the d manifold

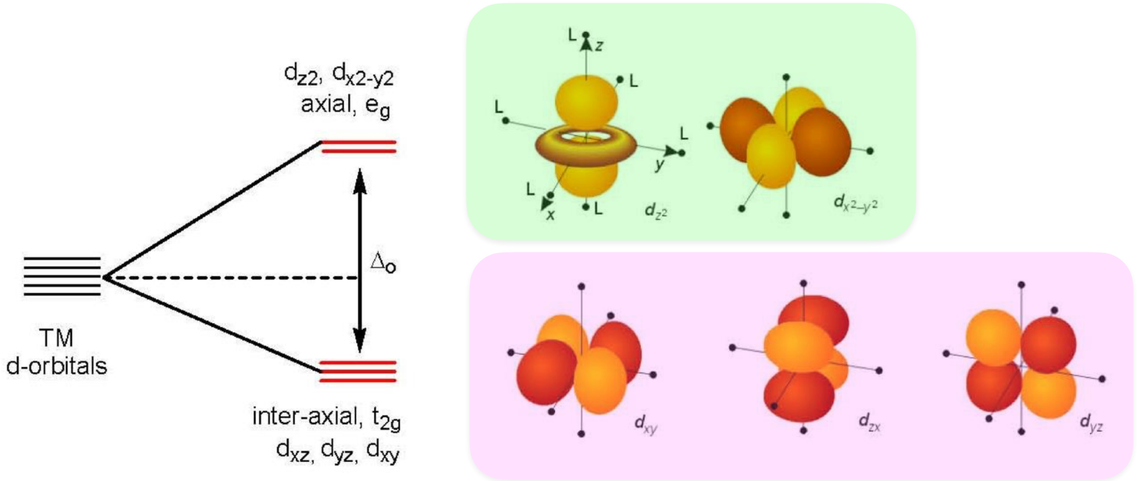

Adiabatic spin energies for Fe(II)-hexacomplexes

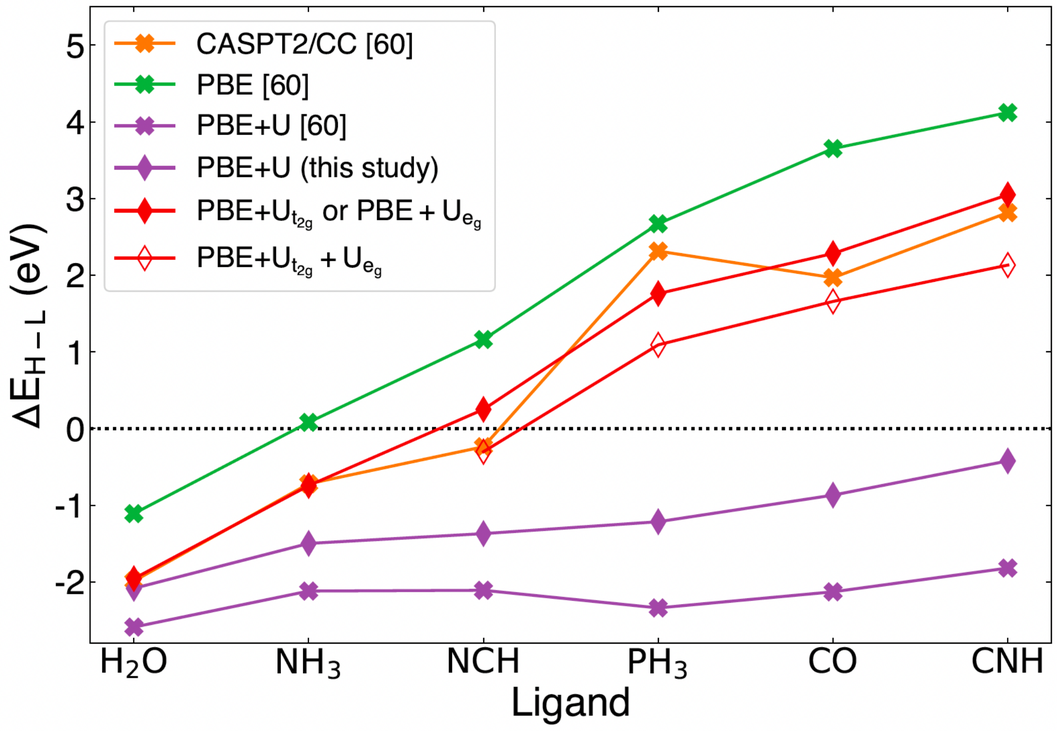

Macke, Timrov, Marzari, Colombi Ciacchi, arXiv:2312.13580

Density-functional perturbation theory +U (DFPT+U)

Band structure of CoO

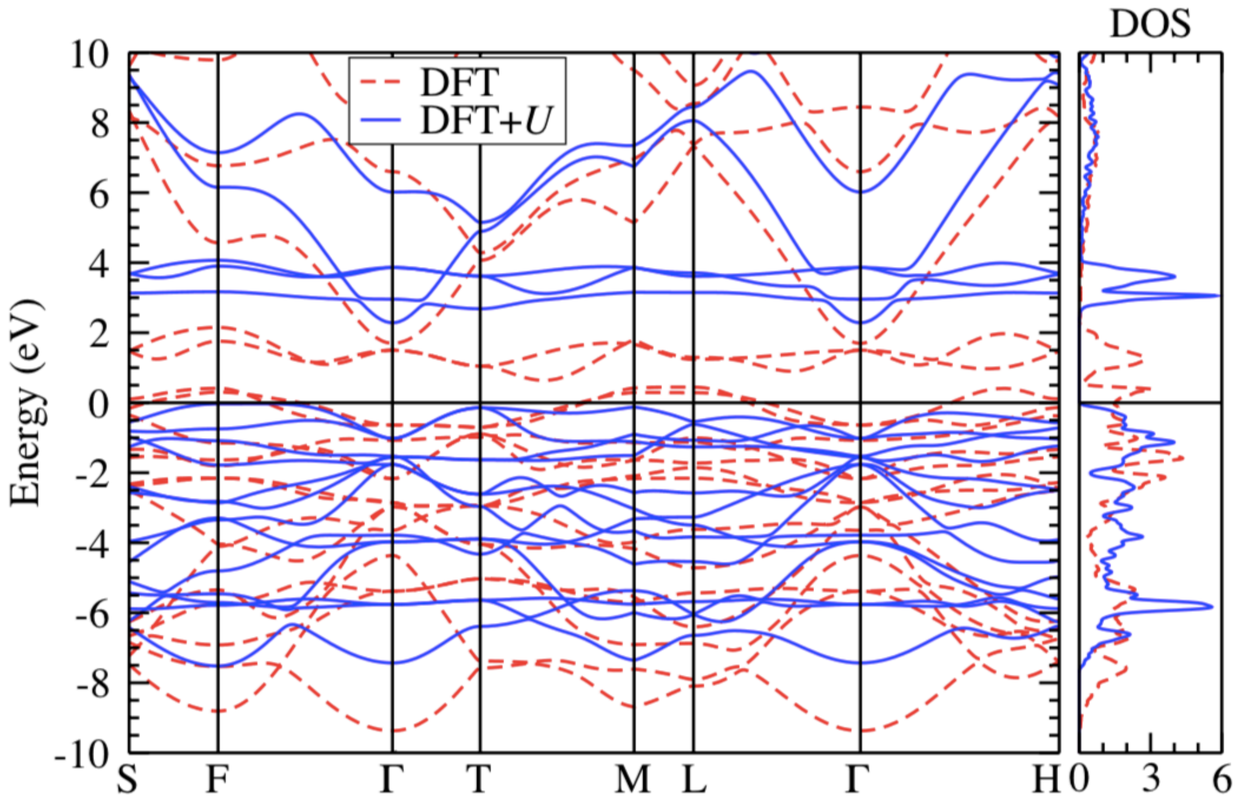

Hubbard corrections are crucial for the correct insulating ground state and dynamical stability of CoO

Floris, Timrov, Himmetoglu, Marzari, de Gironcoli, and Cococcioni, PRB (2020).

Density-functional perturbation theory +U (DFPT+U)

Band structure of CoO

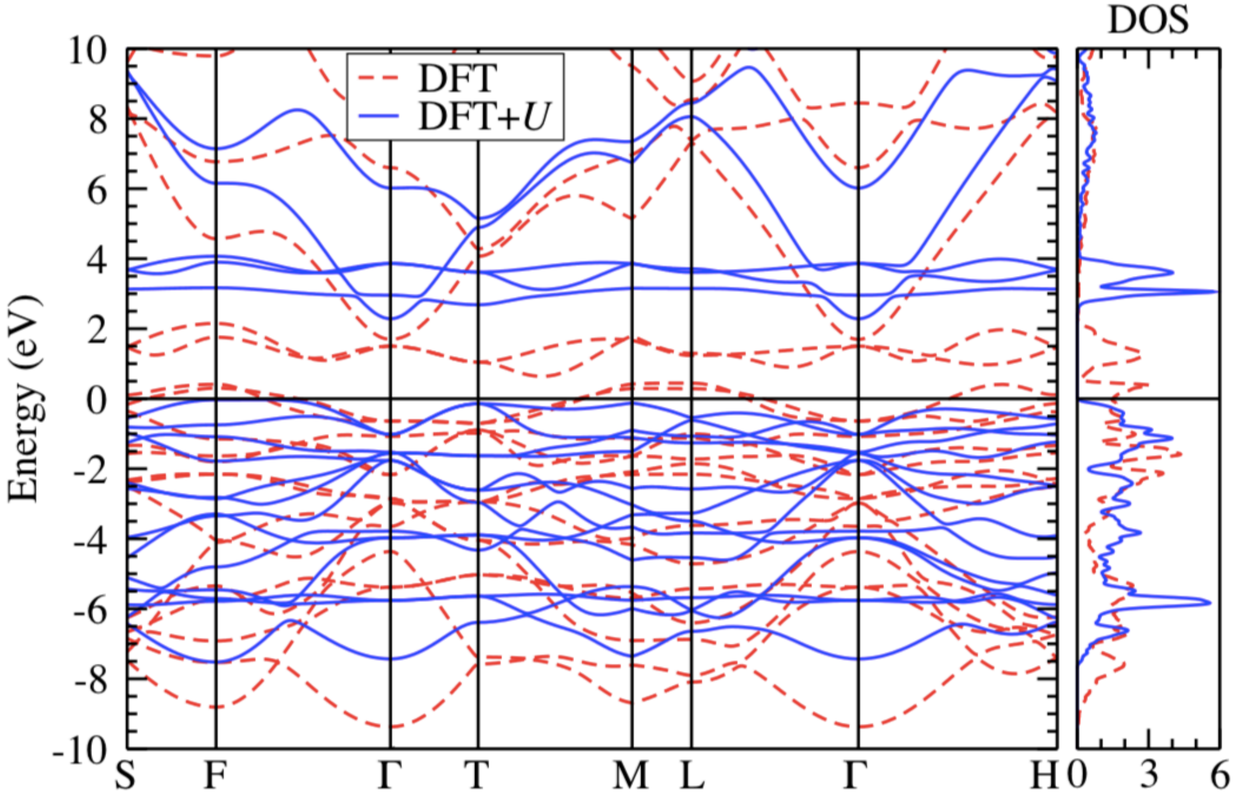

Phonon dispersion of CoO

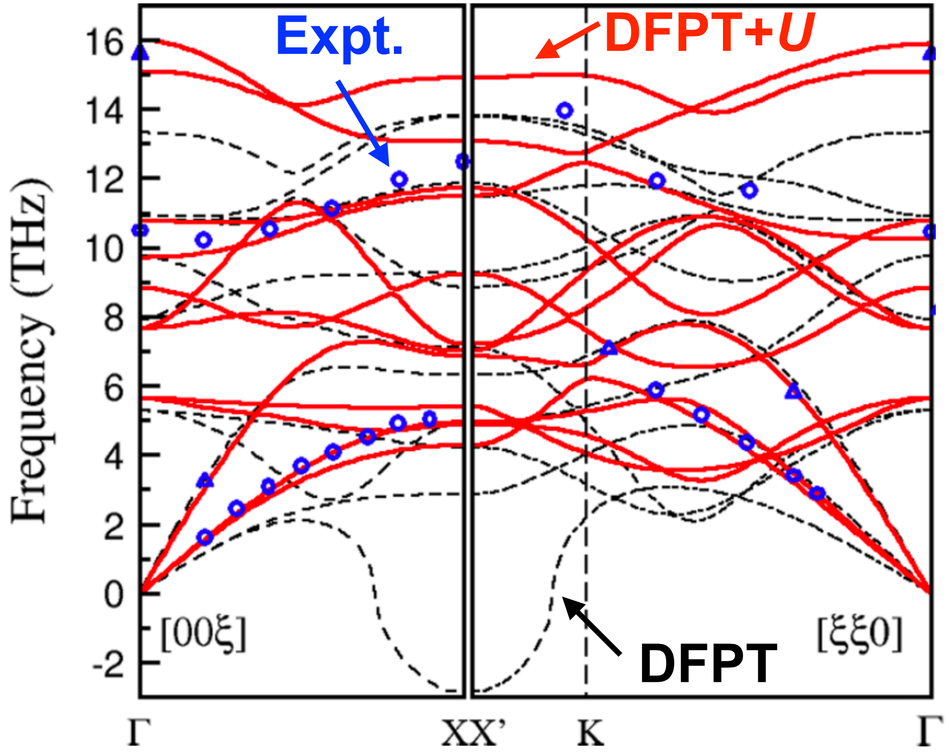

Hubbard corrections are crucial for the correct insulating ground state and dynamical stability of CoO

Floris, Timrov, Himmetoglu, Marzari, de Gironcoli, and Cococcioni, PRB (2020).

Electron-phonon coupling in Mott-Hubbard insulators

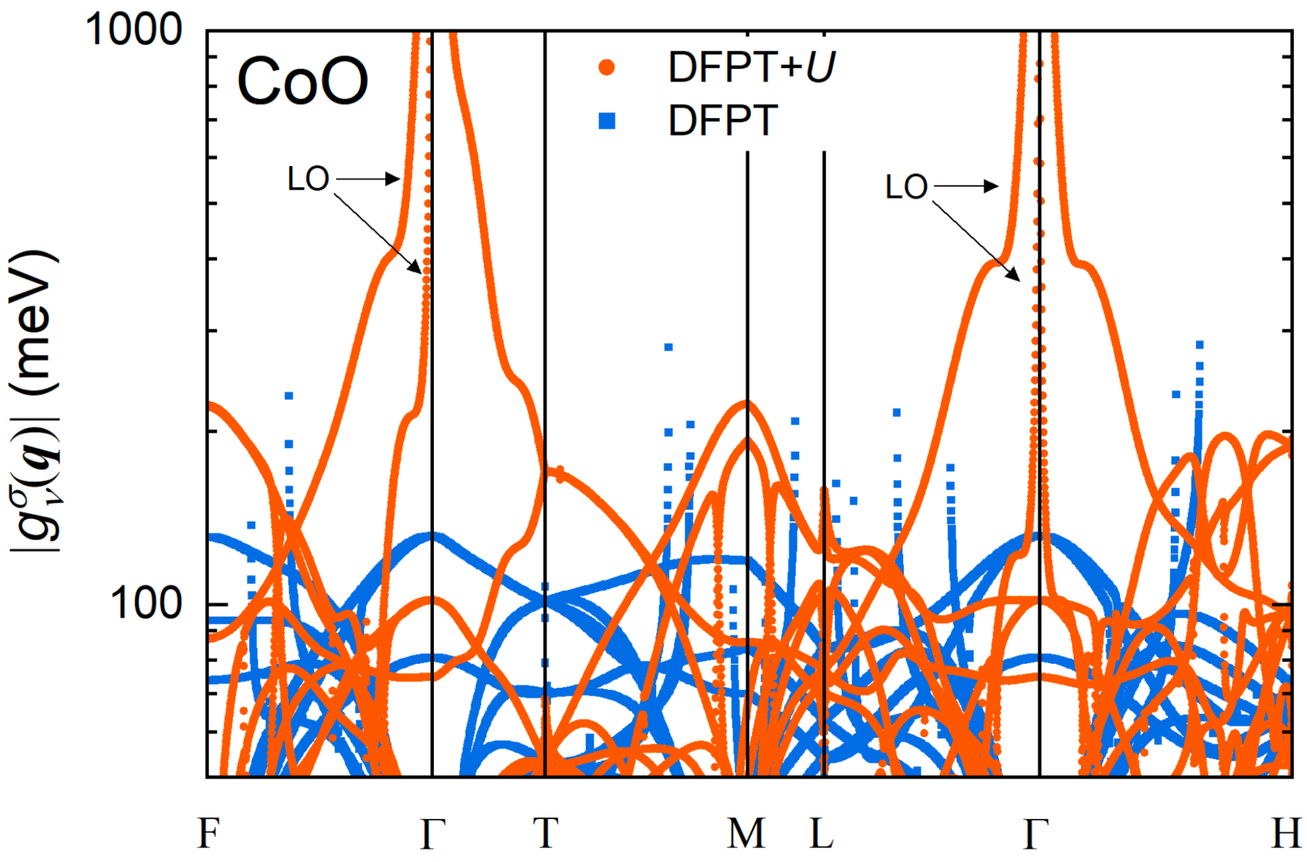

$$|g_\nu^\sigma(\boldsymbol{q})| \equiv \left(\sum_{mn} |g_{mn\nu}^\sigma(\boldsymbol{k}=0,\boldsymbol{q})|^2/N_b\right)^{1/2}$$

Hubbard *U* correction is crucial for the correct description of the electron-phonon coupling in Mott-Hubbard inssulators

Zhou, Park, Timrov, Floris, Cococcioni, Marzari, Bernardi, PRL (2021).

Parent (undoped) cuprate La_2CuO_4

DFT+*U* band structure

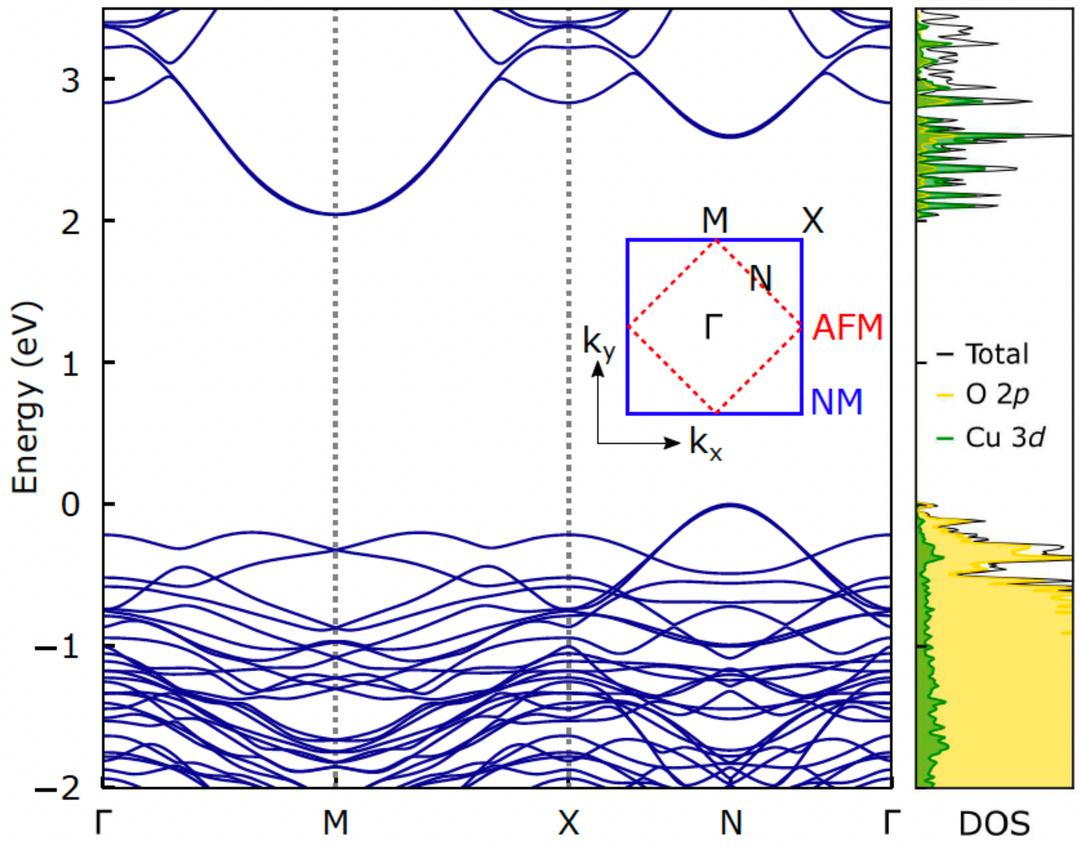

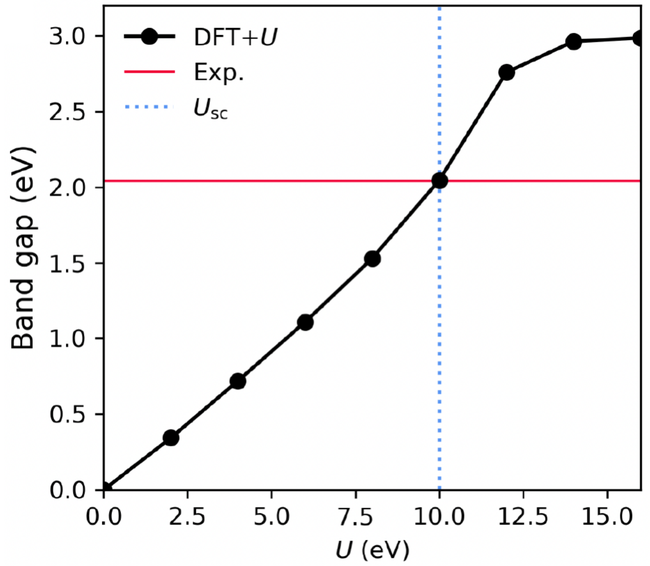

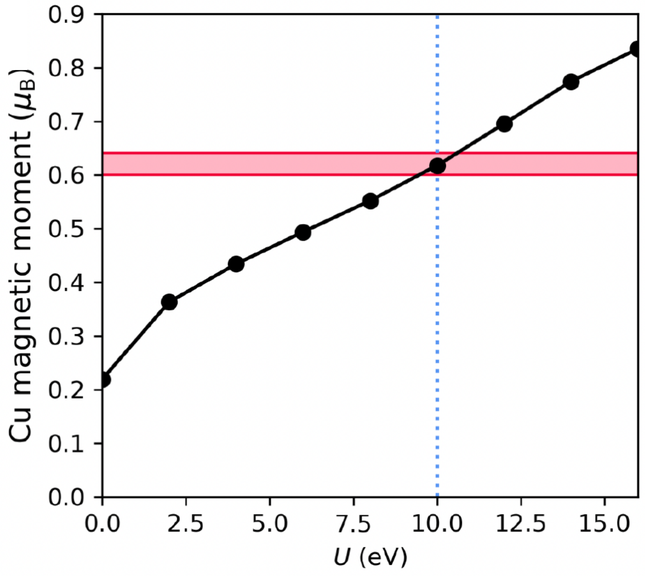

Accurate ground-state properties using the first-principles *U*

Chang, Timrov, Park, Zhou, Marzari, Bernardi, arXiv:2401.11322

Electron-phonon coupling in La_2CuO_4

Phonons

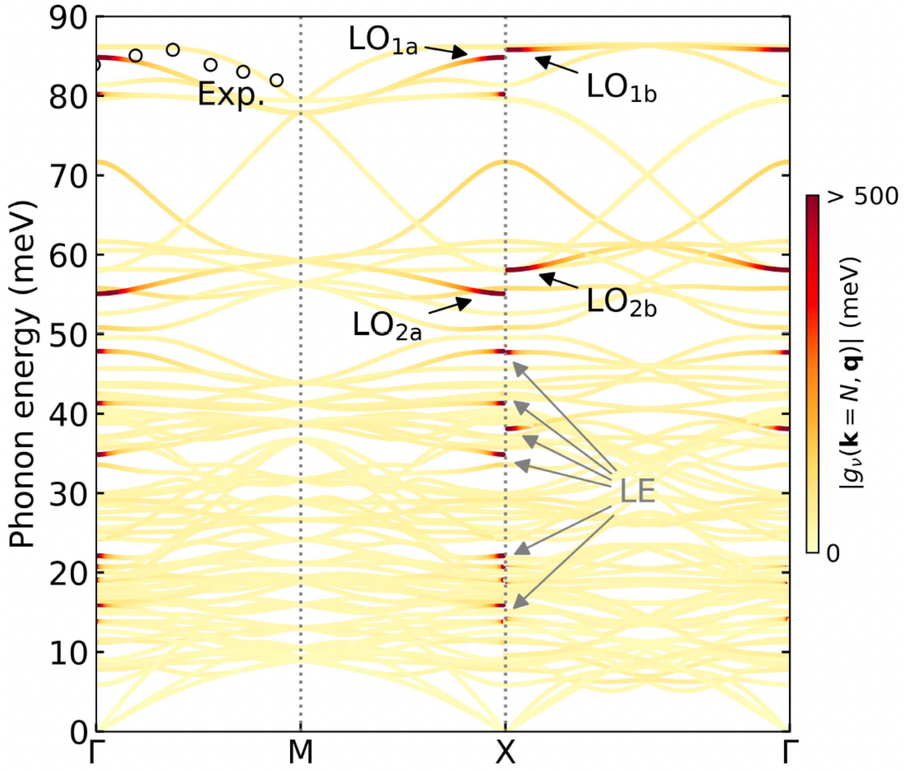

Electron-phonon coupling distribution function

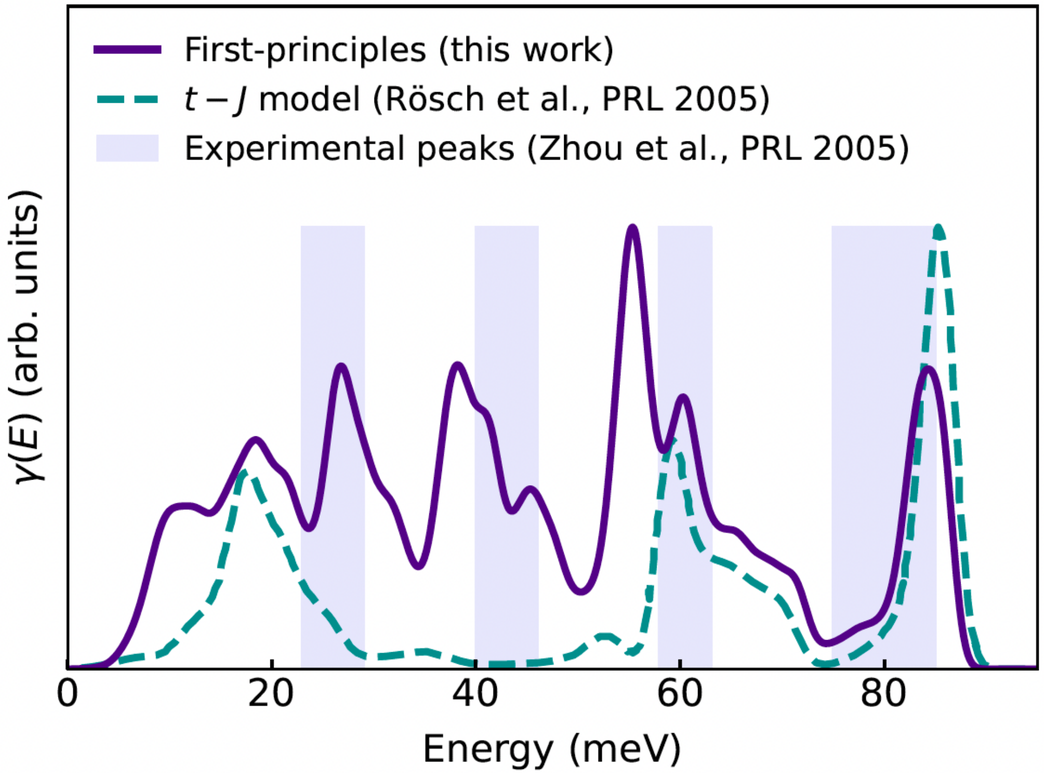

Accurate description of the e-ph coupling to understand the microscopic origin of the high Tc superconductivity

Chang, Timrov, Park, Zhou, Marzari, Bernardi, arXiv:2401.11322

Magnon dispersions from TDDFT+U

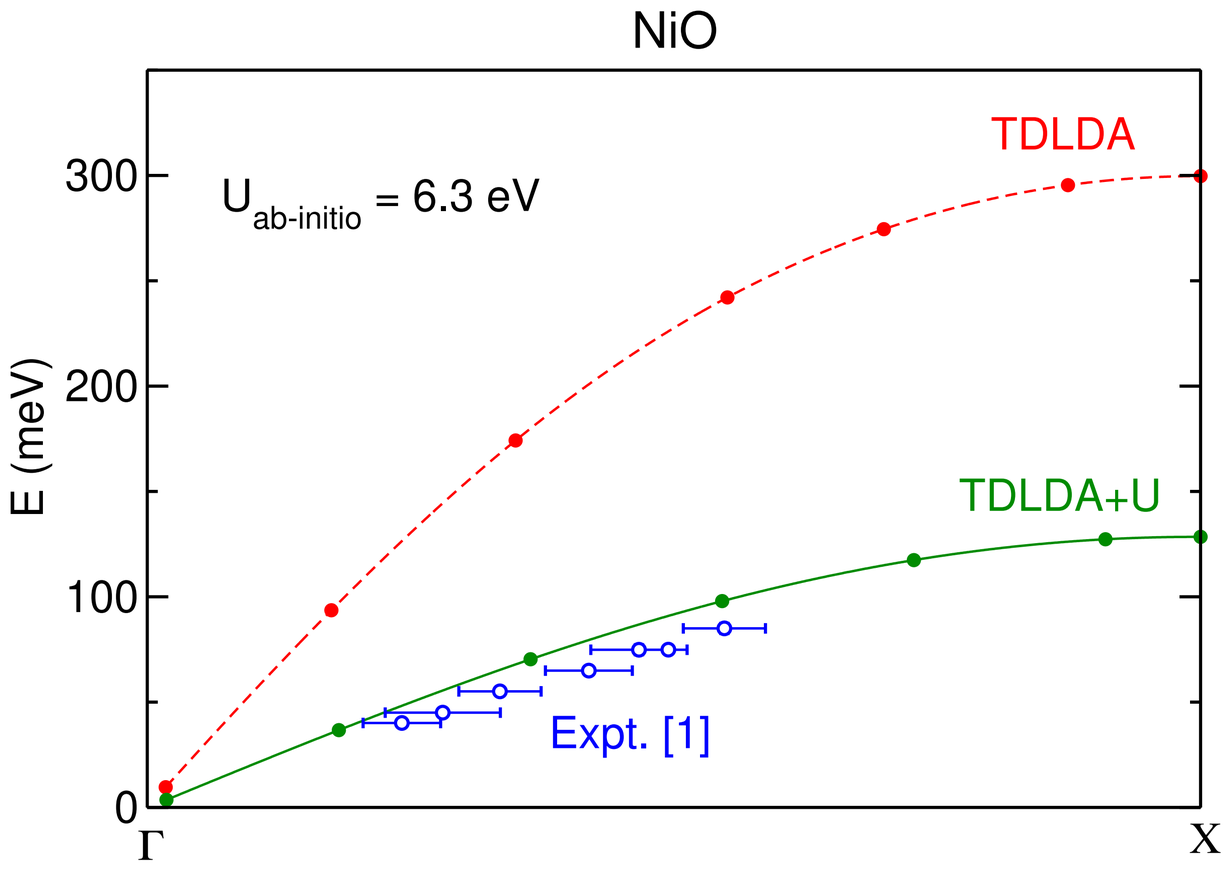

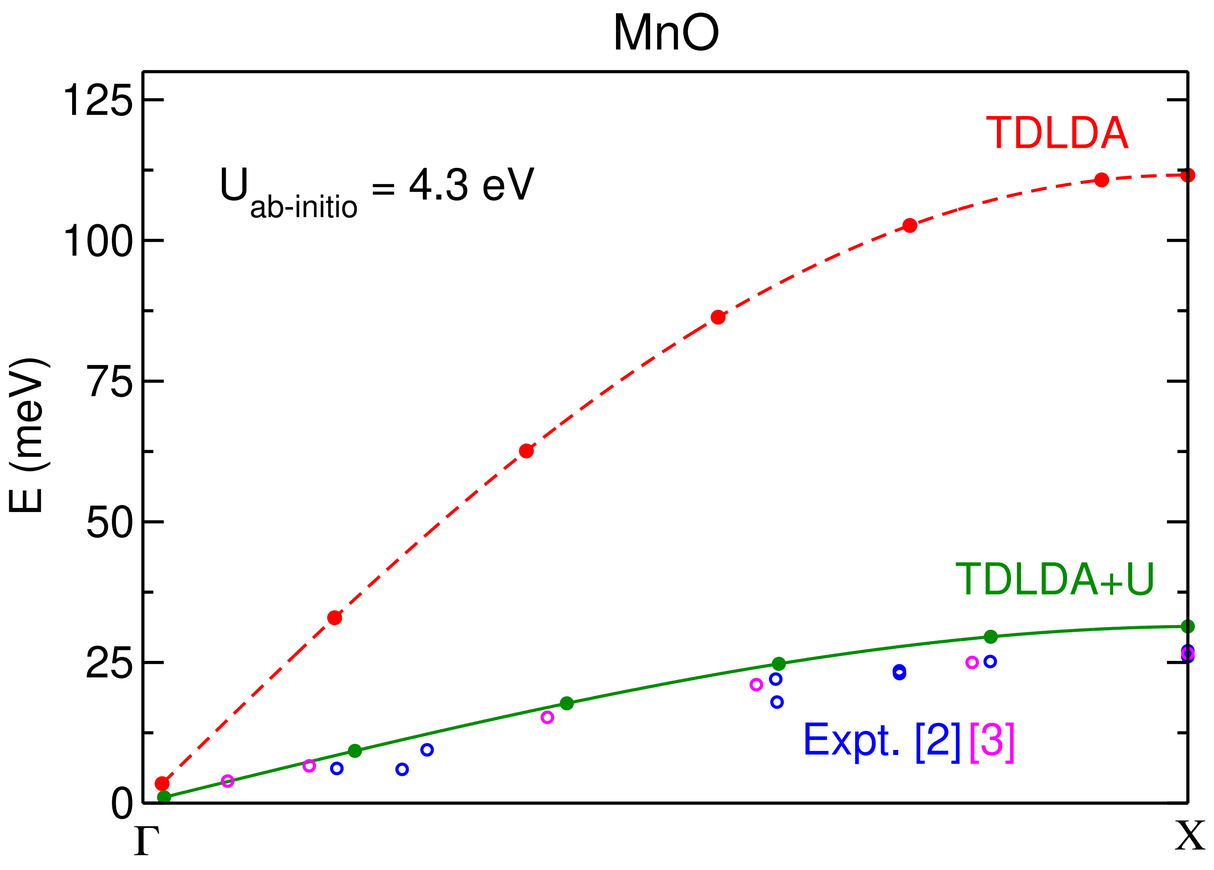

TDDFT@LDA (TDLDA) largely overestimates magnon energies

Remarkable agreement between TDLDA+U calculations and experiments

*[1] M. Hutchings et al., PRB **6**, 3447 (1972), [2] G. Pepy, JPCS **35**, 433 (1974), [3] M. Kohgi et al., SSC **11**, 391 (1972).*

Computational cost

- When *U* (and *V*) are provided, DFT+*U*(+*V*) is only marginally more expensive than DFT
- Calculation of *U* and *V* from DFPT is ~20x more expensive than the ground-state DFT
- *U* and *V* from DFPT ⟶ train the machine learning model [1]
- DFPT calculation of *U* takes less time than HSE06 [2]

Formula	No. of Atoms per Unit Cell	k-Points Mesh	U Calculation q-Points	t_U	HSE06 Calculation q-Points	E_g	t_{HSE06}	Ratio t_{HSE06}/t_U
TiO_2	6	$9\times6\times6$	$4\times3\times3$	3h 46m	$3\times2\times2$	3.30	10h 1m	2.7
NbNO	12	$6\times6\times6$	$3\times2\times2$	7h 35m	$2\times2\times2$	2.68	61h 52m	8.2

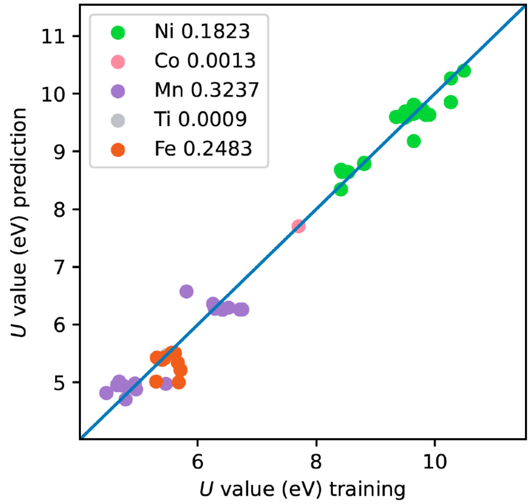

[1] *Uhrin, Zadoks, Binci, Marzari, Timrov, in preparation.*

[2] *Kirchner-Hall, Zhao, Xiong, Timrov, Dabo, Appl. Sci. (2021).*

Limitations/open questions of linear-response theory (LRT) for *U* and *V*

- For closed shells (i.e. fully occupied manifolds) the *U* values from LRT are too large
- *U* and *V* are position-dependent $\longrightarrow$ $dU/dR \neq 0$, $dV/dR \neq 0$ $\longrightarrow$ extra terms in forces
- Hubbard functionals are not variational w.r.t. *U* and *V* (no theorem/proof)
- DFT+*U*(+*V*) is a mean-field single-determinant approach (no strong correlations)
- Piece-wise linearity in the Hubbard manifold is heuristic (no proof)

Hybrid functionals

Main idea

Mixing the Fock energy (of the Hartree-Fock method) with the (semi-)local exchange-correlation functionals

$$E_{\mathrm{x}}^{\mathrm{Fock}} = -\frac{1}{2} \sum_{\mathbf{k}} \sum_{\mathbf{k}'} \sum_{v} \sum_{v'} \int \int \frac{\psi^*_{v,\mathbf{k}}(\mathbf{r}) \psi_{v',\mathbf{k}'}(\mathbf{r}) \psi^*_{v',\mathbf{k}'}(\mathbf{r}') \psi_{v,\mathbf{k}}(\mathbf{r}')}{|\mathbf{r} - \mathbf{r}'|} \, d\mathbf{r} \, d\mathbf{r}'$$

double sum over k points

double sum over bands

E_{Fock} is computationally very expensive in the plane-wave basis set

PBE0 hybrid functional

$$E_{\mathrm{xc}}^{\mathrm{PBE0}} = \alpha E_{\mathrm{x}}^{\mathrm{Fock}} + (1-\alpha) E_{\mathrm{x}}^{\mathrm{PBE}} + E_{\mathrm{c}}^{\mathrm{PBE}}$$

25% of the (non-local) exact-exchange (Fock) energy

75% of the (semi-local) exchange GGA-PBE energy

100% of the (semi-local) correlation GGA-PBE energy

C. Adamo and V. Barone, JCP 110, 6158 (1999).

PBE0 hybrid functional

$$\alpha = 0.25$$

$$E_{\mathrm{xc}}^{\mathrm{PBE0}} = \alpha E_{\mathrm{x}}^{\mathrm{Fock}} + (1-\alpha) E_{\mathrm{x}}^{\mathrm{PBE}} + E_{\mathrm{c}}^{\mathrm{PBE}}$$

25% of the (non-local) exact-exchange (Fock) energy

75% of the (semi-local) exchange GGA-PBE energy

100% of the (semi-local) correlation GGA-PBE energy

C. Adamo and V. Barone, JCP 110, 6158 (1999).

Molecules

Electronic atomization energies (i.e. energy required to completely separate a molecule into its constituent atoms) in kcal/mol

Molecule	PBE	PBE0	Expt.
N_2	244	225	227
O_2	143	124	118
SO	142	128	122

PBE0 hybrid functional gives much more accurate results than PBE compared to experiments for simple molecules

J. Paier, R. Hirschl, M. Marsman, G. Kresse, JCP 122, 234102 (2005).

Solids

Solid	PBE a_0	PBE B_0	PBE0 a_0	PBE0 B_0	Expt.‡ a_0	Expt.‡ B_0
Li	3.438	13.7	3.463	13.7	3.477	13.0
Na	4.200	7.80	4.229	8.22	4.225	7.5
Al	4.040	76.6	4.012	86.0	4.032	79.4
BN	3.626	370	3.600	402	3.616	400
BP	4.547	160	4.520	174	4.538	165
C	3.574	431	3.549	467	3.567	443
Si	5.469	87.8	5.433	99.0	5.430	99.2
SiC	4.380	210	4.347	231	4.358	225
β-GaN	4.546	169	4.481	199	4.520	210
GaP	5.506	75.3	5.446	87.3	5.451	88.7
GaAs	5.752	59.9	5.682	72.7	5.648	75.6
LiF	4.068	67.3	4.011	72.8	4.010	69.8

PBE0 provides more accurate results than PBE for the lattice parameters and bulk modulus of solids

J. Paier, M. Marsman, K. Hummer, G. Kresse, I.C. Gerber, J.G. Angyan, JCP 124, 154709 (2006).

Solids

Direct and indirect band gaps

	PBE	PBE0	Expt.
		GaAs	
$\Gamma_{15v} \rightarrow \Gamma_{1c}$	0.56	2.01	1.52[a]
$\Gamma_{15v} \rightarrow X_{1c}$	1.46	2.67	1.90[a]
$\Gamma_{15v} \rightarrow L_{1c}$	1.02	2.37	1.74[a]
		Si	
$\Gamma'_{25v} \rightarrow \Gamma_{15c}$	2.57	3.97	3.34–3.36,[b] 3.05[c]
$\Gamma'_{25v} \rightarrow X_{1c}$	0.71	1.93	1.13,[d] 1.25[c]
$\Gamma'_{25v} \rightarrow L_{1c}$	1.54	2.88	2.06(3),[e] 2.40(15)[f]
		C	
$\Gamma'_{25v} \rightarrow \Gamma_{15}$	5.59	7.69	7.3[a]
$\Gamma'_{25v} \rightarrow X_{1c}$	4.76	6.66	
$\Gamma'_{25v} \rightarrow L_{1c}$	8.46	10.77	
		MgO	
$\Gamma_{15} \rightarrow \Gamma_1$	4.75	7.24	7.7[g]
$X_{4'} \rightarrow \Gamma_1$	9.15	11.67	
$L_1 \rightarrow \Gamma_1$	7.91	10.38	

- PBE underestimates band gaps
- PBE0 predicts more accurate band gaps, but this is not systematic and there are overestimations
- Overestimation of band gaps in PBE0 is related to the non-optimal fraction of the Fock exchange (see next slides)

J. Paier, M. Marsman, K. Hummer, G. Kresse, I.C. Gerber, J.G. Angyan, JCP 124, 154709 (2006).

B3LYP hybrid functional

$$\alpha = 0.20, \beta = 0.72, \gamma = 0.81$$

$$E_{\mathrm{xc}}^{\mathrm{B3LYP}} = \alpha E_{\mathrm{x}}^{\mathrm{Fock}} + (1-\alpha) E_{\mathrm{x}}^{\mathrm{LDA}} + \beta \Delta E_{\mathrm{x}}^{\mathrm{B88}} + \gamma E_{\mathrm{c}}^{\mathrm{LYP}} + (1-\gamma) E_{\mathrm{c}}^{\mathrm{LDA}}$$

20% of the (non-local) exact-exchange (Fock) energy

80% of the (local) exchange LDA energy

Becke's gradient correction to the exchange functional

81% of the (local) correlation GGA-LYP energy

19% of the (local) correlation LDA energy

A.D. Becke, JCP 98, 1372 (1993).

P.J. Stephens, F.J. Devlin, C.F. Chabalowski, M.J. Frisch, JPC 98, 11623 (1994).

Molecules

Frequencies (ν), dipole strengths (D), rotational strengths (R) of 4-methyl-2-oxetanone

MP2			DFT/B3LYP			expt[b]		
ν	D	R	ν	D	R	ν	D	R
1528	14	−5	1500	13	−5	1453	25	−2
1516	8	4	1489	8	5	1441	3	3
1479	47	−11	1462	43	−11	1419	35	−9
1438	52	11	1422	51	11	1387	58	13
1394	52	27	1389	50	28	1350	40	42
1320	97	9	1316	112	3	1284	161	26
1230	47	−11	1229	44	−4	1198	47	−21
1216	14	0	1204	19	−5	1178	35	−17
1146	191	82	1137	327	99	1118	483	178
1125	219	−40	1113	87	−58	1099	51	−83
1077	10	−12	1076	11	−6	1055	40	−23
1056	271	−50	1041	268	−50	1022	251	−102
973	126	10	966	91	7	959	70	12
914	9	−29	914	8	−27	896	10	−54
873	221	33	850	310	46	836	371	78
829	97	26	817	34	10	812	55	29
714	3	−3	712	2	2	711	13	15

[a] Frequencies, ν, in cm^{-1}, dipole strengths D in 10^{-40} esu^2 cm^2, and rotational strengths R in 10^{-44} esu^2 cm^2. R values are for (R)-(+)-**1**.

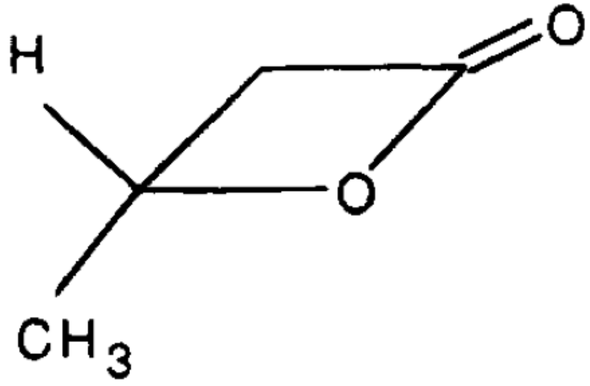

MP2 = second-order Møller-Plesset perturbation theory

B3LYP is very popular in the quantum chemistry community (study of molecules)

P.J. Stephens, F.J. Devlin, C.F. Chabalowski, M.J. Frisch, JPC 98, 11623 (1994).

Range separation

The Coulomb potential is partitioned as a sum of the short-range (SR) and long-range (LR) parts:

$$\frac{1}{|\mathbf{r}-\mathbf{r}'|} = \frac{\mathrm{erfc}(\omega|\mathbf{r}-\mathbf{r}'|)}{|\mathbf{r}-\mathbf{r}'|} + \frac{\mathrm{erf}(\omega|\mathbf{r}-\mathbf{r}'|)}{|\mathbf{r}-\mathbf{r}'|}$$

Range-separated hybrid functionals

From PBE0 to HSE hybrid functional

$$\alpha = 0.25$$

$$E_{\mathrm{xc}}^{\mathrm{PBE0}} = \alpha E_{\mathrm{x}}^{\mathrm{Fock}} + (1-\alpha) E_{\mathrm{x}}^{\mathrm{PBE}} + E_{\mathrm{c}}^{\mathrm{PBE}}$$

$$E_{\mathrm{xc}}^{\mathrm{HSE06}} = \alpha E_{\mathrm{x}}^{\mathrm{Fock,SR}} + (1-\alpha) E_{\mathrm{x}}^{\mathrm{PBE,SR}} + E_{\mathrm{x}}^{\mathrm{PBE,LR}} + E_{\mathrm{c}}^{\mathrm{PBE}}$$

J. Heyd, G.E. Scuseria, M. Ernzerhof, JCP 118, 8207 (2003); JCP 124, 219906 (2006).

HSE03 → HSE06

Solids

Direct and indirect band gaps

	PBE	PBE0	HSE03	Expt.
		GaAs		
$\Gamma_{15v} \rightarrow \Gamma_{1c}$	0.56	2.01	1.29	1.52[a]
$\Gamma_{15v} \rightarrow X_{1c}$	1.46	2.67	1.99	1.90[a]
$\Gamma_{15v} \rightarrow L_{1c}$	1.02	2.37	1.64	1.74[a]
		Si		
$\Gamma'_{25v} \rightarrow \Gamma_{15c}$	2.57	3.97	3.19	3.34–3.36,[b] 3.05[c]
$\Gamma'_{25v} \rightarrow X_{1c}$	0.71	1.93	1.23	1.13,[d] 1.25[c]
$\Gamma'_{25v} \rightarrow L_{1c}$	1.54	2.88	2.13	2.06(3),[e] 2.40(15)[f]
		C		
$\Gamma'_{25v} \rightarrow \Gamma_{15}$	5.59	7.69	6.77	7.3[a]
$\Gamma'_{25v} \rightarrow X_{1c}$	4.76	6.66	5.76	
$\Gamma'_{25v} \rightarrow L_{1c}$	8.46	10.77	9.80	
		MgO		
$\Gamma_{15} \rightarrow \Gamma_1$	4.75	7.24	6.34	7.7[g]
$X_{4'} \rightarrow \Gamma_1$	9.15	11.67	10.79	
$L_1 \rightarrow \Gamma_1$	7.91	10.38	9.49	

J. Paier, M. Marsman, K. Hummer, G. Kresse, I.C. Gerber, J.G. Angyan, JCP 124, 154709 (2006).

What fraction of Fock exchange to use in solids (α parameter)?

From the analogy with the many-body perturbation theory, one can realize that:

$$\cancel{\alpha = 0.25} \quad \Rightarrow \quad \alpha = \frac{1}{\epsilon_\infty}$$

ϵ_∞ is the electronic dielectric constant of a material

J.H. Skone, M. Govoni, G. Galli, PRB 89, 195112 (2014).

Dielectric constant ϵ_∞ of solids

Material	ϵ_∞
Ge	15.9
Si	11.9
AlP	7.54
SiC	6.52
TiO_2	6.34
NiO	5.76
C	5.70
CoO	5.35
GaN	5.30
ZnS	5.13
MnO	4.95
WO_3	4.81

Material	ϵ_∞
BN	4.50
HfO_2	4.41
AlN	4.18
ZnO	3.74
Al_2O_3	3.10
MgO	2.96
LiCl	2.70
NaCl	2.40
LiF	1.90
H_2O	1.72
Ar	1.66
Ne	1.23

J.H. Skone, M. Govoni, G. Galli, PRB 89, 195112 (2014).

Band gaps of solids

Material	PBE	PBE0 ($\alpha = 0.25$)	PBE0 modified ($\alpha = 1/\epsilon_\infty$)	Expt.
Ge	0.00	1.53	0.77	0.74
Si	0.62	1.75	1.03	1.17
AlP	1.64	2.98	2.41	2.51
SiC	1.37	2.91	2.33	2.39
TiO_2	1.81	3.92	3.18	3.3
NiO	0.97	5.28	4.61	4.3
C	4.15	5.95	5.44	5.48
CoO	0.00	4.53	4.01	2.5
GaN	1.88	3.68	3.30	3.29
ZnS	2.36	4.18	3.85	3.91
MnO	1.12	3.87	3.66	3.9
WO_3	1.92	3.79	3.50	3.38

J.H. Skone, M. Govoni, G. Galli, PRB 89, 195112 (2014).

J.H. Skone, M. Govoni, G. Galli, PRB 93, 235106 (2016).

Calculation of the Fock energy in practice

$$E_{\mathrm{x}}^{\mathrm{Fock}} = -\frac{1}{2}\sum_{\mathbf{k}}\sum_{\mathbf{k}'}\sum_{v}\sum_{v'}\int\int\frac{\psi^*_{v,\mathbf{k}}(\mathbf{r})\psi_{v',\mathbf{k}'}(\mathbf{r})\psi^*_{v',\mathbf{k}'}(\mathbf{r}')\psi_{v,\mathbf{k}}(\mathbf{r}')}{|\mathbf{r}-\mathbf{r}'|}\,d\mathbf{r}\,d\mathbf{r}'$$

$$\sum_{\mathbf{q}}$$

auxiliary q point grid ($\mathbf{q} = \mathbf{k} - \mathbf{k}'$)

Replace one sum over k points with a sum over q points ($N_{\mathbf{q}} \leq N_{\mathbf{k}}$)

This allows us to speed up significantly the calculation of $E_{\mathrm{x}}^{\mathrm{Fock}}$

From real to reciprocal space

$$E_{\mathrm{x}}^{\mathrm{Fock}} = -\frac{1}{2}\sum_{\mathbf{k}}\sum_{\mathbf{k}'}\sum_{v}\sum_{v'}\int\int \frac{\psi^*_{v,\mathbf{k}}(\mathbf{r})\psi_{v',\mathbf{k}'}(\mathbf{r})\psi^*_{v',\mathbf{k}'}(\mathbf{r}')\psi_{v,\mathbf{k}}(\mathbf{r}')}{|\mathbf{r}-\mathbf{r}'|}\,d\mathbf{r}\,d\mathbf{r}'$$

From real to reciprocal space

$$E_{\mathrm{x}}^{\mathrm{Fock}} = -\frac{1}{2}\sum_{\mathbf{k}}\sum_{\mathbf{k}'}\sum_{v}\sum_{v'}\int\int \frac{\psi^*_{v,\mathbf{k}}(\mathbf{r})\psi_{v',\mathbf{k}'}(\mathbf{r})\psi^*_{v',\mathbf{k}'}(\mathbf{r}')\psi_{v,\mathbf{k}}(\mathbf{r}')}{|\mathbf{r}-\mathbf{r}'|}\,d\mathbf{r}\,d\mathbf{r}'$$

$$E_{\mathrm{x}}^{\mathrm{Fock}} = -\frac{2\pi}{\Omega}\frac{1}{N_{\mathbf{q}}}\sum_{\mathbf{q}}\sum_{\mathbf{G}}\frac{A(\mathbf{q}+\mathbf{G})}{|\mathbf{q}+\mathbf{G}|^2},$$

$$A(\mathbf{q}+\mathbf{G}) = \frac{1}{N_{\mathbf{k}}}\sum_{\mathbf{k}}\sum_{v,v'}|\rho_{v,\mathbf{k}}^{v',\mathbf{k}-\mathbf{q}}(\mathbf{q}+\mathbf{G})|^2$$

From real to reciprocal space

$$E_{\mathrm{x}}^{\mathrm{Fock}} = -\frac{1}{2}\sum_{\mathbf{k}}\sum_{\mathbf{k}'}\sum_{v}\sum_{v'}\int\int \frac{\psi^*_{v,\mathbf{k}}(\mathbf{r})\psi_{v',\mathbf{k}'}(\mathbf{r})\psi^*_{v',\mathbf{k}'}(\mathbf{r}')\psi_{v,\mathbf{k}}(\mathbf{r}')}{|\mathbf{r}-\mathbf{r}'|}\,d\mathbf{r}\,d\mathbf{r}'$$

$$E_{\mathrm{x}}^{\mathrm{Fock}} = -\frac{2\pi}{\Omega}\frac{1}{N_{\mathbf{q}}}\sum_{\mathbf{q}}\sum_{\mathbf{G}}\frac{A(\mathbf{q}+\mathbf{G})}{|\mathbf{q}+\mathbf{G}|^2},$$

$$A(\mathbf{q}+\mathbf{G}) = \frac{1}{N_{\mathbf{k}}}\sum_{\mathbf{k}}\sum_{v,v'}|\rho_{v,\mathbf{k}}^{v',\mathbf{k}-\mathbf{q}}(\mathbf{q}+\mathbf{G})|^2$$

$$\rho_{v,\mathbf{k}}^{v',\mathbf{k}-\mathbf{q}}(\mathbf{r}) = u^*_{v',\mathbf{k}-\mathbf{q}}(\mathbf{r})\,u_{v,\mathbf{k}}(\mathbf{r})$$

From real to reciprocal space

$$E_{\mathrm{x}}^{\mathrm{Fock}} = -\frac{1}{2}\sum_{\mathbf{k}}\sum_{\mathbf{k}'}\sum_{v}\sum_{v'}\int\int \frac{\psi^*_{v,\mathbf{k}}(\mathbf{r})\psi_{v',\mathbf{k}'}(\mathbf{r})\psi^*_{v',\mathbf{k}'}(\mathbf{r}')\psi_{v,\mathbf{k}}(\mathbf{r}')}{|\mathbf{r}-\mathbf{r}'|}\,d\mathbf{r}\,d\mathbf{r}'$$

$$E_{\mathrm{x}}^{\mathrm{Fock}} = -\frac{2\pi}{\Omega}\frac{1}{N_{\mathbf{q}}}\sum_{\mathbf{q}}\sum_{\mathbf{G}}\frac{A(\mathbf{q}+\mathbf{G})}{|\mathbf{q}+\mathbf{G}|^2},$$

$$A(\mathbf{q}+\mathbf{G}) = \frac{1}{N_{\mathbf{k}}}\sum_{\mathbf{k}}\sum_{v,v'}|\rho_{v,\mathbf{k}}^{v',\mathbf{k}-\mathbf{q}}(\mathbf{q}+\mathbf{G})|^2$$

$$\rho_{v,\mathbf{k}}^{v',\mathbf{k}-\mathbf{q}}(\mathbf{r}) = u^*_{v',\mathbf{k}-\mathbf{q}}(\mathbf{r})\,u_{v,\mathbf{k}}(\mathbf{r})$$

$$\psi_{v,\mathbf{k}}(\mathbf{r}) = \frac{1}{\sqrt{N_{\mathbf{k}}}}e^{i\mathbf{k}\cdot\mathbf{r}}u_{v,\mathbf{k}}(\mathbf{r})$$

From real to reciprocal space

$$E_{\mathrm{x}}^{\mathrm{Fock}} = -\frac{1}{2}\sum_{\mathbf{k}}\sum_{\mathbf{k}'}\sum_{v}\sum_{v'}\int\int \frac{\psi^*_{v,\mathbf{k}}(\mathbf{r})\psi_{v',\mathbf{k}'}(\mathbf{r})\psi^*_{v',\mathbf{k}'}(\mathbf{r}')\psi_{v,\mathbf{k}}(\mathbf{r}')}{|\mathbf{r}-\mathbf{r}'|}\,d\mathbf{r}\,d\mathbf{r}'$$

$$E_{\mathrm{x}}^{\mathrm{Fock}} = -\frac{2\pi}{\Omega}\frac{1}{N_{\mathbf{q}}}\sum_{\mathbf{q}}\sum_{\mathbf{G}}\frac{A(\mathbf{q}+\mathbf{G})}{|\mathbf{q}+\mathbf{G}|^2},$$

$$A(\mathbf{q}+\mathbf{G}) = \frac{1}{N_{\mathbf{k}}}\sum_{\mathbf{k}}\sum_{v,v'}|\rho_{v,\mathbf{k}}^{v',\mathbf{k}-\mathbf{q}}(\mathbf{q}+\mathbf{G})|^2$$

singularity when

$$\mathbf{q}+\mathbf{G}=0$$

$$\rho_{v,\mathbf{k}}^{v',\mathbf{k}-\mathbf{q}}(\mathbf{r}) = u^*_{v',\mathbf{k}-\mathbf{q}}(\mathbf{r})\,u_{v,\mathbf{k}}(\mathbf{r})$$

$$\psi_{v,\mathbf{k}}(\mathbf{r}) = \frac{1}{\sqrt{N_{\mathbf{k}}}}e^{i\mathbf{k}\cdot\mathbf{r}}u_{v,\mathbf{k}}(\mathbf{r})$$

Gygi-Baldereschi method to treat the q+G=0 singulatiry

$$E_{\mathbf{x}}^{\mathrm{Fock}} = -\frac{2\pi}{\Omega}\frac{1}{N_{\mathbf{q}}}\sum_{\mathbf{q}}\sum_{\mathbf{G}}\frac{A(\mathbf{q}+\mathbf{G})}{|\mathbf{q}+\mathbf{G}|^2}$$

F. Gygi and A. Baldereschi, PRB 34, 4405 (1986).

H.-V. Nguyen and S. de Gironcoli, PRB 79, 205114 (2009).

Gygi-Baldereschi method to treat the q+G=0 singulatiry

$$E_{\mathbf{x}}^{\mathrm{Fock}} = -\frac{2\pi}{\Omega}\frac{1}{N_{\mathbf{q}}}\sum_{\mathbf{q}}\sum_{\mathbf{G}}\frac{A(\mathbf{q}+\mathbf{G})}{|\mathbf{q}+\mathbf{G}|^2}$$

$$= -\frac{2\pi}{\Omega}\left\{\frac{1}{N_{\mathbf{q}}}\sum_{\mathbf{q},\mathbf{G}}\frac{A(\mathbf{q}+\mathbf{G})-A(0)e^{-\alpha|\mathbf{q}+\mathbf{G}|^2}}{|\mathbf{q}+\mathbf{G}|^2}+\frac{1}{N_{\mathbf{q}}}\sum_{\mathbf{q},\mathbf{G}}\frac{e^{-\alpha|\mathbf{q}+\mathbf{G}|^2}}{|\mathbf{q}+\mathbf{G}|^2}A(0)\right\}$$

We are adding and subtracting exactly the same term (in red)

F. Gygi and A. Baldereschi, PRB 34, 4405 (1986).

H.-V. Nguyen and S. de Gironcoli, PRB 79, 205114 (2009).

Gygi-Baldereschi method to treat the q+G=0 singulatiry

$$
\begin{aligned}
E_{\mathrm{x}}^{\mathrm{Fock}} &= -\frac{2\pi}{\Omega}\frac{1}{N_{\mathbf{q}}}\sum_{\mathbf{q}}\sum_{\mathbf{G}}\frac{A(\mathbf{q}+\mathbf{G})}{|\mathbf{q}+\mathbf{G}|^2} \\
&= -\frac{2\pi}{\Omega}\left\{\frac{1}{N_{\mathbf{q}}}\sum_{\mathbf{q},\mathbf{G}}\frac{A(\mathbf{q}+\mathbf{G})-A(0)e^{-\alpha|\mathbf{q}+\mathbf{G}|^2}}{|\mathbf{q}+\mathbf{G}|^2}+\frac{1}{N_{\mathbf{q}}}\sum_{\mathbf{q},\mathbf{G}}\frac{e^{-\alpha|\mathbf{q}+\mathbf{G}|^2}}{|\mathbf{q}+\mathbf{G}|^2}A(0)\right\} \\
&= -\frac{2\pi}{\Omega}\left\{\frac{1}{N_{\mathbf{q}}}\left[\sum_{\mathbf{q},\mathbf{G}}{}'\frac{A(\mathbf{q}+\mathbf{G})}{|\mathbf{q}+\mathbf{G}|^2}+\lim_{\mathbf{q}\to 0}\frac{A(\mathbf{q})-A(0)}{\mathbf{q}^2}\right]+D\times A(0)\right\}
\end{aligned}
$$

$$
D=\frac{1}{N_{\mathbf{q}}}\left[-\sum_{\mathbf{q},\mathbf{G}}{}'\frac{e^{-\alpha|\mathbf{q}+\mathbf{G}|^2}}{|\mathbf{q}+\mathbf{G}|^2}+\alpha\right]+\frac{\Omega}{(2\pi)^3}\sqrt{\frac{\pi}{\alpha}}
$$

F. Gygi and A. Baldereschi, PRB 34, 4405 (1986).

H.-V. Nguyen and S. de Gironcoli, PRB 79, 205114 (2009).

Gygi-Baldereschi method to treat the q+G=0 singulatiry

$$
\begin{aligned}
E_{\mathrm{x}}^{\mathrm{Fock}} &= -\frac{2\pi}{\Omega}\frac{1}{N_{\mathbf{q}}}\sum_{\mathbf{q}}\sum_{\mathbf{G}}\frac{A(\mathbf{q}+\mathbf{G})}{|\mathbf{q}+\mathbf{G}|^2} \\
&= -\frac{2\pi}{\Omega}\left\{\frac{1}{N_{\mathbf{q}}}\sum_{\mathbf{q},\mathbf{G}}\frac{A(\mathbf{q}+\mathbf{G})-A(0)e^{-\alpha|\mathbf{q}+\mathbf{G}|^2}}{|\mathbf{q}+\mathbf{G}|^2}+\frac{1}{N_{\mathbf{q}}}\sum_{\mathbf{q},\mathbf{G}}\frac{e^{-\alpha|\mathbf{q}+\mathbf{G}|^2}}{|\mathbf{q}+\mathbf{G}|^2}A(0)\right\} \\
&= -\frac{2\pi}{\Omega}\left\{\frac{1}{N_{\mathbf{q}}}\left[\sum_{\mathbf{q},\mathbf{G}}{}'\frac{A(\mathbf{q}+\mathbf{G})}{|\mathbf{q}+\mathbf{G}|^2}+\lim_{\mathbf{q}\to 0}\frac{A(\mathbf{q})-A(0)}{\mathbf{q}^2}\right]+D\times A(0)\right\}
\end{aligned}
$$

no $\mathbf{q}+\mathbf{G}=0$ singularity, straightforward to compute

non-analytic limit 0/0 can be dealt with using different techniques (e.g. extrapolation)

computed analytically

F. Gygi and A. Baldereschi, PRB 34, 4405 (1986).

H.-V. Nguyen and S. de Gironcoli, PRB 79, 205114 (2009).

meta-GGA functionals

Main idea

$$E_{\mathrm{xc}}[n_\uparrow, n_\downarrow] = \int d^3r\, n(\mathbf{r})\, \varepsilon_{\mathrm{xc}}\Big(n_\uparrow(\mathbf{r}), n_\downarrow(\mathbf{r}), \nabla n_\uparrow(\mathbf{r}), \nabla n_\downarrow(\mathbf{r}), \nabla^2 n_\uparrow(\mathbf{r}), \nabla^2 n_\downarrow(\mathbf{r}), \tau_\uparrow(\mathbf{r}), \tau_\downarrow(\mathbf{r})\Big)$$

$$n(\mathbf{r}) = \sum_\sigma n_\sigma(\mathbf{r})$$ total charge density

$$n_\sigma(\mathbf{r}) = \sum_{v,\mathbf{k}} |\psi^\sigma_{v,\mathbf{k}}(\mathbf{r})|^2$$ spin-charge density

$$\sigma = \{\uparrow, \downarrow\}$$

$$\tau_\sigma(\mathbf{r}) = \frac{1}{2}\sum_{v,\mathbf{k}} |\nabla\psi^\sigma_{v,\mathbf{k}}(\mathbf{r})|^2$$ kinetic energy density

Different meta-GGA functionals

BR89

r^{2}SCAN

MVS

TPSS

SCAN

MGGA_MS2

rSCAN

TASK

revTPSS

HLE17

TM

SCAN-L

SCAN, rSCAN, r²SCAN

$$E_{\mathrm{xc}}[n_\uparrow, n_\downarrow] = \int d^3r\, n(\mathbf{r})\, \varepsilon_{\mathrm{xc}}\Big(n_\uparrow(\mathbf{r}), n_\downarrow(\mathbf{r}), \nabla n_\uparrow(\mathbf{r}), \nabla n_\downarrow(\mathbf{r}), \cancel{\nabla^2 n_\uparrow(\mathbf{r})}, \cancel{\nabla^2 n_\downarrow(\mathbf{r})}, \tau_\uparrow(\mathbf{r}), \tau_\downarrow(\mathbf{r})\Big)$$

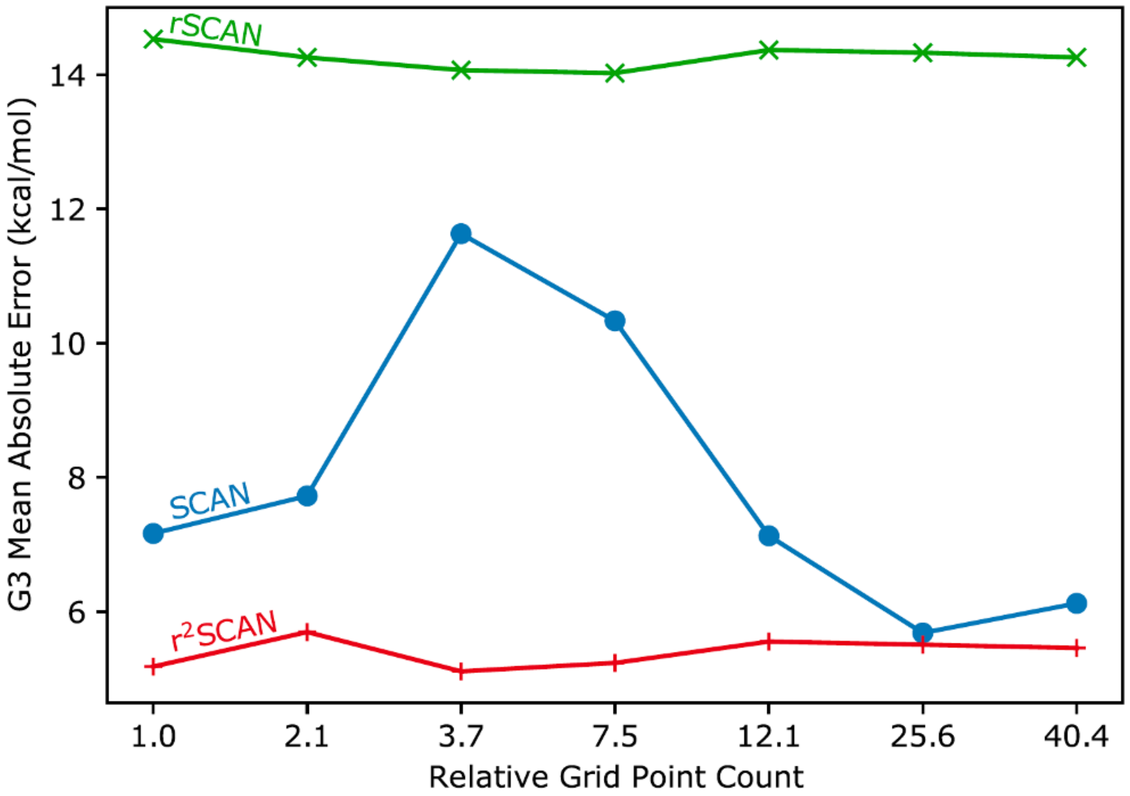

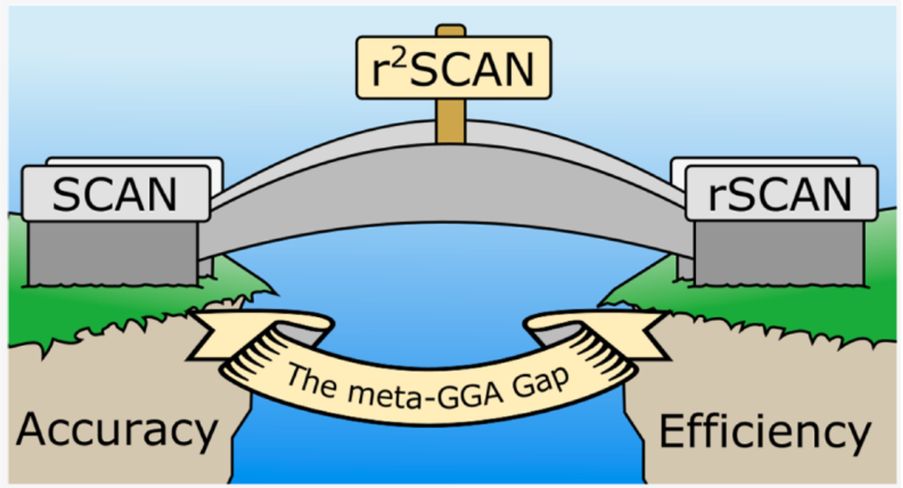

SCAN: J. Sun et al., Phys. Rev. Lett. ***115****, 036402 (2015).*

rSCAN: A. Bartok et al., J. Chem. Phys. ***150****, 161101 (2019).*

r²SCAN: J. Furness et al., J. Phys. Chem. Lett. ***11****, 8208 (2020).*

Accuracy of the SCAN meta-GGA functional

"SCAN" stands for Strongly Constrained and Appropriately Normed functional

SCAN obeys all 17 known exact constraints

	G 3^{HC} (kcal/mol)		G3 (kcal/mol)		BH76 (kcal/mol)		S22 (kcal/mol)		LC20(Å)	
	ME	MAE	ME	MAE	ME	MAE	ME	MAE	ME	MAE
LSDA	−5.6	13.0	−83.7	83.7	−15.2	15.4	2.3	2.3	−0.081	0.081
BLYP	1.8	6.2	3.8	9.5	−7.9	7.9	−8.7	8.8		
PBEsol	−4.1	6.5	−58.7	58.8	−11.5	11.5	−1.3	1.8	−0.012	0.036
PBE	−2.1	6.6	−21.7	22.2	−9.1	9.2	−2.8	2.8	0.051	0.059
TPSS	1.9	3.8	−5.2	5.8	−8.6	8.7	−3.7	3.7	0.035	0.043
M06 L	−0.2	4.6	−1.6	5.2	−3.9	4.1	−0.9	0.9	0.015	0.069
SCAN	−0.8	2.7	−4.6	5.7	−7.7	7.7	−0.7	0.9	0.007	0.016

TABLE II. Mean error (ME) and mean absolute error (MAE) of SCAN and other semilocal functionals for the G3 set of molecules [73], the BH76 set of chemical barrier heights [74], the S22 set of weakly bonded complexes [69], and the LC20 set of solid lattice constants [75]. For the G3-1 subset of small molecules, the SCAN MAE is 3.2 kcal/mol. $G3^{HC}$ is a subset of 46 G3 hydrocarbons, to which we have applied empirical corrections for the C atom as described in the text to show how consistently SCAN describes molecules. For all data sets, zero-point vibration effects have been removed from the reference experimental values. The LSDA results for G3 are from Ref. [25]. Becke-Lee-Yang-Parr (BLYP) [15,76], PBEsol [18], and PBE [6] are GGAs; SCAN, TPSS [7], and M06 L [20] are meta GGAs. We could not locate BLYP in VASP, but Ref. [77] suggests that its LC20 MAE may be more than twice that of PBE. (1 kcal/mol = 0.0434 eV.)

J. Sun, A. Ruzsinszky, J. P. Perdew, PRL 115, 036402 (2015).

Regularized SCAN (rSCAN)

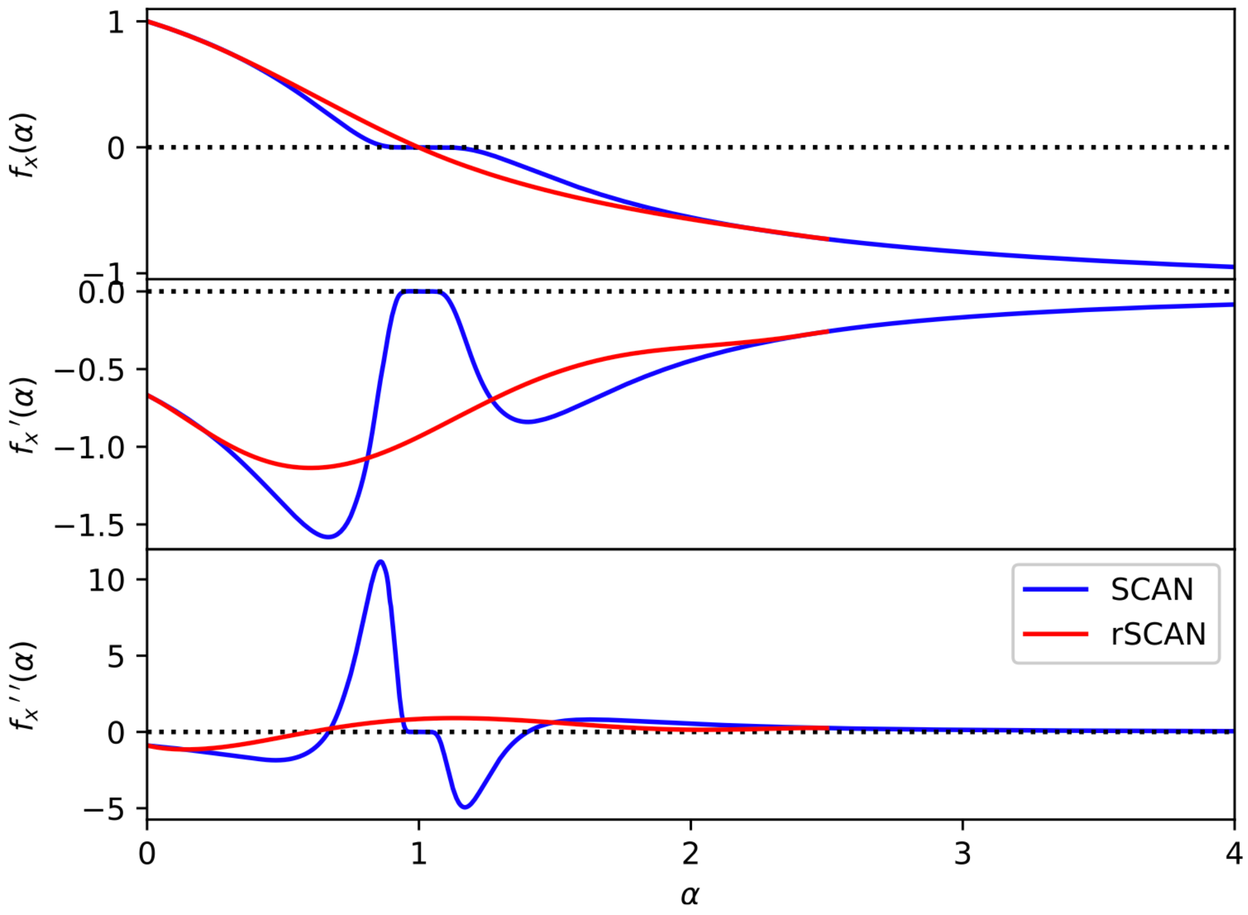

α is the isoorbital indicator function

$f_x,\ f_x',\ f_x''$ are the switching functions

rSCAN has better numerical behavior than SCAN, but it is less accurate than SCAN

A.P. Bartok and J.R. Yates, JCP 150, 161101 (2019).

SCAN vs rSCAN vs r^{2}SCAN

Table 2. Mean Error (ME) and Mean Absolute Error (MAE) of TPSS,[59] SCAN,[7] rSCAN,[22] and r^{2}SCAN for the G3 Set of 226 Molecular Atomization Energies,[28] the BH76 Set of 76 Chemical Barrier Heights,[54] the S22 set of 22 Interaction Energies between Closed Shell Complexes,[55] and the LC20 Set of 20 Solid Lattice Constants[56a]

	G3		BH76		S22		LC20	
	ME	MAE	ME	MAE	ME	MAE	ME	MAE
TPSS	−5.2	5.8	−8.6	8.6	−3.4	3.4	0.033	0.041
SCAN	−5.0	6.1	−7.7	7.7	−0.5	0.8	0.009	0.015
rSCAN	−14.0	14.3	−7.4	7.4	−1.2	1.3	0.020	0.025
r^{2}SCAN	−4.5	5.5	−7.1	7.2	−0.9	1.1	0.022	0.027

[a]Errors for G3, BH76, and S22 sets are in kcal/mol, whereas errors for LC20 are in Å. We did not make corrections for basis set superposition error for the S22 set which used the aug-cc-pVTZ basis set.[60] All calculations for G3 and BH76 used the 6-311++G(3df,3pd) basis set.[28,61] Details of the computational methods are included in Section S1 of the Supporting Information.

J.W. Furness, A.D. Kaplan, J. Ning, J.P. Perdew, and J. Sun, JPCL 11, 8208 (2020).

Success stories of SCAN

Material	Expt.	LDA	PBE	HSE	SCAN
Si	1.17	0.60	0.71	1.11	0.97
InP	1.42	0.50	0.72	1.52	1.06
GaAs	1.52	0.30	0.53	1.41	0.8
BAs	1.60[b]	1.21	1.26	1.71	1.51
CdSe	1.73	0.44	0.71	1.66	1.10
BP	2.10	1.36	1.43	1.79	1.74
GaP	2.35	1.53	1.69	2.09	1.94
CdS	2.48	0.96	1.23	2.27	1.62
β-GaN	3.17	1.70	1.69	2.97	2.03
ZnS	3.72	1.87	2.12	3.32	2.63
C[d]	5.50	4.14	4.17	4.94	4.58

SCAN provides more accurate band gaps than LDA and PBE, but less accurate than HSE

Z.-H. Yang, H. Peng, J. Sun, and J. P. Perdew, PRB 93, 205205 (2016).

Success stories of SCAN

Six polymorphs of MnO_2

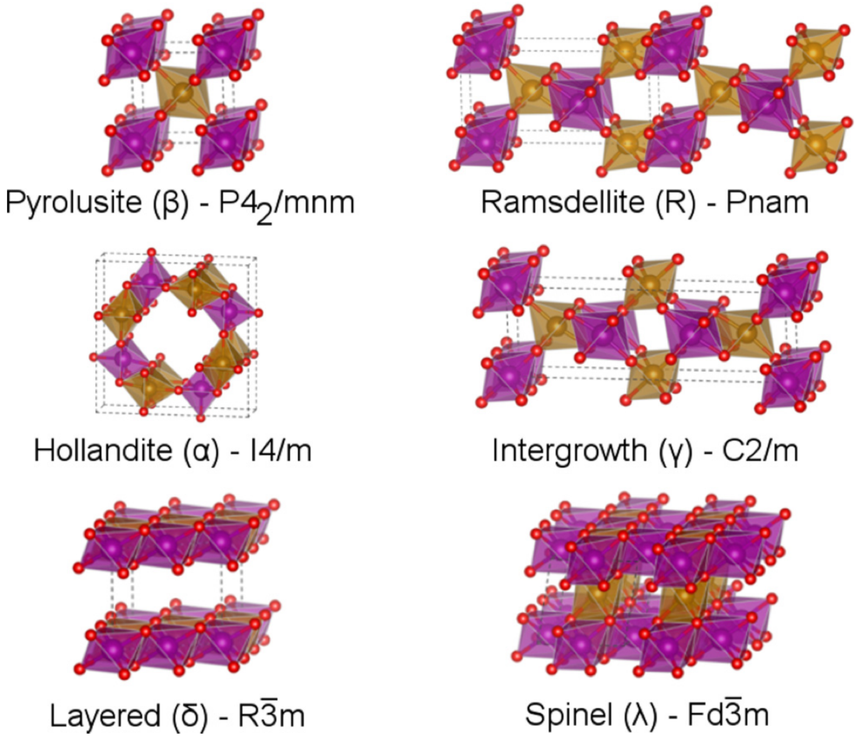

Formation energies relative to the β phase

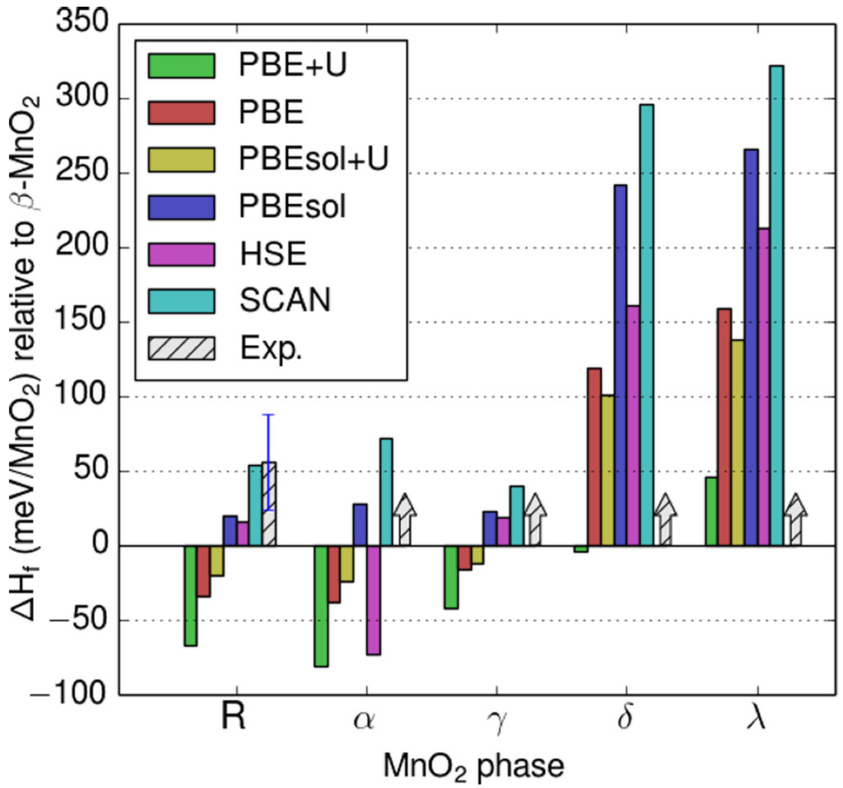

SCAN correctly predicts that the β phase is the lowest-energy phase

D. A. Kitchaev, H. Peng, Y. Liu, J. Sun, J.P. Perdew, and G. Ceder, PRB 93, 045132 (2016).

One of failures of SCAN

		V_0 (Å^3/at)	B_0 (GPa)	B_0' (1)	$m_s(V_0)$ (μ_B)
bcc-Fe	SCAN	11.58	157.5	5.05	2.66
	PBE	11.35	197.7	4.45	2.20
	LSDA	10.36	253.3	4.39	1.95
	Expt.	11.64	175.1	4.6	1.98,[b] 2.08,[c] 2.13[a]
fcc-Ni	SCAN	10.38	230.5	4.79	0.73
	PBE	10.90	199.8	4.76	0.63
	LSDA	10.06	253.6	4.77	0.58
	Expt.	10.81	192.5	4	0.52,[c] 0.55,[d] 0.57[a]
hcp-Co	SCAN	10.45	262.5	4.15	1.73
	PBE	10.91	196.9	4.61	1.61
	LSDA	9.99	237.6	4.95	1.49
	Expt.	10.96	198.4	4.26	1.52,[c] 1.55,[b] 1.58[e]

SCAN overestimates magnetic moments in itinerant ferromagnets

M. Ekholm, D. Gambino, H. J. M. Jönsson, F. Tasnádi, B. Alling, and I. A. Abrikosov, PRB 98, 094413 (2018).

van der Waals functionals

van der Waals (vdW) force

- vdW is a distance-dependent interaction between atoms or molecules
- vdW is weak, and it is different from ionic and covalent bonding
- vdW originate from correlations between charge fluctuations in different parts of an extended system (different fragments)
- vdW interactions are non-local
- vdW are not captured by LDA, GGA, meta-GGA (except SCAN for short-range part of vdW), DFT+U, and hybrids.

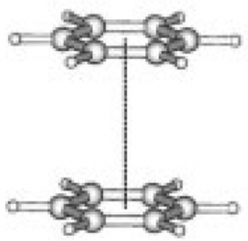

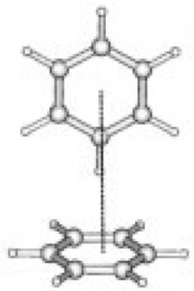

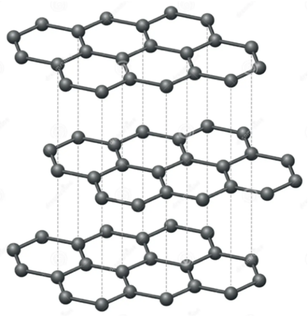

Two types of vdW functionals

vdW functionals

Empirical (or *ab initio*) corrections

$$C_6 R^{-6}$$

Fully nonlocal functionals

$$\frac{1}{2}\int\int n(\mathbf{r})\,\Phi(\mathbf{r},\mathbf{r}')\,n(\mathbf{r}')\,d\mathbf{r}\,d\mathbf{r}'$$

Two types of vdW functionals

vdW functionals

Empirical (or *ab initio*) corrections

$$C_6 R^{-6}$$

Fully nonlocal functionals

$$\frac{1}{2}\int\int n(\mathbf{r})\,\Phi(\mathbf{r},\mathbf{r}')\,n(\mathbf{r}')\,d\mathbf{r}\,d\mathbf{r}'$$

Lennard-Jones potential

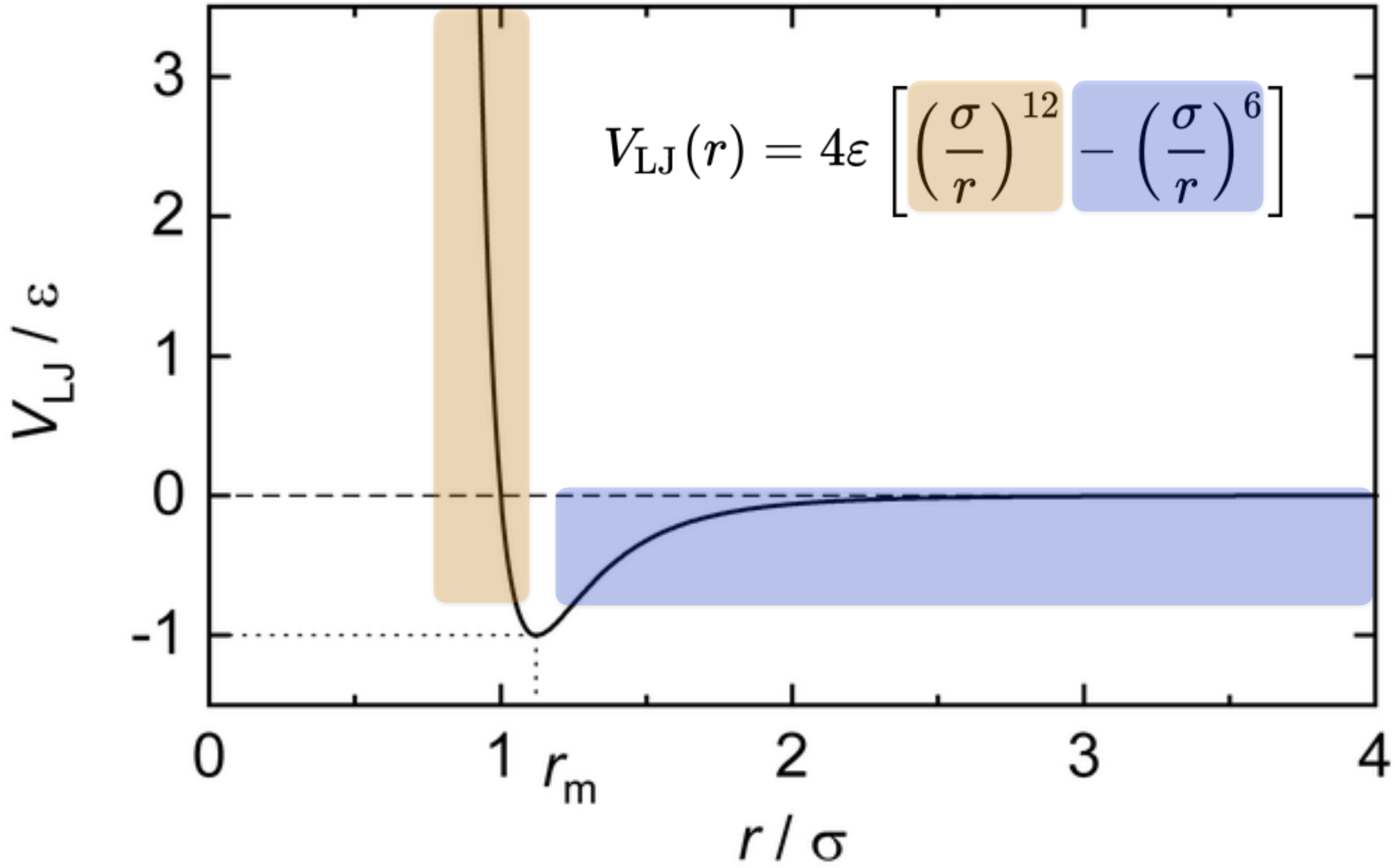

DFT-D functional

$$E_{\mathrm{DFT-D}} = E_{\mathrm{DFT}} + E_{\mathrm{vdW}}, \quad E_{\mathrm{vdW}} = -s_6 \sum_{i=1}^{N_{\mathrm{at}}-1} \sum_{j=i+1}^{N_{\mathrm{at}}} \frac{C_6^{ij}}{R_{ij}^6} f_{\mathrm{dmp}}(R_{ij}), \quad f_{\mathrm{dmp}}(R_{ij}) = \frac{1}{1+e^{-d(R_{ij}/R_r-1)}}$$

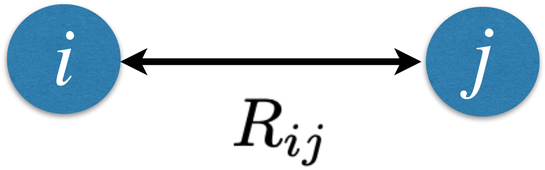

- Dispersion coefficients C_6^{ij} are determined empirically
- f_{dmp} is a damping function to avoid near-singularities for small R_{ij}

Element	C_6	R_0	Element	C_6	R_0
H	0.14	1.001	K	10.80[c]	1.485
He	0.08	1.012	Ca	10.80[c]	1.474
Li	1.61	0.825	Sc–Zn	10.80[c]	1.562[d]
Be	1.61	1.408	Ga	16.99	1.650
B	3.13	1.485	Ge	17.10	1.727
C	1.75	1.452	As	16.37	1.760
N	1.23	1.397	Se	12.64	1.771
O	0.70	1.342	Br	12.47	1.749
F	0.75	1.287	Kr	12.01	1.727
Ne	0.63	1.243	Rb	24.67[c]	1.628
Na	5.71[c]	1.144	Sr	24.67[c]	1.606
Mg	5.71[c]	1.364	Y–Cd	24.67[c]	1.639[d]
Al	10.79	1.639	In	37.32	1.672
Si	9.23	1.716	Sn	38.71	1.804
P	7.84	1.705	Sb	38.44	1.881
S	5.57	1.683	Te	31.74	1.892
Cl	5.07	1.639	I	31.50	1.892
Ar	4.61	1.595	Xe	29.99	1.881

S. Grimme, J. Comput. Chem. 27, 1787 (2006).

V. Barone et al., J. Comput. Chem. 30, 934 (2008).

DFT-D3 functional

$$E_{\text{DFT-D3}} = E_{\text{KS-DFT}} - E_{\text{vdW}}$$

$$E_{\text{vdW}} = E^{(2)} + E^{(3)}$$

S. Grimme, J. Antony, S. Ehrlich, H. Krieg, JCP 132, 154104 (2010).

DFT-D3 functional

$$E_{\text{DFT-D3}} = E_{\text{KS-DFT}} - E_{\text{vdW}}$$

$$E_{\text{vdW}} = E^{(2)} + E^{(3)}$$

Two-body term:

$$E^{(2)} = \sum_{AB} \sum_{n=6,8,10,\ldots} s_n \frac{C_n^{AB}}{r_{AB}^n} f_{d,n}(r_{AB})$$

$$f_{d,n}(r_{AB}) = \frac{1}{1 + 6(r_{AB}/(s_{r,n} R_0^{AB}))^{-\alpha_n}}$$

S. Grimme, J. Antony, S. Ehrlich, H. Krieg, JCP 132, 154104 (2010).

DFT-D3 functional

$$E_{\text{DFT-D3}} = E_{\text{KS-DFT}} - E_{\text{vdW}}$$

$$E_{\text{vdW}} = E^{(2)} + E^{(3)}$$

Two-body term:

$$E^{(2)} = \sum_{AB} \sum_{n=6,8,10,\ldots} s_n \frac{C_n^{AB}}{r_{AB}^n} f_{d,n}(r_{AB})$$

$$f_{d,n}(r_{AB}) = \frac{1}{1 + 6(r_{AB}/(s_{r,n}R_0^{AB}))^{-\alpha_n}}$$

Three-body term:

$$E^{(3)} = \sum_{ABC} f_{d,(3)}(\bar{r}_{ABC}) E^{ABC}$$

$$E^{ABC} = \frac{C_9^{ABC}(3 \cos\theta_a \cos\theta_b \cos\theta_c + 1)}{(r_{AB} r_{BC} r_{CA})^3}$$

S. Grimme, J. Antony, S. Ehrlich, H. Krieg, JCP 132, 154104 (2010).

Tkatchenko-Scheffler (TS) functional

$$E_{\mathrm{vdW}} = -\frac{1}{2}\sum_{A,B} f_{\mathrm{damp}}(R_{AB}, R_A^0, R_B^0) C_{6AB} R_{AB}^{-6}$$

Dispersion coefficients are computed from first principles using the electronic charge density

A. Tkatchenko and M. Scheffler, PRL 102, 073005 (2009).

Tkatchenko-Scheffler (TS) functional

$$E_{\mathrm{vdW}} = -\frac{1}{2}\sum_{A,B} f_{\mathrm{damp}}(R_{AB}, R_A^0, R_B^0) C_{6AB} R_{AB}^{-6}$$

Dispersion coefficients are computed from first principles using the electronic charge density

$$C_{6AB} = \frac{2C_{6AA}C_{6BB}}{\left[\frac{\alpha_B^0}{\alpha_A^0} C_{6AA} + \frac{\alpha_A^0}{\alpha_B^0} C_{6BB}\right]}$$

$$C_{6AA}^{\mathrm{eff}} = \frac{\eta_A^{\mathrm{eff}}}{\eta_A^{\mathrm{free}}} \left(\frac{\kappa_A^{\mathrm{free}}}{\kappa_A^{\mathrm{eff}}}\right)^2 \left(\frac{V_A^{\mathrm{eff}}}{V_A^{\mathrm{free}}}\right)^2 C_{6AA}^{\mathrm{free}}$$

A. Tkatchenko and M. Scheffler, PRL 102, 073005 (2009).

Tkatchenko-Scheffler (TS) functional

$$E_{\mathrm{vdW}} = -\frac{1}{2}\sum_{A,B} f_{\mathrm{damp}}(R_{AB}, R_A^0, R_B^0) C_{6AB} R_{AB}^{-6}$$

Dispersion coefficients are computed from first principles using the electronic charge density

$$C_{6AB} = \frac{2C_{6AA}C_{6BB}}{\left[\frac{\alpha_B^0}{\alpha_A^0}C_{6AA} + \frac{\alpha_A^0}{\alpha_B^0}C_{6BB}\right]}$$

$$C_{6AA}^{\mathrm{eff}} = \frac{\eta_A^{\mathrm{eff}}}{\eta_A^{\mathrm{free}}}\left(\frac{\kappa_A^{\mathrm{free}}}{\kappa_A^{\mathrm{eff}}}\right)^2\left(\frac{V_A^{\mathrm{eff}}}{V_A^{\mathrm{free}}}\right)^2 C_{6AA}^{\mathrm{free}}$$

Hirshfeld partitioning of the electronic charge density:

$$\frac{\kappa_A^{\mathrm{eff}}}{\kappa_A^{\mathrm{free}}}\frac{\alpha_A^{\mathrm{eff}}}{\alpha_A^{\mathrm{free}}} = \frac{V_A^{\mathrm{eff}}}{V_A^{\mathrm{free}}} = \left(\frac{\int r^3 w_A(\mathbf{r}) n(\mathbf{r}) d^3\mathbf{r}}{\int r^3 n_A^{\mathrm{free}}(\mathbf{r}) d^3\mathbf{r}}\right),$$

$$w_A(\mathbf{r}) = \frac{n_A^{\mathrm{free}}(\mathbf{r})}{\sum_B n_B^{\mathrm{free}}(\mathbf{r})},$$

A. Tkatchenko and M. Scheffler, PRL 102, 073005 (2009).

Two types of vdW functionals

vdW functionals

Empirical (or *ab initio*) corrections

$$C_6 R^{-6}$$

Fully nonlocal functionals

$$\frac{1}{2}\int\int n(\mathbf{r})\,\Phi(\mathbf{r},\mathbf{r}')\,n(\mathbf{r}')\,d\mathbf{r}\,d\mathbf{r}'$$

Fully nonlocal vdW functionals

Nonlocal correlation energy: $E_c[n] = E_c^0[n] + E_c^{nl}[n]$

$E_c^{nl}[n]$ is defined to include the longest ranged or most nonlocal terms that give the vdW interaction and to approach zero in the limit of a slowly varying density. The term $E_c^0[n]$ is also nonlocal, but approaches the LDA in this limit.

$$E_c^{nl} = \frac{1}{2} \int \int n(\mathbf{r}) \, \Phi\Big(n(\mathbf{r}), n(\mathbf{r}'), |\nabla n(\mathbf{r})|, |\nabla n(\mathbf{r}')|, |\mathbf{r} - \mathbf{r}'|\Big) \, n(\mathbf{r}') \, d\mathbf{r} \, d\mathbf{r}'$$

nonlocal kernel

There are different numerical methods and approximations how to compute $E_c^{nl}[n]$

Fully nonlocal vdW functionals

vdW-DF M. Dion et al., PRL 92, 246401 (2004).

vdW-DF2 K. Lee et al., PRB 82, 081101(R) (2010).

VV10 O.A. Vydrov and T. Van Voorhis, JCP 133, 244103 (2010).

rVV10 R. Sabatini, T. Gorni, S. de Gironcoli, PRB 87, 041108(R) (2013).

Examples

Binding energy curves for the Ar dimer

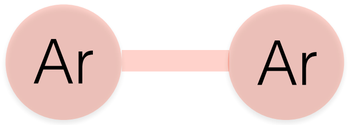

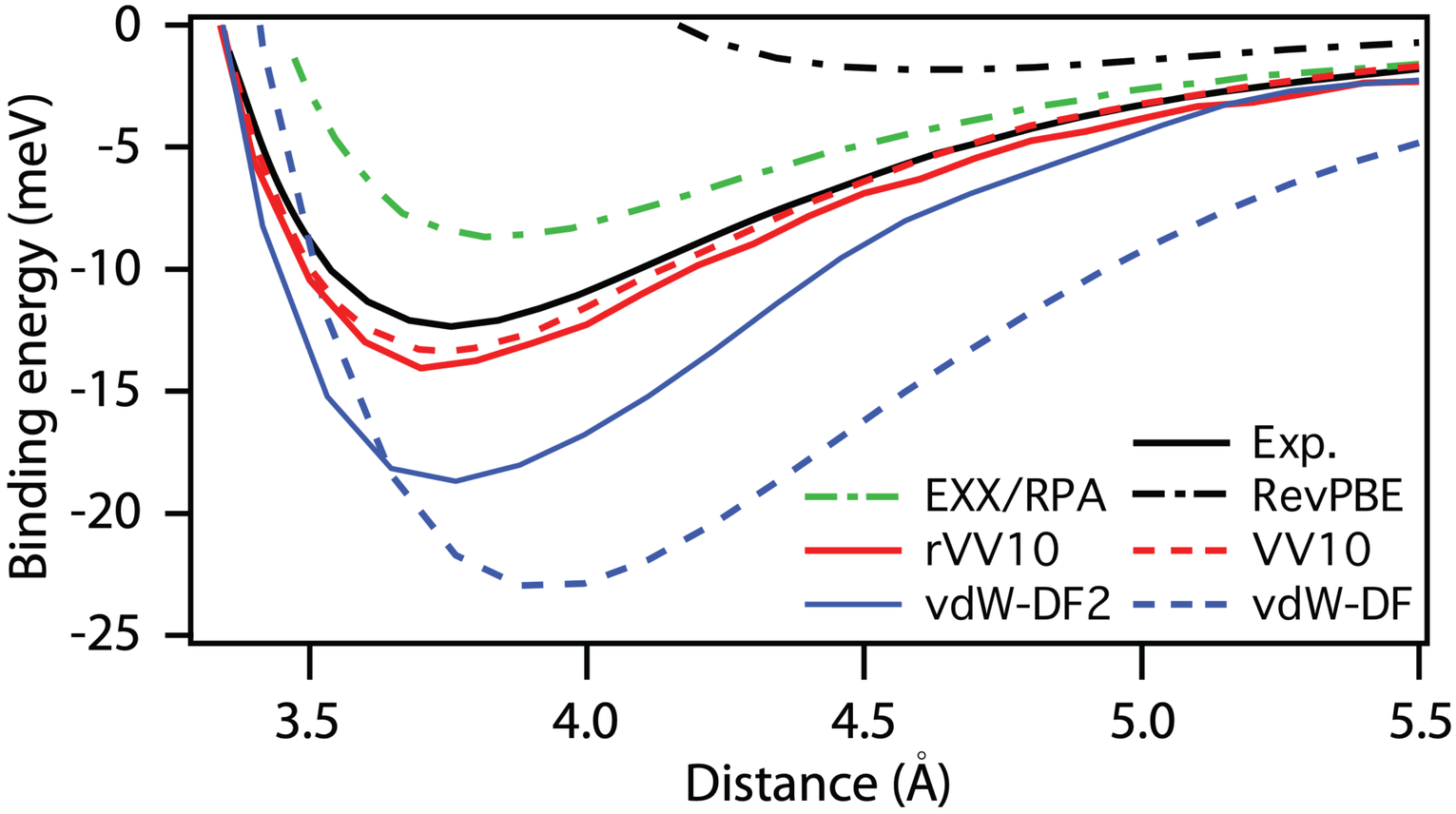

R. Sabatini, T. Gorni, S. De Gironcoli, PRB 87, 041108(R) (2013).

Examples

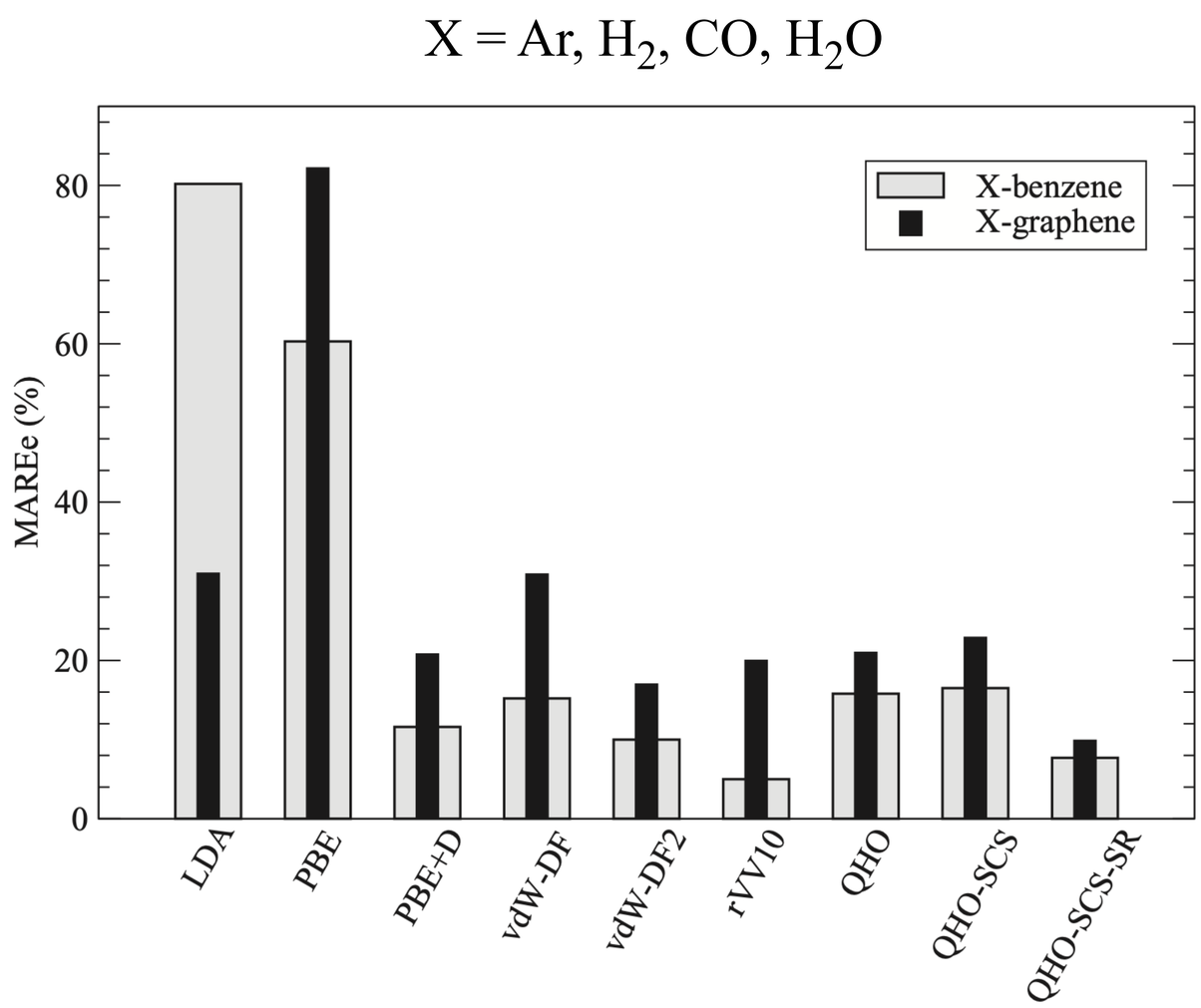

CO molecule

side view

graphene

top view

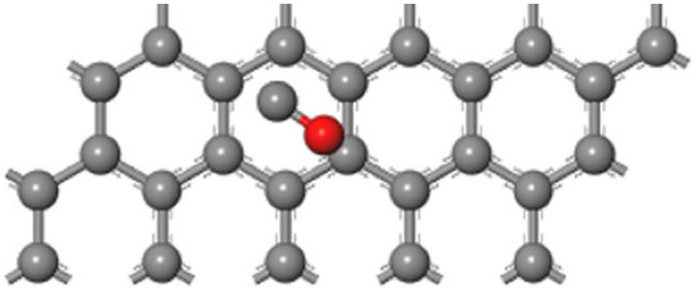

P.L. Silvestrelli and A. Ambrosetti, JCP 140, 124107 (2014).

Can we mix advanced functionals?

(meta-GGA) + (van der Waals) + (Hubbard *U*)

TABLE II. The calculated total energy with respect to the RS phase (ΔE in meV/f.u.), equilibrium volume (Ω_0 in Å^3/f.u.), bulk modulus (B_0 in GPa), and fundamental band gap (E_g in eV) for MnO, FeO, CoO, and NiO in both RS and ZB structures, using PBE+TS+U and SCAN+rVV10+U. The experimental data are collected in Refs. [17,18].

Compound		PBE+TS+U				SCAN+rVV10+U				Experiment		
		ΔE	Ω_0	B_0	E_g	ΔE	Ω_0	B_0	E_g	Ω_0	B_0	E_g
MnO	RS	**0**	21.58	156	1.8	**0**	21.71	164	2.3	21.96	151–162	3.8–4.2
	ZB	88	26.47	102	0.8	138	26.43	120	1.1			
FeO	RS	**0**	20.25	150	1.2	**0**	20.28	163	1.4	20.35	150–180	2.4
	ZB	142	24.34	107	0.3	157	23.15	84	0.8			
CoO	RS	**0**	19.06	184	2.3	**0**	19.08	186	2.9	19.25	180	3.6
	ZB	51	23.53	137	1.4	92	23.45	146	1.7			
NiO	RS	**0**	17.76	205	2.5	**0**	17.94	220	3.5	18.14	166–208	3.7–4.3
	ZB	768	20.55	56	0.9	782	21.16	85	1.5			

H. Peng and J. P. Perdew, PRB 96, 100101(R) (2017).

The Quantum ESPRESSO package

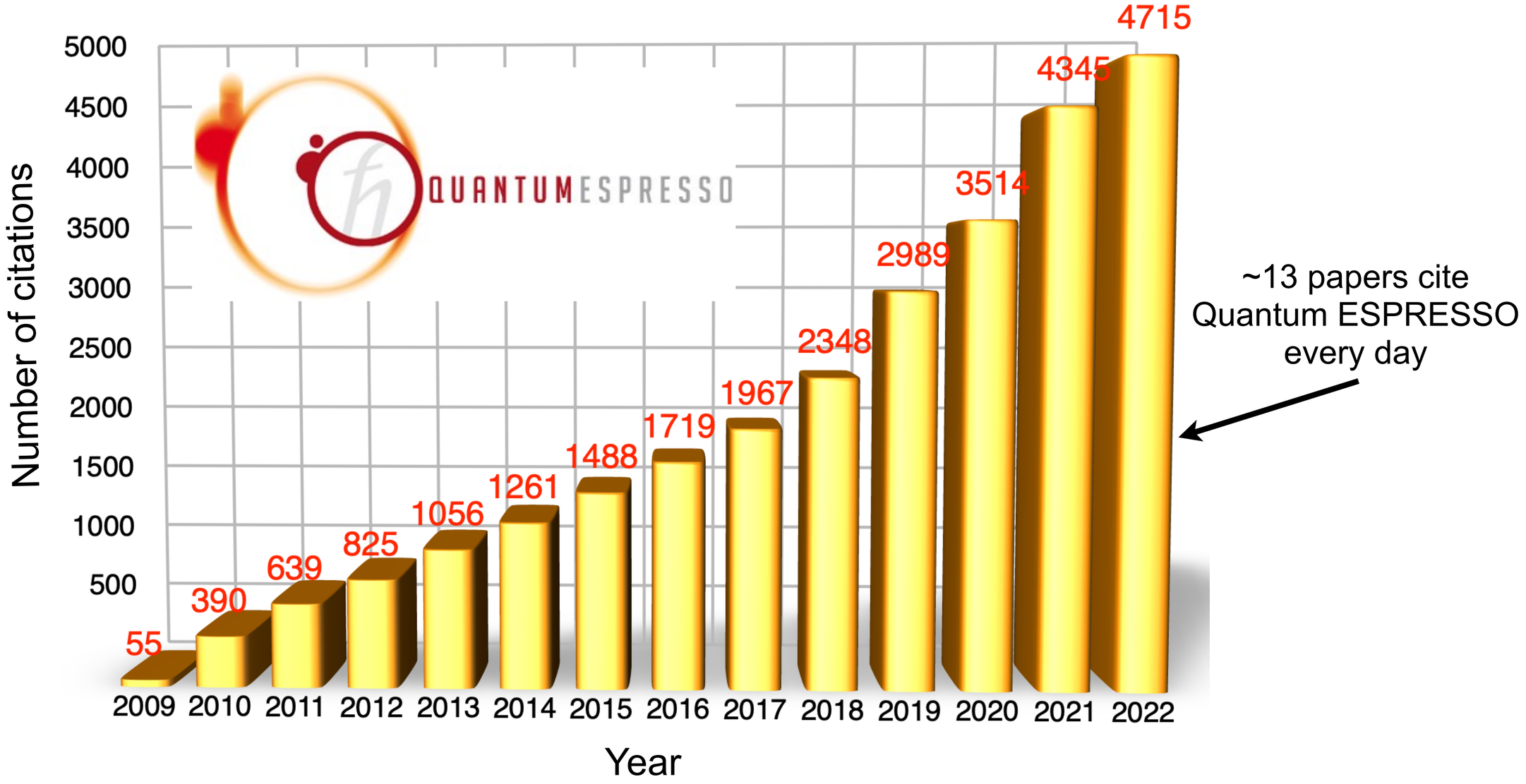

P. Giannozzi et al., JPCM (2009).

P. Giannozzi, …, I. Timrov et al., JPCM (2017) & JCP (2020).

2 PhD positions at PSI

Computational discovery, design, and characterization of novel Na-ion battery cathode materials

- **1st position (Discovery):** Will be between PSI and EPFL and co-supervised by **Dr. Iurii Timrov (PSI)** and **Prof. Nicola Marzari (EPFL/PSI)**. Title "Discovery of novel Na-ion battery cathode materials via high-throughput screening"
- **2nd position (Design):** Will be between PSI and ETH Zurich and co-supervised by **Dr. Iurii Timrov (PSI)** and **Prof. Claude Ederer (ETH Zurich)**. Title "Design of novel Na-ion battery cathode materials via substitutional doping"

Start date: 1 September 2024 (flexible)

To apply: iurii.timrov@psi.ch

PAUL SCHERRER INSTITUT

EPFL

ETH zürich